Studying Neuronal Cytoskeleton Defects and Synaptic Defects in Mouse Model of

Amyotrophic Lateral Sclerosis and Spinal Muscular Atrophy

✍

Die Analyse des neuronalen Zytoskeletts und synaptischer Defekte im Mausmodel der

Amyotrophen Lateralsklerose und der Spinalen Muskelatrophie

Doctoral thesis for a doctoral degree at the Graduate School of Life Sciences,

Julius-Maximilians-Universität Würzburg, Neuroscience section

Submitted by

Preeti Yadav

from

Jhalawar

Würzburg, 2016

Submitted on:…………………………………………………..

Members of the *Promotionskomitee:*

Chairperson: Prof. Utz Fischer

Primary Supervisor: Prof. Michael Sendtner

Supervisor (Second):   Prof. Erich Buchner

Supervisor (Third):   Dr. Robert Blum

Date of Public Defence:…………………………………………..

Date of receipt of Certificates:…………………………………………

For My Parents

Table of contents

List of figures

List of tables

Abbreviations

ALS	Amyotrophic lateral sclerosis
BDNF	Brain-derived neurotrophic factor
CNTF	Ciliary neurotrophic factor
DNA	Deoxyribonucleic acid
dNTP	Deoxyribonucleotriphosphate
E	Embryonic day
IF	Intermediate Filament
kb	Kilobases
kDa	Kilodalton
MN	Motoneurons
MND	Motoneuron disease
MT	Microtubule
nm	Nanometer
Nefl	Neurofilament-light gene mouse
NEFL	Neurofilament-light gene human
NFL	Neurofilament-light protein
NFH	Neurofilament-heavy
NFM	Neurofilament-medium
NMJ	Neuromuscular junction
P	Postnatal day
PBS	Phosphate buffered saline
RNA	Ribonucleic acid
RT-PCR	Reverse transcriptase polymerase chain reaction
SMA	Spinal muscular atrophy
SMN	Survival of motoneuron gene (human)
STAT3	Signal Transducer and Activator of Transcription (human gene)
Stat3	Signal Transducer and Activator of Transcription (mouse gene)
Stat3	Signal Transducer and Activator of Transcription (mouse protein)
TBST	Tris buffered saline-tween
°C	Degrees Celsius
μm	Micrometer

Zusammenfassung

Die Amyotrophe Lateralsklerose und die spinale Muskelatrophie sind die beiden häufigsten Formen der Motoneuronerkrankungen. Sie sind charakterisiert durch eine Destabilisierung der Axonendigungen, durch Axondegeneration und durch Änderungen im neuronalen Zytoskelett. Eine Anhäufung von Neurofilamenten konnte in einigen neurodegenerativen Erkrankungen beobachtet werden. Der genaue Mechanismus, welcher zu einer Destabilisierung des Axons führt, ist bis heute jedoch unklar. Hiermit zeige ich, dass eine gesteigerte Expression von Neurofilamenten in motorischen Nerven von *pmn* mutierten Mäusen zu einer Störung der Mikrotubuli – Dynamik führt. Ein Neurofilamentabbau durch *Nefl* knockout steigert die Anzahl an neu wachsenden Mikrotubuli in *pmn* mutierten Motoneuronen und führt zu erneutem Axonwachstum. Dieser Effekt wird durch eine Interaktion zwischen dem Neurofilament und dem Stathmin Komplex vermittelt. Ein Abbau des Neurofilaments führt zu einer Erhöhung der Stathmin-Stat3 Interaktion und zu einer Stabilisierung der Mikrotubuli. Demzufolge ist die Versorgung der Axone verbessert und die *pmn* mutierten Mäuse überleben länger. Wir vermuten, dass dieser Mechanismus auch für andere neurodegenerative Erkrankungen, bei denen Neurofilamentanhäufung ein dominantes Merkmal ist, relevant sein könnte.

Des Weiteren studierte ich mit Hilfe des $Smn^{-/-}$;*SMN2* Mausmodels, den molekularen Mechanismus der sich hinter dem Synapsenverlust bei SMA verbirgt. SMA ist charakterisiert durch eine Degeneration der unteren α-Motoneuronen im Rückenmark. Es ist jedoch unklar, wie ein Verlust des ubiquitär exprimierten SMN Proteins zu einer MN-spezifischen Degeneration führt. Smn ist involviert in den Prozess des pre-mRNA Splicing (Pellizzoni, Kataoka et al. 1998) und ein Verlust des Proteins führt zu einer Störung des Splicing. Eine Denervierung der motorischen Endplatte führt zu einer Neurodegeneration in SMA. Es gibt jedoch keinen Hinweis auf eine kausale Verbindung zwischen anomalem Splicen von stromabwärts gelegenen Transkripten des Smn und einer Reduktion präsynaptischer Axone, wie man es bei SMA beobachten kann. In dieser Studie konnten wir beobachten, dass Expression und Splicing von *Nrxn2*, welches für ein präsynaptisches Protein kodiert, in SMA Mäusen betroffen ist und dass Nrxn2 ein Kandidat sein könnte, der eine Verbindung zwischen Störungen im Splice Prozess und synaptischen Motoneuron-Defekten in der SMA herstellen könnte.

Abstract

Amyotrophic lateral sclerosis and spinal muscular atrophy are the two most common motoneuron diseases. Both are characterized by destabilization of axon terminals, axon degeneration and alterations in neuronal cytoskeleton. Accumulation of neurofilaments has been observed in several neurodegenerative diseases but the mechanisms how elevated neurofilament levels destabilize axons are unknown so far. Here, I show that increased neurofilament expression in motor nerves of *pmn* mutant mice causes disturbed microtubule dynamics. Depletion of neurofilament by *Nefl* knockout increases the number and regrowth of microtubules in *pmn* mutant motoneurons and restores axon elongation. This effect is mediated by interaction of neurofilament with the stathmin complex. Depletion of neurofilament increases stathmin-Stat3 interaction and stabilizes the microtubules. Consequently, the axonal maintenance is improved and the *pmn* mutant mice survive longer. We propose that this mechanism could also be relevant for other neurodegenerative diseases in which neurofilament accumulation is a prominent feature.

Next, using *Smn*$^{-/-}$;*SMN2* mouse as a model, the molecular mechanism behind synapse loss in SMA is studied. SMA is characterized by degeneration of lower α-motoneurons in spinal cord; however, how reduction of ubiquitously expressed SMN leads to MN-specific degeneration remains unclear. SMN is involved in pre-mRNA splicing (Pellizzoni, Kataoka et al. 1998) and its deficiency in SMA affects the splicing machinery. Neuromuscular junction denervation precedes neurodegeneration in SMA. However, there is no evidence of a link between aberrant splicing of transcripts downstream of *Smn* and reduced presynaptic axon excitability observed in SMA. In this study, we observed that expression and splicing of *Nrxn2*, that encodes a presynaptic protein is affected in the SMA mouse and that *Nrxn2* could be a candidate that relates aberrant splicing to synaptic motoneuron defects in SMA.

1   Introduction

1.1   Neuronal cytoskeleton

Neuronal cytoskeleton helps neurons to maintain their shape and internal organization by separation of cellular constituents, and also provides mechanical support to them. It provides stability and a track for transport of cellular constituents. These functions are achieved by three components of neuronal cytoskeleton; actin microfilaments (6-8 nm), intermediate filaments (10 nm) and microtubules (24 nm) (Fig. 1).
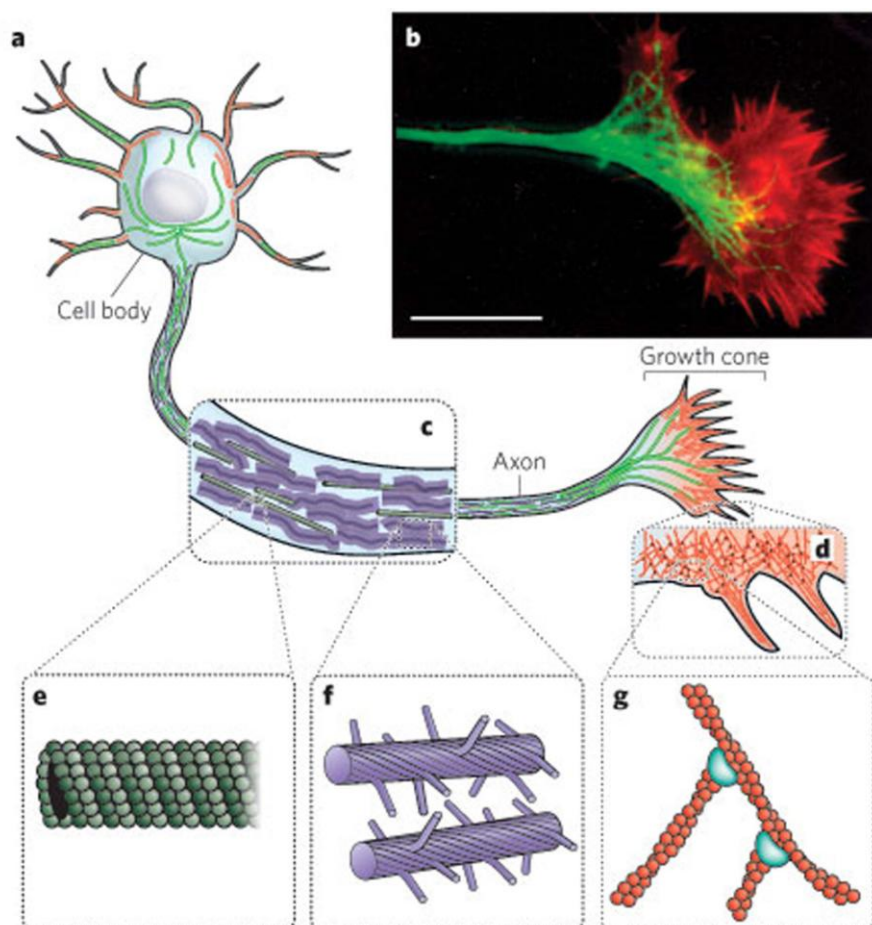
Figure 1: Neurons have elaborate cytoskeleton structure

(a- b) Neurons extend long processes to form connections in the nervous system. Microtubules (green), intermediate filaments (purple) and actin filaments (red) forms the neuronal cytoskeleton. (c) Axonal neurofilaments form a structural matrix that embeds microtubules. (d) Growth cone contains dendritic actin filament networks and parallel actin filament filopodia. (e) Microtubules (f) neurofilaments (g) actin filaments are shown (Fletcher and Mullins 2010).

Microfilaments are the smallest type, most diverse and dynamic component of the cytoskeleton, made up of filamentous actin (F-actin). Intermediate filament proteins, as the name suggests are middle sized and constitute a large gene family that provides mechanical stability to the cells. Microtubules, the largest type, are hollow tubes of protofilaments made of tubulin heterodimers and are associated with several proteins like MAP2, tau protein and stathmin. Microtubules and microfilaments are essential for neuronal development, migration, axon outgrowth, synaptic plasticity and intracellular transport but the functions of IF proteins in neurons remain elusive. Based on molecular structural homology, five types of IFs have been identified in neurons. Neurofilaments belong to type IV IFs together with α-internexin and nestin. Neurons may also express other IF proteins, such as nestin, synemin, syncoilin and vimentin (Perrin, Boisset et al. 2005).

1.1.1   Expression, synthesis and transport of neurofilaments

Neurofilaments are exclusively expressed in neurons and are composed of NF-light (NFL ~68 kd), NF-medium (NFM ~145 kd), NF-heavy (NFH ~200 kd) (Hoffman and Lasek 1975, Liem, Yen et al. 1978) polypeptides and α-internexin in the central nervous system (CNS). In peripheral nervous system, they are composed of NFL, NFM, NFH and peripherin (Beaulieu, Robertson et al. 1999, Yuan, Rao et al. 2006). NFs first appear at embryonic stages when neurite formation starts. The three subunits are differentially expressed during neurogenesis. NFL, α-internexin and peripherin are among the first to be expressed, with their expression starting at the beginning of neuronal differentiation (Carden, Trojanowski et al. 1987). NFM expression starts at the time of neurite formation. NFH is expressed after the axon is well established and has formed synaptic contacts, that is also the time of nervous system maturation when axonal radial growth is required (Shaw and Weber 1982, Julien, Meyer et al. 1986, Carden, Trojanowski et al. 1987, Nixon and Shea 1992). NFH mediates the establishment of stable network that prevents the rapid retraction of neurites. At the final phase of neuronal maturation gradual phosphorylation of C-terminal of NFM and NFH takes place. Several post-translational modifications such as phosphorylation, glycosylation, nitration and ubiquitylation occur in neurofilaments (Perrot, Berges et al. 2008).

After synthesis in the neuronal cell bodies NFs are moved to the axon along microtubules, via slow transport at rates of ~0.2-1 mm/day. There exist two hypotheses for the transport of NFs. Polymer hypothesis states that NF subunits are assembled in the perikarya and are transported as polymeric structure down the axon (Baas and Brown 1997) whereas subunit hypothesis suggests that they are transported as individual subunits (Hirokawa 1997, Nixon

1998, Nixon 1998). Their transport occurs bidirectionally along the axon via microtubules by motor proteins dynein and kinesin but with intermittent long pauses making the overall transport slow (Liu, Xie et al. 2004).

1.1.2 Structure and functions of neurofilament

NFs have a conserved central coiled coil helical rod domain of approximately 310 amino acids, which connects the amino-terminal head and carboxy-terminal tail domains (Fuchs and Weber 1994). Rods from two filaments, for e.g. NFL and NFL, same (homodimers) or NFL and NFM, different (heterodimers), coil around each other like a rope forming a dimer aligning the N and C terminals of each filament. The head domains of NFs contain a microtubule polymerization inhibitory domain that can regulate the number of MTs in the axon (Bocquet, Berges et al. 2009). Two dimers align in an anti-parallel, half staggered manner so that the carboxy and amino terminals project out to form a tetramer protofilament which forms the basic subunit of intermediate filaments. Finally, eight protofilaments are packed longitudinally in a helical array forming a rope like 10 nm filament. The C-termini of NFM and NFH form the fine lateral extensions that increase the spacing between NFs (Heins and Aebi 1994, Herrmann and Aebi 2000). Tail domains of NFH and NFM are also important for making cross-bridge between the neurofilaments which is influenced by their phosphorylation level (Eyer and Leterrier 1988). NFM and NFH by themselves do not form filaments (Elder, Friedrich et al. 1998, Elder, Friedrich et al. 1998). NFL is essential for the assembly of NFs whereas NFM and NFH forms the cross-bridges (Lee, Xu et al. 1993).

NF works in tandem with microtubules, providing strength and support for the fragile tubulin structures. NFs form the cytoskeleton of neurons together with MTs and MFs and provide shape, caliber, support and a platform for transport to the cell. First evidence of neurofilaments being important for the axonal caliber came from a mutant Japanese quail that lacks NFs because of a nonsense mutation and exhibited decreased axon caliber and reduced conduction velocity (Sakaguchi, Okada et al. 1993). The speed of transport in axon depends on caliber of the axon which is dependent on phosphorylation state of the NFs (Sakaguchi, Okada et al. 1993, Zhao, Ohnishi et al. 1994). They are essential for the radial growth of axons (Hoffman, Cleveland et al. 1987) and transmission of electrical impulses along the axons, i.e. velocity of nerve conduction (Friede and Samorajski 1970, Ohara, Gahara et al. 1993, Eyer and Peterson 1994, Zhu, Couillard-Despres et al. 1997).

1.2 Neurofilament accumulation in neurodegenerative diseases

Accumulation of neurofilaments has been observed in the cell bodies, proximal axons and dendrites of neurons in a variety of neurodegenerative diseases, such as ALS (Shankar, Yanagihara et al. 1989, Ishihara, Hong et al. 1999), both sporadic and familial ALS (Corbo and Hays 1992) Parkinson's disease and Alzheimer´s Disease (Schmidt, Lee et al. 1989, Schmidt, Lee et al. 1990, Schmidt, Martin et al. 1996). The cerebrospinal fluid of ALS patients shows high levels of NFL and NFH and auto-antibodies against NFL (Brettschneider, Petzold et al. 2006, Niebroj-Dobosz, Dziewulska et al. 2006). Mouse models of ALS show higher levels of plasma NFH at a later stage of disease progression and treatment response (Lu, Petzold et al. 2012), also the levels of NFL in the CSF of ALS patients are elevated during disease progression (Tortelli, Ruggieri et al. 2012).

Argyrophilic spheroids are usually reported in the cell bodies and axons of neurons in anterior horn of spinal cord of ALS patients and contain NF aggregates (Delisle and Carpenter 1984, Hirano, Donnenfeld et al. 1984, Schmidt, Carden et al. 1987, Sasaki, Maruyama et al. 1989). Alzheimer's disease is characterized by neurofibrillary tangles and senile plaques which results from neurodegeneration in the cell body. Tangles contain phosphorylated NFs and hyper-phosphorylated tau, which could be a result of perturbation in kinases and phosphatase activities. The hyper-phosphorylated tau is unable to bind to MTs and is unable to help in MT assembly *in vitro* (Sternberger, Sternberger et al. 1985, Gong, Lidsky et al. 2000).

Parkinson's disease, caused by degeneration of pigmented neurons in substantia nigra of the brain, is characterized by Lewy bodies which are composed of altered NFs, MTs, ubiquitin and other proteins. Mutations of NFM rod domain have been identified in cellular aggregates in Parkinson's disease patients (Lavedan, Buchholtz et al. 2002). Several families with Charcot Marie Tooth disease, characterized by degeneration of motoneurons and sensory neurons affecting skeletal muscles, show mutation in *NEFL* gene that affects NF assembly, axonal transport or NF phosphorylation. Intermediate filament accumulation is also a prominent feature in giant axonal neuropathy (GAN), neurofilament inclusion disease (NFID), diabetic neuropathy, spinal muscular atrophy (SMA) and spastic paraplegia (Mersiyanova, Perepelov et al. 2000, De Jonghe, Mersivanova et al. 2001, Georgiou, Zidar et al. 2002, Jordanova, De Jonghe et al. 2003, Abe, Numakura et al. 2009, Perrot and Eyer 2009, Szaro and Strong 2010).

1.2.1 Mouse models of neurofilament deletion

Several transgenic and knockout mouse models with neurofilament overexpression or deletion have been produced to support the idea that NF accumulation is a cause of neurodegeneration rather than just a consequence. NFL has been considered as an obligate subunit for the assembly of NF triplet proteins. But *Nefl* knockout mice (Zhu, Couillard-Despres et al. 1997) develop no overt disease phenotype and only show a scarcity of IF structures and severe axonal hypotrophy. Levels of other two neurofilament proteins; NFH and NFM are heavily reduced in brain and sciatic nerve; tubulin and GAP-43 levels are increased in the *Nefl* knockout mouse. Cerebral cortex of *Nefl* knockout mice shows a significant reduction in phosphorylated and dephoshphorylated NFs. ClassIII neuron-specific β-tubulin and microtubule-associated protein 2 were increased and β-actin levels were decreased at postnatal day 4 in this mouse (Liu, Staal et al. 2013). This mouse model confirmed the importance of NFL in IF assembly.

Nefm knockout mice show increased levels of NFH and nearly 50% reduced levels of NFL; the mice exhibit reduced axonal caliber and increased velocity of axonal transport of NF proteins (Elder, Friedrich et al. 1998). *Nefh* null mice, on the other hand, have no change in number and packing density of neurofilaments (Elder, Friedrich et al. 1998) but show a decrease in nerve conduction velocity and increase in microtubule density in the large ventral root axons (Zhu, Lindenbaum et al. 1998, Kriz, Zhu et al. 2000). Also, an increase in the transport velocity of newly synthesized neurofilaments is observed. Caliber of both large and small diameter myelinated axons is diminished in *Nefh* null mice and large diameter axons do not develop in such mice showing the importance of NFH in development of large diameter axons (Elder, Friedrich et al. 1998). When *Nefh* null mice are treated with the toxin IDPN (β, β′-Iminodipropionitrile) that segregates microtubules and retards neurofilament transport, the mice did not develop NF swellings in motoneurons as is seen in wild-type mice (Zhu, Lindenbaum et al. 1998). These findings suggested that NFH might not be important for the radial growth of axons but it is required for its interaction with the microtubules.

The double knockout mouse for *Nefm* and *Nefh* showed reduction in axonal IFs and NFL proteins. NFL was enhanced in the cell body but was nearly absent in axons and the number of microtubules was increased (Elder, Friedrich et al. 1999, Jacomy, Zhu et al. 1999), indicating that NFL needs NFM and NFH to translocate to axons and to establish filaments at this cellular site.

1.2.2 Mouse models that overexpress neurofilament

Direct evidence for the ability of aberrant neurofilaments to cause neurodegeneration came from studies with transgenic mice that overexpress different neurofilament proteins. Mice that overexpress *Nefl* show ALS- like symptoms, such as extensive neurodegeneration, massive accumulation of NFs, axonal degeneration, swellings in proximal axon and severe skeletal muscle atrophy. Most of these mice die during the third week after birth suggesting a direct role of NFL accumulation in neurodegeneration (Xu, Cork et al. 1993).

Nefm overexpression in mice leads to proportionate decrease in NFH levels, probably to maintain the stoichiometry of NF. No neuronal loss is observed but the mouse exhibits axons with reduced cross-sectional area and filamentous swellings (Wong, Marszalek et al. 1995). Mice that overexpress *Nefh* do not show any neurodegeneration but the radial growth of axons is reduced, NF transport along the axons is slowed, NFs are accumulated in perikarya and motoneurons exhibit proximal axon swellings (Marszalek, Williamson et al. 1996). When the hNFH gene is introduced in mouse, a progressive neuropathy with swellings containing NFs and muscular atrophy develops (Cote, Collard et al. 1993). Increasing NFH and or NFM levels in the mouse inhibited dendritic arborization of motoneurons and caused dissociation of the NF network from microtubules causing NF aggregation which could be rescued by increasing NFL levels. This suggests the importance of stoichiometry of NF proteins and NFL as the important subunit (Kong, Tung et al. 1998).

1.2.3 Neurofilament deletion in mouse with neurodegenerative diseases

To investigate the direct influence of neurofilament accumulation in diseases, different neuro-filament genes were knocked out from the respective mouse models. When *Nefl* was deleted from tau transgenic mice overexpressing human tau protein (T44 mice), the pathological symptoms were reduced. Tau and NF containing spheroids were reduced and the mice showed reduced motor weakness, improved motor behavior and increased viability (Ishihara, Higuchi et al. 2001). When *Nefl* was deleted from ALS linked mutant *tg(SOD1*G85R)* mice, the disease was delayed and life span of mouse was increased. These mice showed delayed axonal degeneration, motoneurons showed reduced levels of NFM and NFH subunits in ax-onal compartment and increased NF in the cell bodies (Williamson, Bruijn et al. 1998). In order to study the effect of NF stoichiometry, one allele for all the three NFs were removed from an ALS linked mutant *tg(SOD*G37R)* mouse, that reduced the NF content but main-tained the stoichiometry of NFs, the mice showed reduced caliber of large axons but no rescue from neurodegeneration (Nguyen, Lariviere et al. 2000). When the *tg(SOD1*G37R)* mouse

model was crossed with mice expressing human *Nefh*, the resulting mice showed a 65% increase in lifespan, and neurodegeneration was reduced (Couillard-Despres, Zhu et al. 1998).

1.3   Progressive motoneuropathy or *pmn* mutant mouse

Pmn mouse is a model of amyotrophic lateral sclerosis that carries a mutation in the tubulin-specific chaperone E (*tbce*) gene. The mouse suffers from a severe motoneuron disease, leading to axonal trafficking defects and axonal degeneration (Bommel, Xie et al. 2002, Martin, Jaubert et al. 2002, Selvaraj, Frank et al. 2012). Homozygous *pmn* mice are healthy at birth but start to show the first symptoms of weakness in third postnatal week. By the attainment of fourth week, the disease reaches an advanced stage and most of the *pmn* homozygous mice die at the age of 5-6 weeks (Schmalbruch, Jensen et al. 1991, Sendtner, Schmalbruch et al. 1992). The disease progresses in a dying back fashion in which hind limb muscles show neurogenic atrophy and the gastrocnemius muscle shows postsynaptic fold with degenerating axons (Schmalbruch, Jensen et al. 1991). Phrenic nerve and facial nucleus of *pmn* mutant mice show loss of myelinated axons and motoneurons (Sendtner, Schmalbruch et al. 1992, Sagot, Tan et al. 1996).

A tryptophan to glycine substitution at position 524 (t1682g) in the *tbce* gene leads to production of a destabilized Tbce protein which results in unstable MTs that causes neurodegeneration in *pmn* mutant mouse (Bommel, Xie et al. 2002, Martin, Jaubert et al. 2002). The protein binds to α-tubulin and is required for formation of α-tubulin and β-tubulin heterodimers, which are essential for microtubule polymerization. Number of microtubules in phrenic nerve from one week old mice are normal but in the second postnatal week 20% of axons show loss of microtubules and by the end of fourth week, all microtubules are lost, whereas intermediate filaments are still present (Martin, Jaubert et al. 2002).

Isolated motoneurons from *pmn* mutant mice, cultured for 7 days *in vitro* show reduced axon outgrowth. This reduction in axon length of motoneurons can be rescued by CNTF application which also enhances both the rate and speed of axonal mitochondrial transport (Selvaraj, Frank et al. 2012). *In vitro* cultured motoneurons from *pmn* mice show a reduction in microtubule density in the proximal part of the axon (Selvaraj, Frank et al. 2012). *Pmn* mutant motoneurons exhibit reduced microtubule regrowth after nocodazole treatment which is also rescued by CNTF application (Selvaraj, Frank et al. 2012). These studies suggested a close relationship between *tbce* mutation in *pmn* mice and dysregualtion of microtubule network.

1.4 Microtubule dynamics in neurons

1.4.1 Synthesis and assembly of microtubules

Neurons are polar cells with a long axon and multiple short dendrites. In axons, orientation of microtubules plus end is towards the axon tip but in dendrites the plus end of microtubules could be facing either cell body or the axon tip. MTs are polymers made of α- and β-tubulin heterodimers and maintain the intracellular transport, shape, polarity and division of a cell. Synthesis of microtubules is a complex process that involves several chaperons. Nascent α- and β- tubulins interact with prefoldin that transports them to cytosolic chaperonin CCT. Here, α- tubulin is captured by cofactor B (TBCB) (Lewis, Tian et al. 1997), and β -tubulin by cofactor A (TBCA) (Campo, Fontalba et al. 1994). At the next step, α -tubulin is captured by cofactor E (TBCE) and β -tubulin by cofactor D (TBCD) to form a super-complex with which the cofactor C (TBCC) interacts, and finally the αβ-tubulin heterodimers are released upon GTP hydrolysis (Fontalba, Paciucci et al. 1993). These heterodimers assemble in head-to-tail fashion such that all the β -tubulin subunits face towards the faster growing end (plus end) and α -tubulin faces the slower-growing end (minus end) to form a protofilament. γ-tubulin, serves as a template for the correct assembly of microtubules. 10-15 protofilaments associate laterally to form a 24 nm hollow cylinder called microtubule (Desai and Mitchison 1997, Tuszynski, Carpenter et al. 2006). Catalytic domain of α-tubulin of a free dimer contacts the E site (nucleotide exchange site) of the β-subunit in the protofilament. Plus end contains GTP cap that stabilizes the microtubule structure but minus end has no GTP cap since E-site of new dimer binds to the catalytic region of the last subunit. When the GTP cap of plus end is lost the protofilaments splay apart and microtubules depolymerize. After polymerization, GTP is hydrolyzed and cannot be exchanged.

1.4.2 Post-translational modifications of microtubules

Post-translational modifications of tubulin are important for neuronal differentiation and axon guidance (Janke and Bulinski 2011). Most of the tubulin modifications occur on polymerized tubulin i.e. on the tubulins that has been incorporated into the microtubules (Kumar and Flavin 1981, Gundersen, Khawaja et al. 1987, Matten, Aubry et al. 1990) (Fig. 2). Both microtubules and tubulins undergo several post-translational modifications which determine their functions, diversity and properties and are dependent upon development state, differentiation state and cellular compartment where the microtubules are present (Song and Brady 2015) (Fig. 3).
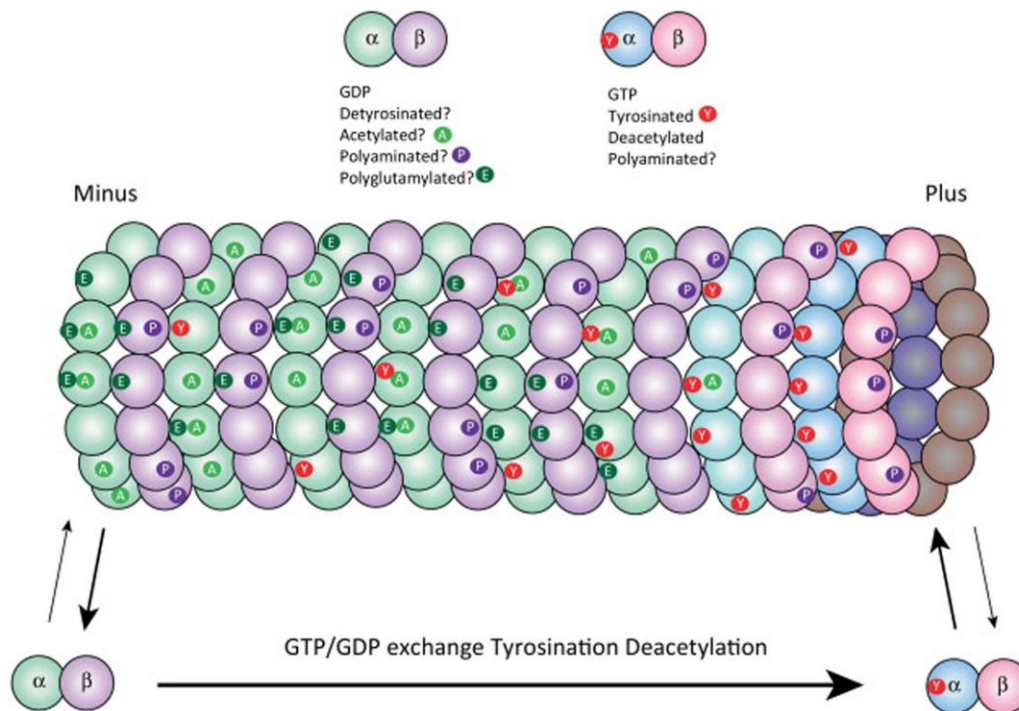
Figure 2: Post-translational modifications of microtubules and tubulins
Tubulin dimers are GTP-rich (blue-pink shading) in the soluble pool and on the plus end of the microtubule, but polymeric tubulin gradually hydrolyzes GTP and becomes GDP-rich (green/purple shading). Some modifications are associated specifically with tubulin polymerized in microtubules including acetylation (A), detyrosination, and polyglutamylation (E), while others may occur only on soluble tubulin like tyrosination (Y), or on either soluble or polymerized tubulin like polyamination (P) (Song and Brady 2015).

The detyrosination-retyrosination of α- tubulin at the C terminus is a reversible post-translational modification (Barra, Rodriguez et al. 1973). It is accomplished by carboxypeptidase that catalyzes the removal of tyrosine residues (Hallak, Rodriguez et al. 1977) preferentially acting on the polymerized tubulin (Kumar and Flavin 1981) and tubulin tyrosine ligase (TTL) that adds the tyrosine residue acting only on the monomeric tubulin (Raybin and Flavin 1977). Stathmin and TTL compete for binding on tubulin dimers; stathmin may thus regulate TTL function and can inhibit tyrosination of tubulin (Steinmetz 2007, Szyk, Deaconescu et al. 2011). The monomer pool of tubulin is completely tyrosinated in cultured cells (Gundersen, Khawaja et al. 1987, Webster, Gundersen et al. 1987). Microtubules are formed from tyrosinated tubulin monomers therefore proliferating non-differentiated cells are mainly composed of tyrosinated tubulin. Once the cells start differentiating, MTs become stabilized and the carboxypeptidase can act on them and hence differentiated cells are mainly composed of glutamylated (Glu) tubulin (Gundersen, Kalnoski et al. 1984, Gundersen, Khawaja et al. 1987, Schulze, Asai et al. 1987, Webster, Gundersen et al. 1987). Detyrosinated tubulins are en-

21

riched in the proximal axons and tyrosinated tubulins are concentrated at the tips of the neu-rites and at the growth cones (Geuens, Gundersen et al. 1986, Brown, Li et al. 1993). Motor protein kinesin preferentially binds to Glu tubulin as compared to the tyrosinated tubulin (Liao and Gundersen 1998). Detyrosinated tubulin acts as a signal for the recruitment of in-termediate filaments to the MTs and affects their interaction through a mechanism that in-volves the motor protein kinesin (Kreitzer, Liao et al. 1999). Motor protein kinesin binds to tyrosinated tubulin and depolymerizes the MTs suggesting that detyrosination protects the MTs (Peris, Wagenbach et al. 2009, Ghosh-Roy, Goncharov et al. 2012). The neurites where microtubules are highly unstable or tyrosinated tubulin is predominant develop into dendrites (Witte, Neukirchen et al. 2008).
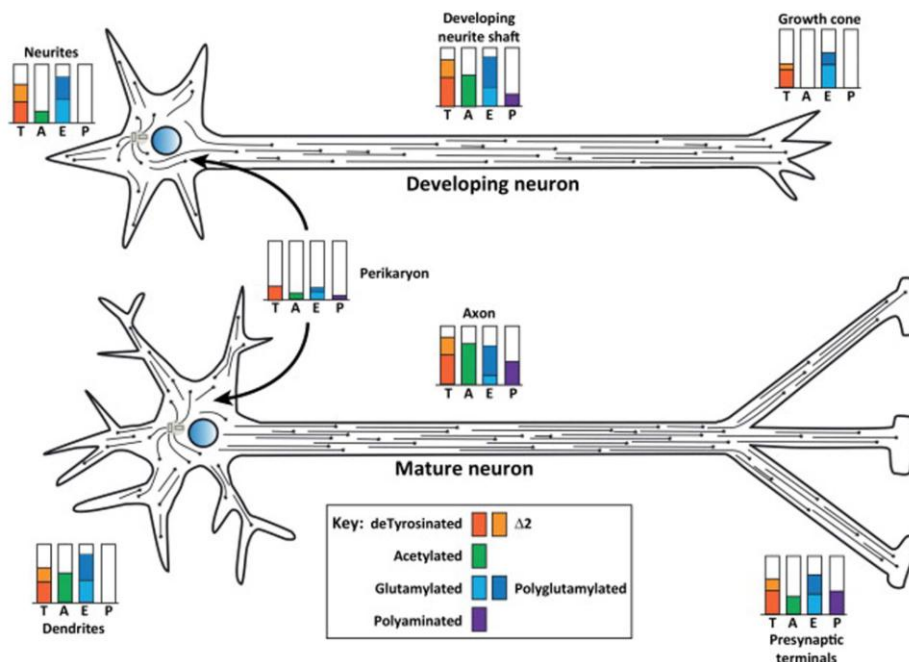
Figure 3: Post-translational modifications of microtubules and tubulins in neurons
PTMs vary in different regions of a neuron and change during neuronal differentiation. In developing neuron (upper), microtubules in all neurites are plus end out. In a mature neuron, microtubules from dendrites exhibit mixed polarity while axonal microtubules remain plus end out. (Song and Brady 2015)

Acetylation of tubulin occurs stochastically at α-tubulin Lys40 (L'Hernault and Rosenbaum 1985), on the surface of microtubules by tubulin acetyltransferase (TAT), not only at the ends but is distributed along the MT surface. Acetylation is not essential for cell survival because some cells and organisms are completely deficient of acetylated tubulin (Perdiz, Mackeh et al. 2011). Surprisingly, mice that lack αTAT1 or acetylated MTs showed an increase in MT sta-bility and were more resistant to nocodazole treatment (Kalebic, Sorrentino et al. 2013).

Acetylation predominantly occurs in long-lived MTs because soluble tubulin dimers are rapidly deacetylated. Direct tests showed no effect of acetylation on MT dynamics (Janke and Bulinski 2011). Acetylation occurs on polymerized tubulin incorporated in MTs whereas when tubulin dimers are released from the MTs they are rapidly deacetylated (Perdiz, Mackeh et al. 2011). Taxol treatment stabilizes the MTs and aids in regeneration of axons after spinal cord injury (Hellal, Hurtado et al. 2011). It increases total polymerized tubulin and decreases tyrosinated tubulin and thus helps in regeneration of axons after lesion. This suggests that regulation of MT stability and turnover are controlled by local regulatory mechanisms and they are important for regeneration and degeneration as in motoneuron diseases.

1.4.3   Role of microtubules in axonal transport

Motoneurons are polarized cells with their axons reaching very far from the cell body where vital components required for cell maintenance and growth are synthesized. Transport of the vital components such as mitochondria, vesicles, proteins, RNA, cytoskeletal components such as NFs from the cell body to the axons is essential for the growth and maintenance of motoneurons. Impairment in this transport is related to various motoneuron diseases such as mutant SOD1 mice show impaired mitochondrial transport (Williamson and Cleveland 1999, Marinkovic, Reuter et al. 2012) and *pmn* mutant mice show reduced mitochondrial transport (Selvaraj, Frank et al. 2012). Axonal transport occurs along the microtubule network with the help of motor proteins; Dyneins and Kinesins. Mutation in the genes coding for these motor proteins are also related to motoneuron degeneration (Zhao, Takita et al. 2001, Reid, Kloos et al. 2002, Hafezparast, Klocke et al. 2003). Disruption of transport leads to accumulation of cargoes in the proximal part of axons and perikarya of the neurons, thus representing a characteristic feature of motoneuron diseases.

1.4.4   Proteins interacting with microtubules

MAPs are microtubule associated proteins that induce microtubule polymerization, e.g. Tau and MAP1B interacts with microtubule near the growth cone and promote axon outgrowth. On the other hand, stathmins constitute a family of microtubule destabilizing proteins that includes stathmin1, SCG10, SCLIP and RB3. MAP2 is found associated with MTs in dendrites whereas tau is present in axons.

1.4.5 Microtubule associated protein stathmin

Stathmin or OpI8 is a 17 kDa highly conserved microtubule dynamics regulator protein, ubiquitously expressed in the cell (Sobel, Boutterin et al. 1989) and abundantly expressed in the developing nervous system. It is cytoplasmic and is present in various phosphorylated and unphosphorylated forms. Stathmin is phosphorylated in response to various extracellular signals regulating cell differentiation and proliferation. Stathmin is important to control the dynamics of microtubules through the cell cycle in a phosphorylation-dependent manner (Belmont, Mitchison et al. 1996, Marklund, Larsson et al. 1996). It interacts with the tubulin heterodimers to form a tight ternary T2S complex that cannot polymerize in microtubules. It acts as a pure tubulin sequestering protein and lowers the concentration of soluble tubulin that disturbs the microtubule assembly (Jourdain, Curmi et al. 1997). *In vivo* studies of decreasing stathmin levels have shown to result in reduced numbers of microtubule catastrophes and increased levels of polymerized microtubules (Howell, Deacon et al. 1999). Stathmin is inactivated by phosphorylation which also inactivates its MT- binding capacity. Stathmin levels are increased in many types of cancer cells.

1.4.6 Signal transducer and activator of transcription 3

Stat3 (signal transducer and activator of transcription 3) is a transcription factor important in cytokine signaling. It is phosphorylated upon cytokine stimulus and the activation involves cytokine induced receptor subunit multimerization and activation of receptor-associated Jak protein kinase at the intracellular domain (Darnell 1994). Jak kinase phosphorylation of the receptor subunits recruits Stat3 from the cytoplasm. Stat3 is then phosphorylated, dimerized and translocated to the nucleus where it binds to the CTGGGA motif of DNA and directs the transcription of several genes like c-myc, Bcl-2 etc. (Heim, Kerr et al. 1995). These genes may be required for cell cycle regulation and migration for Stat3 mediated tumorigenesis. Stat3 functional motifs include an amino terminus involved in dimerization, coiled coil domain for protein-protein interactions, a central DNA binding domain, a SRC homology domain (SH2) containing the conserved tyrosine phosphorylation site at 705, and a C-terminus which plays a roles in transcription activation (Reich and Liu 2006). *Stat3* knockout in mice causes early embryonic lethality indicating that Stat3 plays an important role in early embryonic development before implantation (Takeda, Noguchi et al. 1997). Also, the conditional s*tat3* knockout mice showed impairment in the survival of motoneuron after axotomy (Schweizer, Gunnersen et al. 2002).

1.4.7   Role of Stat3- stathmin interaction in neuronal growth

Most of the activated Stat3 remains localized in cytoplasm where it performs its transcriptional independent functions. Stat3 directly binds to the COOH-terminal tubulin interacting domain of MT-destabilizing protein stathmin and modulates MT dynamics. Fibroblasts that are deficient in Stat3 show impaired microtubule network, suggesting a role of Stat3 in regulation of microtubule dynamics (Ng, Lin et al. 2006). This interaction also plays a role in microtubule dynamics for T-cell migration (Verma, Dourlat et al. 2009). Stat3 may compete for the tubulin-binding site of stathmin and thus antagonizes its MT-destabilizing activity. CNTF receptor signaling activates Stat3 and activated Stat3 then interacts with stathmin and inhibits its microtubule-destabilizing activity in *in vitro* cultured *pmn* mutant motoneurons. This leads to the restoration of axon growth and axon maintenance in these neurons (Selvaraj, Frank et al. 2012). Genetic depletion of Stat3 in *pmn* mice abolishes the CNTF mediated rescue of axon length. CNTF mediated restoration of axon length and maintenance of *pmn* motoneurons has been shown to be mediated via local axonal function of Stat3.

1.5   Spinal muscular atrophy

Spinal muscular atrophy (SMA) is characterized by severe muscular atrophy due to degeneration of anterior horn motoneurons in the spinal cord (Lefebvre, Burglen et al. 1995), subsequently paralyzing the limbs and body (Werdnig 1971). Proximal spinal muscular atrophy (SMA) is an autosomal recessive disorder in which α- motoneurons of spinal cord degenerate. With an incidence of 1 in 10,000 live births, it is estimated to be the second most common cause of inherited child mortality (Pearn 1973, Pearn 1978) in the world. SMA could be of varying severity and clinical course according to which it could be divided into three groups (Roberts, Chavez et al. 1970, Munsat and Davies 1992). Type I SMA or Werding-Hoffman disease is the most severe form characterized by severe muscle weakness and hypotonia at birth or before the age of 6 months causing death within the first 2 years. Type II SMA is of intermediate severity arises around 18 months of age in affected children. The patients are able to sit but eventually die before they could attend the ability to walk at around 4 years of age. Type III SMA or Kugelberg- Welander disease is the mildest form in which proximal muscle weakness arises after the age of 2 and the patients are able to stand and walk; they survive more than 4 years.

Humans possess 2 genes for SMN; telomeric *SMN1* and centromeric *SMN2,* that differ in a single nucleotide (C →T base) change in exon 7 of the *SMN2* gene (Lefebvre, Burglen et al.

1995, Monani, Lorson et al. 1999). This base difference changes the splicing pattern of the gene because of which the majority of transcript produced by *SMN2* gene lacks exon7 (SMNΔ7) encoded domains and is unstable, whereas *SMN1* produces full length transcripts (Coovert, Le et al. 1997, Lefebvre, Burlet et al. 1997, Kashima and Manley 2003). SMA is caused by mutations in the telomeric *SMN1* gene which results in low levels of full-length SMN transcript and hence low levels of functional SMN protein (Bussaglia, Clermont et al. 1995, Lefebvre, Burglen et al. 1995, Parsons, McAndrew et al. 1996, Hahnen, Schonling et al. 1997, Talbot, Ponting et al. 1997).

Mouse genome contains only one copy of *Smn* gene which is equivalent to *SMN1* in humans (DiDonato, Chen et al. 1997, Viollet, Bertrandy et al. 1997) and the knockout of this *Smn* gene is embryonic lethal in mouse (Schrank, Gotz et al. 1997). Therefore, entire human *SMN2* gene was introduced in low copy number into the mouse null *Smn*$^{-/-}$ background to mimic the human type I SMA condition (Monani, Sendtner et al. 2000). The exact reason why motoneurons are particularly affected by the reduction of a ubiquitously expressed SMN protein remains unclear. Two hypotheses have been put forward to understand the role of SMN in the pathology of SMA (Burghes and Beattie 2009).

1.5.1   Role of Smn in pre-mRNA splicing

First hypothesis involves the interaction of Smn with spliceosomal snRNP core proteins. Smn is a ubiquitously expressed 38 kD protein found both in the nucleus and cytoplasm. Inside the nucleus Smn is concentrated in the form of structures called Gemini of coiled bodies or "gems" (Liu and Dreyfuss 1996). Smn protein is found in a complex associated with Smn-interacting protein 1 SIP1 (now called gemin 2) and several Sm proteins which are components of spliceosomal snRNPs. Sm proteins combine with the snRNAs in the cytoplasm and are translocated to the nucleus where these snRNPs function in the pre-mRNA splicing. Smn is involved in the assembly and recycling of RNA-protein complexes of the pre-mRNA processing system (UsnRNPs) which form the spliceosomal complexes involved in pre-mRNA splicing (Pellizzoni, Kataoka et al. 1998). Its deficiency has been shown to affect the splicing machinery, and reduces the snRNPs in SMA mice. This reduction correlates with the severity of the disease (Gabanella, Butchbach et al. 2007). Injection of purified U snRNPs prevents motoneuron degeneration in *Smn* deficient zebrafish (Winkler, Eggert et al. 2005). The reduced U snRNP assembly in SMA could affect splicing especially of transcripts important for motoneurons and might play a role in SMA phenotype.

1.5.2 Role of Smn in mRNA transport

Another hypothesis involves the role of Smn in transport of mRNA in motoneurons. Smn is found to be accumulated in the growth cones and NMJs during neuronal differentiation and neuromuscular maturation where it does not colocalize with Sm proteins (Jablonka, Bandilla et al. 2001), suggesting that it acts in another cellular function not related to pre-mRNA splicing (Fan and Simard 2002). Wild-type Smn is found to interact with hnRNPR and hnRNPQ, the proteins involved in RNA processing during pre-mRNA splicing. Notably these proteins do not interact with mutated or truncated Smn. Both hnRNPR and Smn colocalize in axons of motoneurons (Rossoll, Kroning et al. 2002). hnRNPR associated with the Smn is involved in the translocation of β-actin mRNA to growth cones along the axons of motoneurons (Rossoll, Jablonka et al. 2003) which might be required for local translation at the growth cone. Also, a dysregulation in local translation of β-actin mRNA was observed in the growth cone of SMA motoneurons (Rathod, Havlicek et al. 2012).

1.5.3 SMA, a neuromuscular junction disorder

In SMA, denervation of neuromuscular junctions occurs even before neurodegeneration starts and the density and release of synaptic vesicles at NMJ is reduced in SMA mice. The immature motor unit could be responsible for muscle weakness in SMA (Kong, Wang et al. 2009). SMA is a dying back disease in which abnormalities in motor terminals precedes the motoneuron loss in spinal cord. It has been proposed to be a synaptopathy with impaired maturation of NMJ. Maintenance of NMJ function can be a promising method of treatment in SMA. Besides reduced β-actin mRNA and protein in the distal axon, SMA motoneurons also show reduced axon growth and reduced growth cone size. The global spontaneous excitability in cell bodies and proximal axon is normal but the spontaneous calcium transients in distal axon and growth cones are reduced as a result of defective $Ca_v2.2$ clustering in SMA motoneurons (Jablonka, Beck et al. 2007). The electrical excitability of muscle fiber and polyinnervation is preserved in SMA but postsynaptic potentials and neurotransmitter release are decreased. An increased intracellular calcium concentration at mutant terminals causes anomalous increase in asynchronous transmitter release (Ruiz, Casanas et al. 2010). Maturation of acetylcholine receptor clusters into 'pretzels' is impaired causing reduced size of AChR clusters and small myofibers. At the presynapse intermediate filaments aggregates are formed and quantal content and synaptic vesicle density is reduced causing defective synaptic transmission (Kariya, Park et al. 2008, Kong, Wang et al. 2009). Together these pre-

and post-synaptic defects can lead to failed maturation of the motor units causing muscle weakness and neurodegeneration in SMA.

1.6   Presynaptic cell surface protein; neurexins

Neurexins constitute a family of highly polymorphic, neuron specific presynaptic cell surface proteins with a putative role in cell recognition at the nerve terminals. They were discovered as a receptor for α-latrotoxin, the venom from black widow spider which causes massive neurotransmitter release on binding to the presynaptic surface (Ushkaryov, Petrenko et al. 1992). In mammals, there are 3 genes for neurexins, each containing two independent promoters encoding a larger α-isoform and a shorter β-isoform (Ushkaryov and Sudhof 1993). All neurexins contain evolutionary conserved alternative splice sites (SS), SS1-5 in α-neurexins and SS4 and 5 in β-neurexins. Therefore, each neurexin can undergo extensive alternative splicing and possesses the potential to produce hundreds of alternative spliced isoforms that are developmentally and spatially regulated. This also provides them a potential for specificity during synaptogenesis (Missler and Sudhof 1998) suggesting a role of neurexins in cell-cell interaction (Ushkaryov, Petrenko et al. 1992, Ullrich, Ushkaryov et al. 1995).

Neurexins show high polymorphism, receptor-like structure and have developmentally and spatially regulated expression that makes them a putative candidate for cell adhesion and recognition molecules. The α-neurexins contain a large extracellular domain that contains six laminin -neurexin -sex hormone-binding globulin (LNS) domains and 3 epidermal growth factor-like (EGF-like) regions whereas β-neurexins contain one LNS domain and no EGF-like domain. LNS domain is followed by a glycosylation sequence, a transmembrane domain and a short intracellular tail. Extracellular domain of β-neurexins but not α-neurexins can bind to neuroligin, a postsynaptic molecule (Ichtchenko, Hata et al. 1995) and thus stabilize the synaptic structure (Nguyen and Sudhof 1997, Scheiffele, Fan et al. 2000) (Fig. 4). Neurexins also bind with dystroglycan in the postsynapse which could mediate cell-cell adhesion (Sugita, Saito et al. 2001). The intracellular tail of neurexins interacts with Ca^{2+} channels modulating proteins CASK (Hata, Butz et al. 1996), Mint (Biederer and Sudhof 2000) and synaptotagmin (Petrenko, Perin et al. 1991). Double α-neurexin knockout mice show decreased presynaptic calcium current and impaired neurotransmitter release in CNS synapses. This signifies the role of α-neurexins in functioning of synaptic voltage gated N and P/Q type Ca^{2+} channels connecting cell adhesion of neurexin from the extracellular domain to

presynaptic secretory machinery (Missler, Zhang et al. 2003, Zhang, Rohlmann et al. 2005). The quantal contents of motor nerve terminals are reduced at the NMJ of double *α-nrxn* knockout mice (Sons, Busche et al. 2006) showing that α-Nrxns are important for transmitter release even in the absence of a postsynaptic partner.
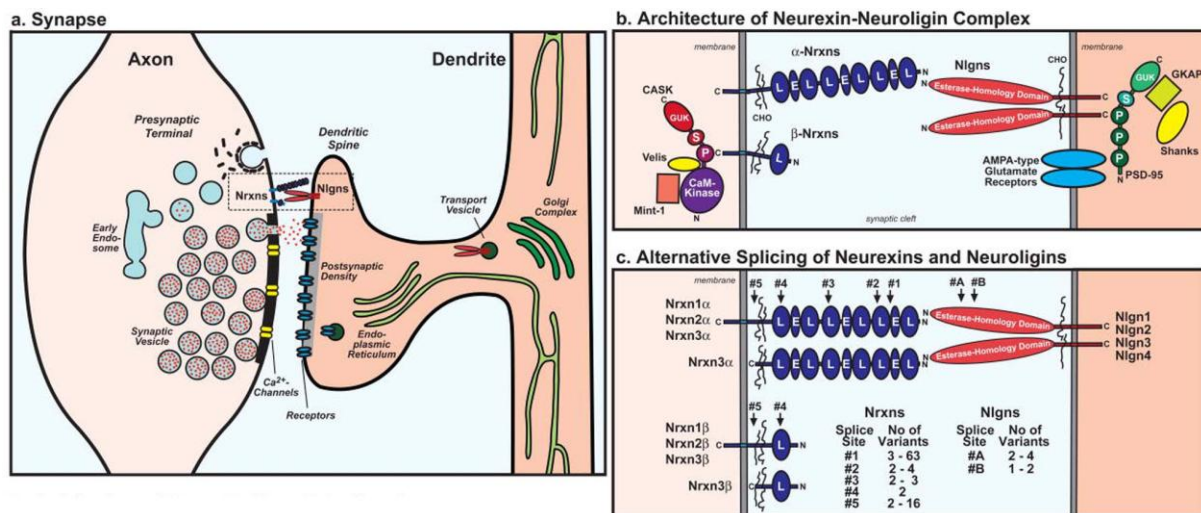
Figure 4: Architecture of trans-synaptic neurexin-neuroligin complex

a. Cartoon of the structure of an excitatory synapse and the putative locations of Nrxns and Nlgns in the synapse. b. Schematic diagram of Nrxn/Nlgn junction including selected pre- and postsynaptic binding proteins: CASK, Velis, and Mints on the presynaptic side and PSD-95, GKAP, and Shanks on the postsynaptic side. Note that Nrxns and CASK could be, at least in part, also postsynaptic, and that Shank may also be presynaptic (Sudhof 2008).

1.6.1   Alternative splicing of neurexins

Neurexins are highly alternatively spliced with a potential to form thousands of possible isoforms and each splice isoform exhibit different functions and properties (Missler and Sudhof 1998, Rozic-Kotliroff and Zisapel 2007). Expression of different neuroligin and neurexin isoforms specifies a trans-synaptic signaling code (Chih, Gollan et al. 2006). On depolarization, calcium-dependent neurotransmitter release is observed in primary rat cortical neurons and the splicing of Nrxn2α at SS#1 and SS#3 (exon 11 exclusion) is also affected (Rozic-Kotliroff and Zisapel 2007). This exclusion of exon 11 in rat (which corresponds to the exon 12 in mouse) at SS3 was dependent on the levels of Ca^{2+} present. SS#2, #3 and #4 of Nrxnα are located in the LNS domains which function as autonomous ligand binding sites with a high degree of specificity (Missler, Fernandez-Chacon et al. 1998) and exon 11 exclusion changes the specificity of Nrxn2 binding to trans-synaptic ligands.

1.7   Goal of the thesis

Destabilization of axon terminals and axonal degeneration is a common prominent feature in amyotrophic lateral sclerosis (ALS) and spinal muscular atrophy (SMA) (Sendtner 2014). Though the genetics behind the two diseases has been studied, the cellular mechanisms responsible for NMJ defects and degeneration of neurons in these diseases are not fully understood. Both are characterized by dysfunction and degeneration of neuromuscular endplates early in the disease (Munoz, Greene et al. 1988, Cifuentes-Diaz, Nicole et al. 2002). Accumulation of intermediate filaments and alteration of axonal cytoskeleton are symptoms of both the diseases. The increased density of intermediate filaments and destabilization of microtubules could be functionally connected but there is no direct evidence for this phenomenon. Depletion of axonal neurofilaments improves axonal transport (Perrot and Julien 2009) and increases life span in SOD1 mutant mice (Williamson, Bruijn et al. 1998) and attenuates the neurodegeneration in tau transgenic T44 mice (Ishihara, Higuchi et al. 2001). However, the molecular mechanism how neurofilament depletion prevents or delays axon degeneration remained unclear. In order to study this relation, I used *pmn* mutant mice as a model for ALS and showed that *pmn* mutant mice also exhibit neurofilament accumulation during neurodegeneration. To study the effect of neurofilament accumulation and its role in neurodegeneration, the *Nefl* gene was deleted from *pmn* mice. Further, the possible mechanism involved in delay of neurodegeneration in *pmn* mutant mice upon *Nefl* deletion is studied. Further, an interaction partner of neurofilament and microtubules and a possible mechanism that might be involved in stabilization of microtubules upon neurofilament depletion is proposed.

Spinal muscular atrophy (SMA) is characterized by degeneration of lower α-motoneurons (MN) in spinal cord; however, how reduction of a ubiquitously expressed SMN protein leads to MN-specific degeneration remains unclear. SMN protein is involved in pre-mRNA splicing and its deficiency also causes neuromuscular denervation (Kariya, Park et al. 2008, Kong, Wang et al. 2009), eventually leading to neurodegeneration. However, the link between aberrant splicing and reduced excitability at NMJ has not been found. Here we observed that the expression and splicing of a presynaptic protein Nrxn2α is affected upon Smn deficiency in mice. We propose that Nrxn2 could be candidate that connects aberrant splicing with presynaptic defects in SMA.

2   Materials and Methods

2.1   Materials

2.1.1   Materials for protein biochemistry method

Table 1: Solutions and chemicals used for western blotting
NaCl: sodium chloride; SDS: sodium dodecyl sulphate; EDTA: ethylene diamine tetra acetic acid; PIPES: piperazine-diethane-sulfonic acid; HEPES: hydroxyethyl-piperazineethane-sulfonic acid; EGTA: ethylene glycol tetraacetic acid; TEMED: tetramethyl-ethylene-diamine.

RIPA buffer (protein lysis buffer)	50mM Tris HCl pH 7.6	Roth, 9090.3
	150 mM NaCl	Sigma, 31434
	1% TritonX-100	Sigma, T8787
	1% SDS	Biorad, 161-0418
	2 mM EDTA	Roche, 04693159001
	Protease inhibitor 1X (complete mini, EDTA free)	Roche, 04693159001
	1 mM Sodium fluoride	Sigma, S6776
	10 mM Sodium pyrophosphate	Sigma, 221368
	1 mM Okadaic acid	LC laboratories; O-5857
	2 mM Sodium orthovanadate	Sigma, S6508
Immunoprecipitation buffer	50 mM Tris HCl pH 7.4	
	150 mM NaCl	
	Protease inhibitor 1X	
	1% TritonX-100	
	2 mM EDTA	
	1 mM Sodium fluoride	
	10 mM Sodium	

	pyrophosphate	
	1 mM Okadaic acid	
	2 mM Sodium orthovanadate	
Laemmli buffer (5X)	125 mM Tris HCl pH 6.8	
	10% β-Mercaptoethanol	Sigma, M7154
	4% SDS	
	20% Glycerol	Calbiochem, 356350
	0.02% Bromophenol blue	
Resolving gel	30% Acrylamide (29:1)	Applichem, A0951
	1.5 M Tris-HCl pH 8.8	
	10% SDS	
	10% Ammonium persulfate	Sigma, A3678
	TEMED	Merck, 1.10732
	Water Ampuwa® Aqua ad injectabilia	DeltaSelect; 8771004
Stacking gel	30% Acrylamide (29:1)	
	1 M Tris-HCl pH 6.8	
	10%SDS	
	10% Ammonium persulfate	
	TEMED	
	Water	
SDS Running buffer (10X)	30.3 g Tris Base	Applichem, A2264
	144 g Glycine	Roth, 3790.3
	10 g SDS	
	Water make up to 1 L	
Transfer buffer	900 ml 1X SDS Running	

	buffer	
	100 ml Methanol	Sigma, 32213
Tris Buffered Saline (TBS) (10X) pH 8.0	0.2 M Tris Base	
	1.5 M NaCl	
TBST (1X)	1 L TBS(1X)	
	0.1% Tween 20	Sigma, P7949
Blocking solution	5% milk powder in 1X TBST	Roth, T145.3
Stripping buffer	Restore plus western blot SB	Thermo, 46430
Protein ladder	Pre-stained Protein Ladder	PageRulerTM #SM0671 Fermentas
Transfer membrane	Nitrocellulose	Protran Protran BA83
X-ray films		Fuji Film, 47410-19230
ECL reagent	Western blotting detection	GE Healthcare, RPN2209
ECL Prime reagent		GE Healthcare, RPN2232
Protein estimation kit	Protein assay	Pierce
PHEM buffer (microtubule regrowth assay)	60 mM Pipes	Applichem, A3495
	25 mM Hepes	Roth, HN77.4
	10 mM EGTA	Sigma, E8145
	2 mM MgCl2	Merck, 5833
SDS polyacrylamide gel electrophoresis	Mini Protean Tetra Cell	BioRad, Munich, Germany
Semi-dry western blot chamber		Peqlab
Power supplies	Standard Power Pack P25	Biometra/Biorad
Protein-A beads	Immunoprecipitation	Roche, 1171940801

2.1.2   Materials for DNA method

Table 2: Solutions and chemicals used for DNA work

Tail lysis buffer	10 mM Tris pH 8.0 150 mM NaCl 0.5% SDS 10 mM EDTA pH 8.0 Add 20 µl of 20 mg/ml stock Proteinase K per 1 ml of lysis buffer	
Tail lysis buffer (quick Chelex)	10 ml 5 M NaCl. 25 ml 10% Sarcosyl solution 25 g Chelex beads Water up to 500 ml	
50X TAE	2 M Tris Base. 50 mM EDTA pH8.0. 5.71% Glacial acetic acid	
6X loading dye	30% Glycerol, 0.15% Bromophenol blue. 0.15% Xylene cyanol. 1X TAE	
Sodium borate buffer (20X)	137 mM NaCl, 725 mM Boric acid. Adjust pH 8.0 by NaOH	
DNA ladder	GeneRulerTM 100 bp DNA Ladder	Fermentas
dNTPS	dNTP set 100 mM Gene Craft Germany	
Taq Polymerase	5' Prime,	

Ethidium bromide	10 µg/ml	Merck, Darmstadt Germany
Thermocycler	Thermocycler personal Thermocycler gradient	Eppendorf, Hamburg, Germany
Horizontal agarose gel	PEQLAB Biotech. GMBH electrophoresis chamber	Erlangen, Germany
X-ray developer		X-Omat 2000, Stuttgart, Germany
Photometer		BioPhotometer, Eppendorf, Hamburg, Germany
Tissue sonication	For protein lysates	UP50H - Compact Lab Homogenizer, Hielscher Ultrasound Technology, Teltow, Germany
Nanodrop	Spectrophotometer	PEQLAB Biotech. GMBH Erlangen, Germany

2.1.3   Material for RNA work

Table 3: Chemicals for RNA work
DEPC: Diethyl-pyro-carbonate; EB-BSA: EDTA-Bovine serum albumin

RNA easy mini kit		Qiagen
QIA shredder		Qiagen
Reverse Transcriptase kit	SuperScript First-Strand Synthesis system for RT-PCR	Invitrogen
SYBr Green kit	LightCycler FastStart DNA Master SYBR Green I	Roche, 12239264001
DEPC water	0.1 ml Diethyl-pyrocarbonate in 100 ml	

	water	
Rnase away		
EB-BSA	BSA in Tris-HCl	
RNA gel		
Light cycler 1.5	real time light cycler PCR machine	Roche

2.1.4   Materials for motoneuron cell culture

Table 4: Chemicals for motoneuron culture
BDNF = brain-derived neurotrophic factor; CNTF = ciliary neurotrophic factor, HBSS: Hank's Balanced Salt Solution; NB: Neurobasal medium.

Borate buffer	150 mM Boric acid in water, pH 8.35	AppliChem,
Tris-HCl	10 mM Tris, pH 9.5	
Depolarizing solution	30 mM KCl, 0.8 % NaCl, 2 mM CaCl2, in water	
ß-Mercaptoethanol	100 µM stock	Sigma, M7522
1% Trypsin	1 g in Trypsin in 100 ml HBSS (1%), 250 µl 1 M HEPES (pH 7.4)	Worthington, LS003707
0.1% Trypsin inhibior	0.5 g Trypsin inhibitor 9.75 ml HBSS, 250 µl 1 M HEPES (pH 7.4)	Sigma, T-6522
Laminin-221	2.5 µg / ml in HBSS	Invitrogen, 23017-015
Poly-D, L-Ornithin	50 mg 1 ml 150 mM borate buffer pH 8.35, PORN working 0.5 mg/ml	Sigma, P8638
B27-supplement	1X	Invitrogen, Gibco, 17504-044
Horse serum	Heat inactivated at 55 °C, 30 min	Linaris, SHD3250ZK

Hank's balanced salt solution (HBSS)		Invitrogen
p75 antibody MLR2	45 ng/ml monoclonal, Abcam	Biosensis, M-009-100
Neurobasal media		Gibco, 21103-041
L-Alanyl-L-Glutamin (Glutamax)	1X	Gibco, 35050-038
Full media for motoneuron culture	NB media with 1X Glutamax 2% horse serum 1X B27 supplement BDNF 5 ng/ml (or CNTF 10 ng/ml)	Prof. Sendtner, Wuerzburg
Falcon tubes		Greiner
Cell culture dishes		
Panning solution	Anti-p75 antibody(MLR2) (1:2000) 10 mM Tris buffer (pH 9.5)	Biosensis, M-009-100
Aqua polymount		Polysciences, 18606-20
Square four well dishes for MT regrowth assay		
Glass coverslip		

2.1.5 Materials for histology and electron microscopy

Table 5: Chemicals for histology
PBS = Phosphate buffered saline; PFA: Paraformaldehyde; GLA: Glutaraldehyde.

Fixant for motoneuron for electron microscopy (4 ml)	0.1 M Cacodylate buffer pH7.5 (2 ml 0.2 M stock). 2.5% Glutaraldehyde (400 µl of 25% stock).0.8% tannic acid (320 µl of 10% tannic acid (dissolved in water)). 1280 µl water	

Dishes for motoneuron culture	Falcon dishes	BD Falcon™ - Dish 35X10mm non-TC Petri EZGrip 500cas - BD Biosciences
4% PFA pH7.4 (100 ml)	4 g paraformaldehyde, 50 ml water, Few drops of NaOH dissolved at 60 °C, 41 ml of 0.2 M Na_2HPO_4, 9 ml of 0.2 M NaH_2PO_4	
PBS 1X 1 L	8 g NaCl, 0.2 g KCl, 1.44 g Na_2HPO_4. 0.24 g Na_2HPO_4	
Heparin	0.5 ml from stock solution 5000 1U/ml for 1L.	Ratiopharm
0.1 M Cacodylate buffer (1L)	21.4 g of cacodylic in 1 L water	
Perfusion 4%PFA + 2%GLA in Cacodylate buffer	40 g of PFA is dissolved in 900 ml of 0.1 M cacodylate buffer at 70 °C. Few drops of NaOH, Cool 4 °C, pH 7.4, Add 2% GLA (final). Make up to 1L.	

2.1.6 Materials for histology and for laser-microdissection

Table 6: Chemicals for laser microdissection
OCT: Optimal Cutting Temperature compound; POL: Polyesther; DTT: Dithiothreitol.

Tissue Tek	O.C.T Mount medium	Tissue Tek, Sakura
Cryostat		Modell CM 1950, Leica, Wetzlar, Germany
Slides	POL-membrane frame slide	Leica; 11505188
Cresyl violet for staining	70% EtOH (in DEPC	

	water), Cresylviolet stain (1% CV dissolved in 100% EtOH), 100% EtOH	
Laser microdissection system		Leica DM6000B
Freezing the tissue	N-pentane cooled in Liquid nitrogen.	
Direct cDNA synthesis Lysis Buffer (RT buffer)	1X First Strand Buffer	
	1X RT Buffer (made below)	
	1 mM Tris/HCl pH 8.0	Invitrogen (18080093)
	10 mM DTT	ROCHE (11332473001)
	0.5% NP-40	Fermentas (R0551)
	20 μg Glycogen	Promega (N2611)
	10 U RNasin Plus RNAse inhibitor	
	RNAse free water	
Direct cDNA synthesis 10XRT Buffer	6 mM Tris-HCl pH 8.0	
	2 mM dNTPs Invitrogen	Invitrogen (18080093)
	1 mM Random Primer	ROCHE (11034731001)
	Make upto 2 μl by DEPC water	

2.1.7 Antibodies used in the study

Table 7: Antibodies used for western and immunocytochemistry

Name	Species	Dilution	Use	Company
NFL	Rabbit	1:20,000	WB	Abcam; ab9035
Stathmin mAb (EP1573Y)	Rabbit	1:2000	WB	Abcam; ab52630

Stat3	Mouse	1:2000	WB	Cell signaling; 9139S
		1:5000	IF	
pStat3 ^{Y705} (Y705)(D3A7)	Rabbit	1:2000	WB	Cell signaling; 9145S
Calnexin	Chicken		WB	
GAPDH	Mouse	1:5000	WB	Calbiochem;CB1001
anti-tau	Rabbit	1:1000	IF	Sigma, T6402
α-tubulin	Mouse	1:5000	WB	Sigma; T5168
		1:2000	IF	
Acetylated tubulin	Mouse	1:2000	IF	Sigma
γ-tubulin	Rabbit	1:1000	IF	Abcam; Ab11317
Tyrosinated tubulin	Rat	1:2000	WB	Abcam; Ab6160
		1:2000	IF	
NFH	Chicken	1:20,000	WB	Millipore, AB5539
Histone-3	Rabbit	1:20,000	WB	Abcam
DAPI (4,6-diamidino-2-phenylindole dihydrochloride)		1 mg/ml stock	IF	Sigma Aldrich

2.1.8 Primers used in the study

Table 8: Primers used for genotyping and RT-PCR

Pmn line 017	*pmn*-fw	5´ – TGA CCA ACC AAA TCA CTG TAG TG – 3´
	pmn -rev	5´ – TAG CAT GCA CCA TCA GAT CG- 3'
Pmn line 017 (modified by me)	*pmn*2fw	5' – GAGGGTGGCATGGATAGC – 3'
	*pmn*2-rev	5' –CTACTCTGCCTTGCCTGATATGT - 3'
NFL WT line 127	*Nefl* ex2a	5' - TCT GAG CCT TCC CGC TTC - 3'
	Nefl ex2b	5' - CTT TCC GAC ACC TCG TCC TT -3'

NFL KO line 127	Nefl ex1a 5' - CTT CTC CCC CGT TCT TCT CT - 3'	
	Neo b.fw 5' - AGG TGA GAT GAC AGG AGA TC - 3'	
Smn WT line 30	Smn wt fw 5'- CTGGAATTCAATATGCTAGACTGGCCTG -3'	
	Smn rev 5' - AATCAATCTATCACCTGTTTCAAGGGAGTTG-3'	
Smn KO line 30	Smn ko fw 5' - CTGGAATTCAATATGCTAGACTGGCCTG -3'	
	Smn ko rev 5' - GATGTGCTGCAAGGCGATTAAGTTG – 3'	
Mouse Nrxn1α (NM_020252)	ACAACTTTATGGGCTGTCTCAA	148 bp, intron-spanning, real time qRT-PCR
	ACAACTTTATGGGCTGTCTCAA	
Mouse Nrxn2α (NM_020253)	TTAAACAGCGAAGTAGGGTC	185 bp, intron span-ning, real time qRT-PCR
	GCCAGTGTGATCTCGTCA	
Mouse Nrxn3α (NM_001198587)	CACTGGCTATGGTGGCACAC	165 bp, intron span-ning, real time qRT-PCR
	TCGCTGCTGCTCTGGATG	
Mouse Nrxn2β	CCACTTCCACAGCAAGCACG	133 bp, intron span-ning, real time qRT-PCR
	GGGAGGCCATGTATAGGTGAT	
Mouse Nrxn2α exon11 (semi-quantitative PCR)	GCTGACACTCTGCGTCT	alternative splicing at SS3 of mouse Nrxn2a
	CCGCAAACAGTGTCTC	
Mouse Gapdh (NM_008084)	GCAAATTCAACGGCACA	141 bp, real time qRT-PCR
	CACCAGTAGACTCCACGAC	
Mouse Hmbs (NM_013551)	AGTGGGCACCCGTAAGAG	118 bp, intron span-ning, real time qRT-PCR
	GTCTCCCGTGGTGGACATAG	
Mouse Hprt1 (NM_013556)	TTATGCCGAGGATTTGGAA	118 bp, intron span-ning, real time qRT-PCR
	ACAGAGGGCCACAATGTGAT	
Mouse exon11 (q-RT PCR)	TGCTGCCCACTGCGATGCAC	179 bp
	GCAGCCGACGCGCAGGCAGT	

2.1.9 Software and other instruments used

Table 9: Software and instruments used

Adobe Photoshop CS3	Adobe Systems, San Jose, CA, USA
Oligo 6	MedProbe
ApE - plasmid editor	M. Wayne Davis
Image J	WS Rasband, ImageJ, US National Institute of Health, Bethesda,
LAS AF Lite	Leica confocal
Graph Pad prism 4.0	GraphPad, SanDiego, CA
Rotarod	Ugo Basile
Grip strength meter	Chatillon, Columbus Instruments

2.2 Methods

2.2.1 Animal husbandry

All experimental procedures were approved by animal care and ethic committee of the University of Wuerzburg, the Veterinäramt of the City of Wuerzburg and the Regierung von Unterfranken, and were performed according to the guidelines of the European Union. All mice were maintained under a 12 h light/dark cycle with food and water ad libitum. The transgenic mice used in the study are as follow:

(a) Smn$^{+/-}$;SMN2: FVB background

(b) Progressive motoneuropathy or *pmn mutant* mice: A spontaneous Trp524Gly substitution of the *Tbce* (tubulin-specific chaperone E) gene in the NMRI/Pan outbred line at the Panum Institute (Kopenhagen, Denmark) led to the first identification of *pmn* mice (Schmalbruch, Jensen et al. 1991). These mice are maintained in the animal facility at Institute of clinical neurobiology, wuerzburg, Germany.

(c) NFL knockout mice: Mice lacking one or both the alleles for *Nefl* are maintained on C57Bl/ 6 genetic backgrounds.
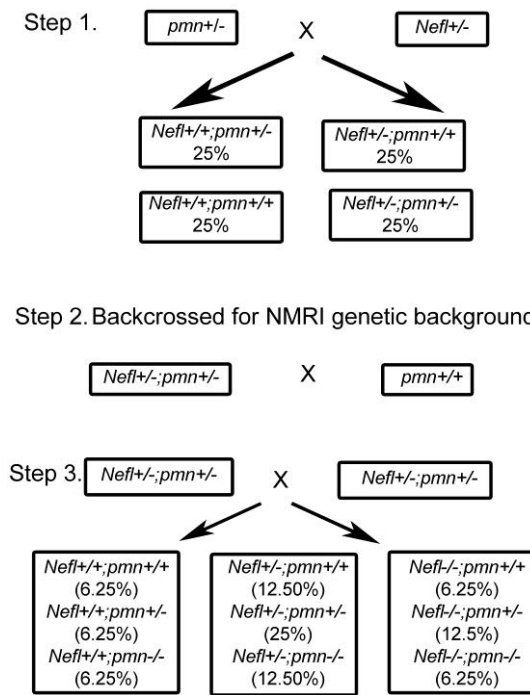
Figure 5: Production of *Nefl* knockout *pmn* mouse

The 3-step mating scheme used to produce *Nefl-/-;pmn* mice. A total of 9 different genotypes with varying frequencies were obtained.

(d) *Nefl-/-;pmn* : Heterozygous *pmn* mutant mice originally maintained on Naval Medical Research Institute (NMRI) (Schmalbruch, Jensen et al. 1991) genetic background were crossed with heterozygous *Nefl* knockout mice on a C57Bl/6 genetic background (Zhu, Couillard-Despres et al. 1997) to produce double heterozygous *Nefl+/-;pmn+/-* mice. These mice were then backcrossed with NMRI genetic background for at least three generations to obtain a uniform NMRI genetic background. Subsequently, the heterozygous *Nefl+/-;pmn+/-* were intercrossed to obtain the mice investigated in this work. *Nefl* knockout and corresponding control wild-type mice on a C57BL/6 genetic background were used for the immunoprecipitation experiments. The crossing scheme is as shown in fig. 5.

2.2.2 Genomic DNA isolation

For using phenol-chloroform method, animal tissue (tail or half head) collected in 300 µl of DNA lysis buffer with 20 µl Proteinase K (20 mg/ml) were dissolved overnight on a thermoshaker at 60 °C. An equal volume of phenol : chloroform mixture was added, mixed on a vortex and centrifuged at 12,000 g for 5 min. Upper aqueous layer was collected and an equal volume of phenol : chloroform mixture was added, lysate was mixed on a vortex and centri-

fuged. The upper aqueous layer was collected in a fresh tube and 1 ml isopropanol was added to it to precipitate DNA. The contents were mixed by shaking up and down several times and the tubes containing the lysate were centrifuged at maximum speed for 10 min to obtain the precipitated DNA as a pellet. The pellet was washed with 500 µl of 70 % ethanol followed by centrifugation for 2 min at maximum. Pellet was air dried and DNA was dissolved in TE buffer.

For chelex- quick method (for Smn genotyping), tissue was dissolved in chelex lysis buffer containing Proteinase K at 55 °C for 2 hours, followed by heating at 99 °C for 15 min. The lysate was centrifuged at full speed for 5 min and 2 µl of supernatant was used for PCR.

2.2.3   Genotype of mouse

***Pmn* genotype**: A T1570G transversion in the *tbce* (tubulin-specific chaperone E) gene led to an extra *MnlI* restriction site in the mutants, which is utilized for their identification. A DNA segment of 441 bp across the mutation is amplified from the genomic DNA by using *pmn* PCR primers and is digested by *MnlI* restriction enzyme. Wild-type DNA contains only one *MnlI* site in the amplified region and hence shows only products of 226 bp and 215 bp in a 3 % agarose gel. In contrast, the mutant DNA contains two *MnlI* sites resulting in three products of 226 bp, 136 bp and 79 bp. Heterozygous mice show four bands of size 226, 215, 136 and 79 bp.

***MnlI* restriction digestion:**

PCR product	20 µl
Buffer Green	2.5 µl
MnlI enzyme	0.2 µl
Water	2.3 µl

Reagants	Volume (µl)
DNA	1
10X 5' buffer	2
dNTP mix (10 mM)	1
5' Taq polymerase	0.3
Forward primer (50 pmol/µl)	0.2
Reverse primer (50 pmol/µl)	0.2
Water	Upto 20

Step	Cycle condition	Duration
Denaturation	94 °C	2 min
Amplification (30 cycles)	94 °C	10 sec
	53 °C	15 sec
	72 °C	30 sec
Melting	72 °C	7 min
Termination	4 °C	5 min

NFL genotype: *Nefl* gene was disrupted by generating a targeting vector replacing a 720 bp PvuII fragment from the first exon by a 1.1 Kb neo-cassette from pMC1neo-polyA.
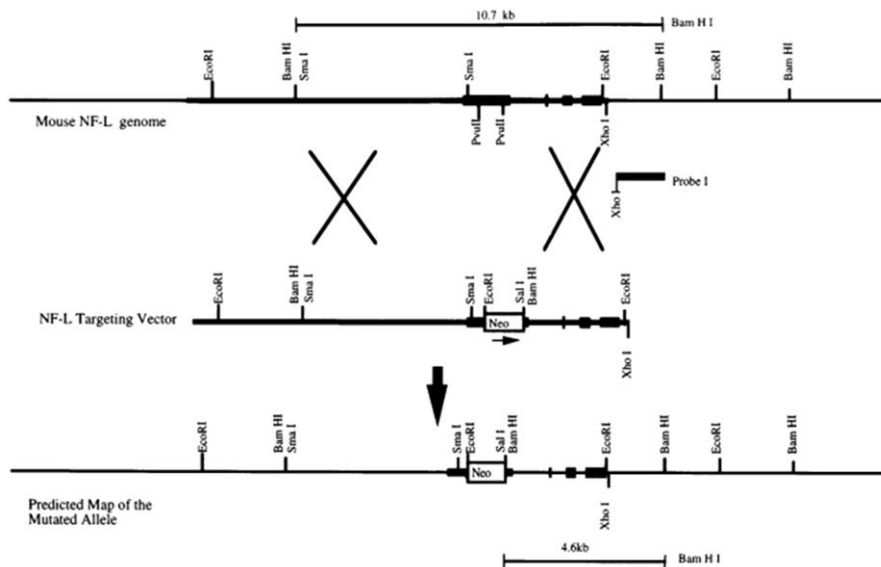
Figure 6: Restriction map of NFL targeting vector
The restriction map of mouse genome and targeting vector (Zhu, Couillard-Despres et al. 1997).

It included 8 Kb of 5' NFL sequence and 3.1 Kb of internal and 3' sequences (Zhu, Couillard-Despres et al. 1997). The restriction map of mouse genome and targeting vector used by (Zhu, Couillard-Despres et al. 1997), is as shown in fig 6.

The PCR primers for knockout are designed such that the reverse primer is on the neo cassette and gives a product of size 1050 bp, whereas the wild- type primers are designed after the neo cassette insertion site to give a product of 540 bp.

Reagants	Volume (µl)
DNA	1
10X 5' buffer	2
dNTP mix (10mM)	0.5
5' Taq polymerase	0.3
Forward primer (50 pmol/µl)	0.4
Reverse primer (50 pmol/µl)	0.4
Water	Upto 20

Step	Cycle (KO)	Cycle (WT)	Dura-tion
Denaturation	94 °C	94 °C	5 min
Amplification (30 cycles)	94 °C	94 °C	30 sec
	66 °C	61 °C	30 sec
	68 °C	68 °C	1 min
Melting	72 °C	72 °C	7 min
Termination	4 °C	4 °C	5 min

Smn genotype: The product size for the genotyping is 600 bp for $Smn^{-/-}$;*SMN2* and 879 bp for $Smn^{+/+}$;*SMN2*.

Reagants	Volume (µl)
DNA	1
10X 5' buffer	5
dNTP mix (10 mM)	1
5' Taq polymerase	0.3
Forward primer (10 pmol/µl)	1
Reverse primer (10 pmol/µl)	1
Water	Upto 50

Step	Cycle condition	Duration
Denaturation	94 °C	3 min
Amplification (35 cycles)	94 °C	30 sec
	59 °C	30 sec
	72 °C	1 min
Melting	72 °C	5min
Termination	4 °C	5 min

2.2.4   *In vitro* mouse motoneuron culture

Culture dishes containing glass coverslips were coated with poly-D, L-ornithine (PORN) solution and incubated overnight at 4 °C. On the following day, the dishes were gently washed three times with water or HBSS and coated with laminin, an extracellular matrix protein that mediates cell growth and differentiation of growth cone, for at least 1 hour. A panning plate was prepared by coating 24-well Nunclon surface dishes with antibody against p75^{NTR} (diluted to a final concentration of 1–5 ng/ml in 10 mM, pH 9.5 TRIS-buffer) and incubated at room temperature for minimum one hour.

Lumbar spinal cord was dissected from embryonic day 13.5 mice (Wiese, Herrmann et al. 2010) and collected in 180 µl HBSS. The isolated spinal cord from each embryo was cleaned and trypsinized at 37 °C for 15 min by adding trypsin (20 µl of 1%) to a final concentration of 0.1%. Trypsinization reaction was stopped by adding trypsin inhibitor to a final concentration of 0.1% (20 µl of 1%). Tissue was gently triturated to obtain single cells. Cell suspensions including motoneurons expressing p75^{NTR} receptor were then transferred to panning dishes to allow the motoneurons to bind to antibody coated surface of the dish for 45 min. Unbound

cells were removed by gently washing the surface three times with neurobasal medium. Motoneurons attached to the surface of the dish were detached by adding depolarizing solution (300 µl) for 15 sec followed by 1 ml of full medium (NB + 2% HS + 1X B-27) and collected in 1 ml tubes. Cells are counted using a Neubauer chamber and plated on PORN-laminin coated dishes (as per the requirement). After one hour of incubation, cells are attached to the laminin coated dish and are provided with full media containing BDNF. These motoneurons are incubated at 37 °C temperature and 5% CO_2 for 7 (or 5) days and culture media is changed on day 1, 3 and 5, after plating.

2.2.5   Fixation and staining of *in vitro* cultured mouse motoneurons

Growth medium was removed from cultured motoneurons and cells were fixed with 4% PFA (freshly prepared) in PBS for 15 minute at room temperature. PFA was washed away with 1X TBST, three times for 5 min and motoneurons were incubated with blocking (also permeablizing) solution (0.3% Triton X-100, 15% goat serum in PBS) for one hour. Primary antibody diluted in the blocking solution was added to the cells and incubated overnight at 4 °C. On the following day, cells were washed 3 times with 1X TBST and incubated with secondary antibody diluted in TBS for 1 hour at room temperature. Cells were then washed 3 times with 1X TBST and the coverslip containing motoneurons was mounted on object glass slides using aqua polymount.

For axon length measurement, cells were stained with anti-*tau* antibody for identifying axons and Map2 for dendrites. Mounted cells were imaged at 20X magnification under a Leica TCS SP2 microscope. For survival assays, 1500 cells were plated on polyorinithin- laminin coated 4-well dishes (without coverslips) and were provided with full media (2% horse serum) with BDNF or without BDNF (for control cells). Viable cells were counted 2 hour after plating, and after day 3, 5 and 7 of plating. Survival of cells with and without neurotrophic factor was compared.

2.2.6   Isolation of RNA and reverse transcription- PCR

RNAeasy kit (Qiagen) was used for RNA isolation from motoneurons and spinal cord. Motoneurons isolated from each embryo were cultured in individual wells of a 24-well dish. After 7 days *in vitro* culture, cells were washed with warm PBS (RNAse free or freshly opened bottle) and 350 µl of RLT buffer was added immediately to each well. Cells were then scrapped off using a 1 ml tip.

For RNA isolation from spinal cord, isolated lumbar spinal cord was collected in an RNAse free tube and was immediately frozen in liquid nitrogen. Before proceeding for isolation, the tissue was washed once with RNAse free PBS and 350 µl of RLT buffer (10 µl β-mercaptoethanol was added to 1 ml RLT buffer) was added. Tissue was homogenized by pipetting and lysate was loaded on a QIA shredder column (Qiagen) and centrifuged for 2 min at full speed. 350 µl of 70% ethanol (made in DEPC water) was added and immediately mixed by pippeting in and out several times. Lysate was loaded on a RNA easy column and centrifuged for 15 sec at 8000 g such that the RNA could bind to the column. The column was then washed with 700 µl RW1 and two times with RPE, by centrifugation at 8000 g for 15 sec. Column was placed in a fresh tube and centrifuged at full speed for 1 min, to remove all the ethanol. 30-50 µl RNAse-free water is added to the column to dissolve the RNA. After 30 sec, RNA was eluted in a fresh tube by centrifuging at 8000 g for 1 min. All the abbreviations used for the buffers are as mentioned in the kit.

RNA quality and quantity was measured by using the Nanodrop instrument. Nucleic acid has a maximum absorbance at 260 nm; protein, phenol or other contaminants absorb strongly near 280 nm whereas EDTA, carbohydrates and phenol absorb near 230 nm. A 260/280 value of 2-2.02 and 260/230 ratio of nearly 2.2 is generally accepted as pure for RNA.

Preparing cDNA from RNA (reverse transcription): RT-PCR is used to reverse transcribe the RNA of interest into its DNA complement through the use of reverse transcriptase enzyme. Superscript III First-Strand Kit (Cat no. 18080-05, Invitrogen) was used for this purpose. The reaction set up was 2 µl 10 mM dNTP mix, 1 µl RNAse out, 1 µl random hexamer N6, 200 ng of RNA were mixed in a tube and the total volume was made up to 12 µl by adding DEPC water. This mix was incubated at 65 °C for 5 min and was immediately put on ice. 2 µl 10X RT buffer, 1 µl DTT, 2 µl $MgCl_2$ was then mixed into this tube and incubated at 37 °C for 5 min. 1 µl superscript III enzyme was added to the RT reaction but not to the negative RT control and the mix was incubated at 37 °C for 2 hours. RNaseH was added and incubated for 20 minutes at 37 °C. The reverse transcription reaction was stopped by incubation at 70 °C for 10 min and cDNA was stored at -20 °C. Prior to use, cDNA was diluted 1:10 in EB-BSA.

2.2.7 Quantitative PCR (qPCR) or real time PCR

Quantitative PCR is used for studying gene expression levels. Relative quantification is based on internal reference genes to determine fold-differences in expression of the target gene. Quantification is expressed as the change in expression levels of mRNA interpreted as cDNA.

In relative quantification the amount of studied gene is compared to the amount of a control housekeeping gene.

Real-time PCR was performed using a FastStart SYBR green Master kit. SYBR Green I is a DNA double-strand-specific dye and it intercalates to the amplified PCR product during each cycle of DNA synthesis. The amplicon is detected by its fluorescence by light cycler and thus the amplification is monitored by measuring fluorescence increase. Number of cycles at which the fluorescence exceeds the threshold is called threshold cycle or crossing point. Heat-labile blocking groups on some of the amino acid residues of FastStart Taq DNA Polymerase make the modified enzyme inactive at room temperature. Therefore, there is no elongation during the period when primers can nonspecifically bind. FastStart Taq DNA Polymerase is activated by removing the blocking groups at a high temperature (*i.e.* a pre-incubation step at 95 °C).

Reagent	1X(ul)
MgCl (50 mM)	x
Primerrev (10 pmol)	x
Primerfw (10 pmol)	x
Sybr-green	2
Water	Upto 18µl
cDNA	2µl

Step	Cycle condition	Duration
Denaturation	95 °C	10 min
Amplification (50 cycles)	95 °C	1 sec
	X °C	5 sec
	72 °C	x sec
	85 °C	5 sec
Melting	65 °C	15 sec
Termination	40 °C	40 sec

MgCl concentration and primer concentration required is primer specific and was standardized by running a test PCR using different primer concentration of 20, 30 and 40 pmol per primer per reaction and different volume of MgCl (50 mM) 1.6 µl and 2.4 µl, using a test cDNA. The minimum quantity of MgCl and primer concentration that gives the lowest cross-

ing point was used for that primer set for all further runs. PCR primers were designed using Oligo6 software and annealing temperature was primer specific and used as determined by Oligo6. Duration of amplification is PCR product length (x) specific and was used as x/25°C, so for an amplicon of 130 length amplification step of 6 (or 7) sec was used.

2.2.8   Protein isolation and estimation of protein concentration

Tissue (sciatic nerve) was dissected from mouse and collected in RIPA buffer on ice; it was immediately lysed by sonication followed by centrifugation (4 °C, full speed); supernatant was collected for further use. Protein concentration was determined by using BCA kit as per the instruction manual. Laemmli (5X) was added to 20 µg of protein and the mixture was boiled at 99 °C for 5 min.

Desired proteins were loaded on SDS-PAGE gel where they are separated according to their molecular weight. Transfer of the proteins to nitrocellulose membrane was done using a Peqlab transfer apparatus, semi-dry blotting technique was used at a constant current 120 mA (2X area of gel) for 2 hours. Membrane was blocked by 5% milk in TBST for one hour and was incubated with desired primary antibody diluted in blocking solution at 4 °C overnight. Blots were washed 3 times with TBST (10 min each) and secondary antibody diluted in blocking solution was added for one hour at room temperature. Blots were washed again 3 times with TBST (10 min each wash) and ECL reagent was used to detect the protein on X-ray films. Bands on the film were later quantified using the Image J software.

2.2.9   Immunoprecipitation of proteins

To study protein-protein interactions in a cell lysate, immunoprecipitation technique was used. Sciatic nerves from each mouse were collected in 500 µl of IP buffer, homogenized by glass hand homogenizer, and the supernatant was collected after centrifugation at 14,000 rpm for 10 min at 4 °C. Protein estimation was performed using BCA kit. A minimum of 200 µg of protein lysate was used as the initial material for IP. Protein was diluted to a concentration of 1 µg/µl and was incubated with 20 µl of protein-A beads (prewashed with PBS and equilibrated with lysis buffer) for an hour at 4 °C in a rotor wheel for preclearing. Cleared lysate was obtained as the supernatant by centrifugation at 500 rpm for 3 min at 4 °C. 20 µg of protein was taken out as input and stored at -20 °C. Remaining lysate was incubated with 5 µl of anti- stathmin antibody overnight at 4 °C in a rotor wheel. For IgG control, lysate was incubated with irrelevant rabbit antibody. On the next day, antibody and lysate mix was coupled

to beads by incubation with 20 µl of protein-A (because stathmin is anti-rabbit antibody therefore protein-A beads are used) beads for 1 hour at 4 °C in the rotor wheel. Protein coupled beads were collected after centrifugation at 500 rpm for 3 min at 4°C and supernatant was stored at -20 °C. Beads were then washed 3 times using IP buffer. 40 µl of 2X Laemmli was added and beads were boiled at 99 °C for 10 min, centrifuged at full speed for 5 min. The supernatant after centrifugation was used as eluate of IP for western blot. For western blot analysis, a gradient gel (Biometra 12cm x 13cm) (lower 12%, 5 cm, upper 7%, 5 cm and 4% stacking gel 2 cm) was made and 20 µg of input and 40 µl of eluate was loaded on the gel. Gel was run at constant current of 20 mA. The following antibodies were used for western blot, mouse anti-Stat3 (clone 124H6 #9139 cell signaling), dilution 1: 2000; rabbit anti stathmin (abcam 52630) dilution 1:2500. Secondary antibody, goat anti mouse, 1: 5000 Jackson's immunoresearch #115-035-003, Goat anti rabbit POD, 1: 5000 Jackson's immunoresearch #111-035-003.

2.2.10 Perfusion of mice for electron microscopy

Mice were killed by excessive carbon dioxide; transcardially perfused with a mixture of 4% PFA and 2% glutaraldehyde in cacodylate buffer (CB). Distal phrenic nerves were collected and postfixed in the same fixative overnight at 4 °C. Next day, nerves were washed with CB and treated with 2% OsO_4 in CB for 2 hours, dehydrated in ascending concentration of ethanol and embedded in Epon. Transverse ultrathin sections of nerve were transferred to Formvar-coated nickel grids and contrasted with uranyl acetate and lead citrate. Electron micrographs were obtained with a transmission electron microscope (LEO 912 AB; Carl Zeiss). At least 3 mice from each genotype were investigated and the number of microtubules was counted in transverse sections of 10 axons from each mice. Microtubules were counted manually and the area was calculated using Image J.

2.2.11 Laser microdissection of motoneurons from spinal cord

Laser capture microdissection (Leica DM6000B laser microdissection system) was used to isolate motoneuron cell bodies from spinal cord of adult mice or 2-days-old postnatal mice. Mice were killed by cervical dislocation and the lumbar spinal cord was dissected carefully without distorting the anatomy. From 2 days old pubs, the spinal cord was dissected with bone cavity around the spinal cord to preserve the anatomy of the tissue. Tissue was put in optimum cutting temperature compound (Tissue-Tek); immediately immersed in isopentane

cooled in liquid nitrogen for rapid freezing and stored at -80 °C until it was used. Tissue stored at -80 °C was used for cryosectioning as soon as possible. About 100 -150 cross-sections of 10 µm thickness were prepared from each spinal cord on a Leica cryostat, and collected on 0.9 µm POL membranes (Leica). Spinal cord sections were fixed in 70% ethanol (made in DEPC water) for 2 min and stained in cresylviolet (1% CV dissolved in 100% ethanol) for 1 min. Sections were washed once with 70% ethanol and once with 100% ethanol, followed by drying at room temperature for 5 min and then in a desiccator for 45 minutes. Dried slides with cryosections were immediately put in 50 ml falcon and tightly closed to avoid any moisture contact and stored at -80 °C till use. All containers used for staining were cleaned with RNAse away and rinsed with DEPC water to avoid any RNA degradation.

At laser capture microdissection system, 1500- 2000 motoneuron cell bodies were dissected from each spinal cord and collected on the cap of a PCR tube. Total RNA was purified from the samples and real-time RT-PCR was performed (Grundemann, Schlaudraff et al. 2008). 9.7 µl of RNA lysis buffer (see material and method for composition) was added to each cap, on ice. Tubes were incubated (on lid) for 2 min at 72 °C on a heater. They were then incubated on lid for 1 min on ice and centrifuged at 13,000 rpm for 1 min. 0.3 µl of Superscript III reverse transcriptase was added to 8 µl of lysis buffer and rest 2 µl was used as negative control. Tubes containing both control and RT samples were transferred to a mastercycler with following settings; Lid 105 °C, 2 hours at 38 °C followed by 8 hours at 39 °C and finally at 4 °C. Tubes containing cDNA was then stored at -20 °C till use. The resulting cDNA was diluted 1:10 in EB-BSA before use. The cDNA was used to compare the expression level of Neurexin2α in wild-type versus Smn MNs, GAPDH expression served as denominator and relative expression was calculated.

2.2.12 Fixation of motoneuron for electron microscopy

Motoneurons were cultured on special Falcon dishes (BD Falcon™-Dish 35X10mm non-TC Petri EZGrip 500cas - BD Biosciences) for 7 days following the protocol described for motoneuron culture above. Neurons were fixed with 2.5% glutaraldehyde and 0.8% tannic acid in 0.1M cacodylate buffer pH 7.5 (CB), for 5 min at 37 °C followed by 90 min at room temperature. Fixed neurons were then washed three times with CB and treated with 1%OsO_4 in CB for 1 hour. These neurons were subjected to dehydration in 30%, 50% ethanol for 5 min each, followed by 30 min 0.5% uranyl acetate in 70% ethanol, followed by 90%, 96%, 100% ethanol for 5 min each, and were finally embedded in a thin sheet of Epon (Serva,

Heidelberg, Germany) resin. After polymerization, the resin sheets were stained with methylene blue for light microscopic identification of motoneurons. Resin pieces containing identified motoneurons were mounted on empty Epon blocks, ultrathin sections of ca. 80 nm were prepared, transferred to Formavar-coated nickel grids and contrasted with uranyl acetate and lead citrate (Reynolds 1963). Electron micrographs were obtained with a transmission electron microscope (LEO 912 AB; Carl Zeiss). Intermediate filaments have a diameter of 11.29 ± 0.46 nm. Proximal axons (within 50 μm distance to the cell body), distal axons (less than 100 μm distance to the axon tip), intermediate axons (in-between these two regions), growth cones and cell bodies of motoneurons were imaged with the electron microscope.

2.2.13 Microtubule regrowth assay

An established MT regrowth assay (Ahmad and Baas 1995) with following modifications was used to study the MT regrowth in cultured motoneurons. 6,000 cells were plated on polyornithin-laminin coated 12 mm coverslips and incubated at 37 °C for one hour. Cells were then provided with full medium (2% horse serum, 1X B-27 and 5 ng BDNF) containing 10 μM nocodazole to depolymerize the microtubule network. After 6 hours of depolymerization, cells were washed 5 times with warm neurobasal (NB) media and incubated at 37 °C for 5 min with 500 μl of warm NB to investigate the regrowth of microtubules. These cells were then washed with MT stabilizing buffer PHEM (60 mM Pipes, 25 mM Hepes, 10 mM EGTA, and 2 mM $MgCl_2$) and MTs were extracted by adding PHEM with 0.5% triton X-100 and 10 μM paclitaxel for 3 min at 37 °C. Cells were rinsed with PHEM and were fixed in 4% PFA + PHEM (1:1). These motoneurons were then stained for α-tubulin to label polymerized MT and γ-tubulin to label microtubule organizing center (MTOC). Images were taken at a SP5 confocal microscope with 63X oil immersion objective, 4X magnification and 1.4 N.A. Image J was used to quantify the regrowth of microtubules. After background subtraction of radius 50, similar threshold was set for all the images and Sholl analysis was performed to quantify the number of microtubule intersections at a step size of 1 μm. Total length of MT for each cell was determined by multiplying the number of intersections at each step by its distance from the MTOC, starting from the periphery to the center. Mean length was calculated by summing up the length of MTs obtained and divided by the total number of MTs measured: $\Sigma ((nx - (nx + 1)) \times \Delta MTOCx)/N$, in which n is the number of intersections, x is the circle of interest, $x + 1$ is the next outer circle, $\Delta MTOCx$ is the distance from MTOC to the circle of interest, and N is the total number of MTs.

2.2.14 Behavior analysis of mice

Motor coordination and disease severity of mice were tested using a rotarod (accelerating rotarod, Ugo Basile) that records the latency (time from beginning of the trial until the mouse falls off) to fall off the rotating rod. 6 mice from each genotype *pmn*, *Nefl+/-;pmn* and *Nefl-/-;pmn* were tested for three consecutive days at the age of 27, 28 and 29 days for both constant speed (4 rpm) and accelerating speed rotarod (linear acceleration from 4-40 rpm). The latency to fall off from the rotating rod (in seconds) was recorded for each mouse for three trials spaced by 10 min each. Average latency for all the 9 trials for each mouse for three consecutive days is plotted. Fore limb grip strength of mice was measured using the automatic grip strength meter (Chatillon). Mice were allowed to grasp a horizontal metal grid and pulled by their tail until the grip was released. The peak pull-force (Newton) was recorded on the digital display. This test was performed for 6 trials per day for three consecutive days (age of 27, 28 and 29 days). Average of the results from three days is plotted. Only female mice were used for rotarod and grip strength tests.

2.2.15 Structure illumination microscopy

SIM microscopy was performed to study the tubulin dynamics in *in vitro* cultured motoneurons. Structure illumination is a widefield technique used for optical sectioning, and forms the basis for higher resolution techniques. It relies on a grid pattern superimposed on the specimen during imaging. The grid pattern is rotated in steps at a certain angle (for e.g. 5 steps) during imaging. A sinusoidal excitation wavefield is generated that can be used to extract information from the image focal plane that rejects the out-of-focus blur. A special algorithm is used by the program to process the raw data producing an image with an axial resolution between 150-300 nm and lateral resolution approximately twice that of diffraction limited instruments.

Motoneurons cultured for 3 days were fixed and stained with the above described protocol. Neurons were labeled by indirect immunofluorescence using secondary antibodies labeled with Alexa Fluor 488, Cy3 and Cy5. Specimens were imaged using a SIM Zeiss ELYRA S.1 microscope system with a 63x/1.40 oil immersion objective in x-y-z stacks. Raw images (16 bit) were processed to reconstruct high-resolution information using the provided commercial software package (Zeiss). Three-color images were aligned using a transformation matrix and were later processed with ImageJ. SIM images shown in the result section are maximum-intensity projections of 5 z-stacks.

3   Results

3.1   Neurofilament depletion improves microtubule dynamics via modulation of Stat3/stathmin signaling

3.1.1   Increased intermediate filaments in *pmn* mutant mouse neurons

Axonal accumulation of neurofilaments is a pathological hallmark in many forms of motoneuron disease. *Pmn* mutant mice suffer from a severe form of motoneuron disease which starts in the third postnatal week and leads to death within 3-4 weeks (Schmalbruch, Jensen et al. 1991). In order to investigate the axonal pathology in *pmn* mice, the ultrastructure of phrenic nerves of 34 days old *pmn* mice were analyzed using electron microscopy. A drastic increase in the number and density of intermediate filaments with typical diameter of 10 nm in cross sections of phrenic nerve from *pmn* mutant mice was observed (Fig. 7B and 7D) as compared to the wild-type (Fig. 7A and 7C).
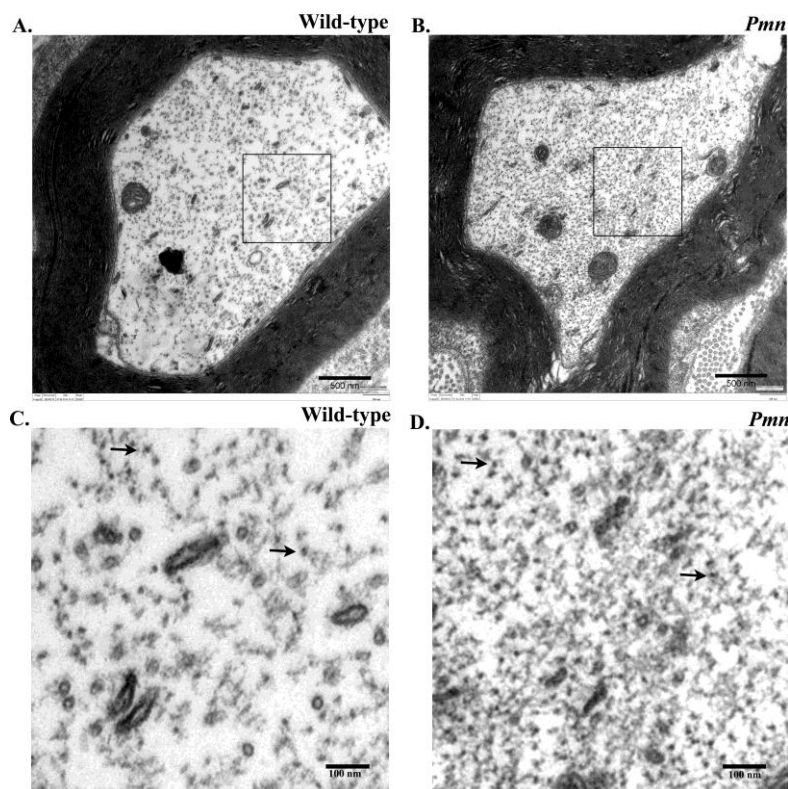

Figure 7: Intermediate filament accumulation in distal phrenic nerve of adult *pmn* mice

Electron micrograph of distal phrenic nerve from 34 days old (A) wild-type mouse (B) *pmn* mouse. Zoomed- in image of boxed area in (C) wild-type (D) *pmn* nerve. Arrows show 10 nm intermediate filaments in the nerve sections. Scale bar upper lane : 500 nm. Scale bar, lower lane: 100 nm.

Next, I analyzed the ultrastructure of isolated embryonic motoneurons which were cultured for 7 days *in vitro*. Analysis of proximal, intermediate and distal compartments of axons showed increased intermediate filaments in *pmn* mutant motoneurons (Fig. 8).
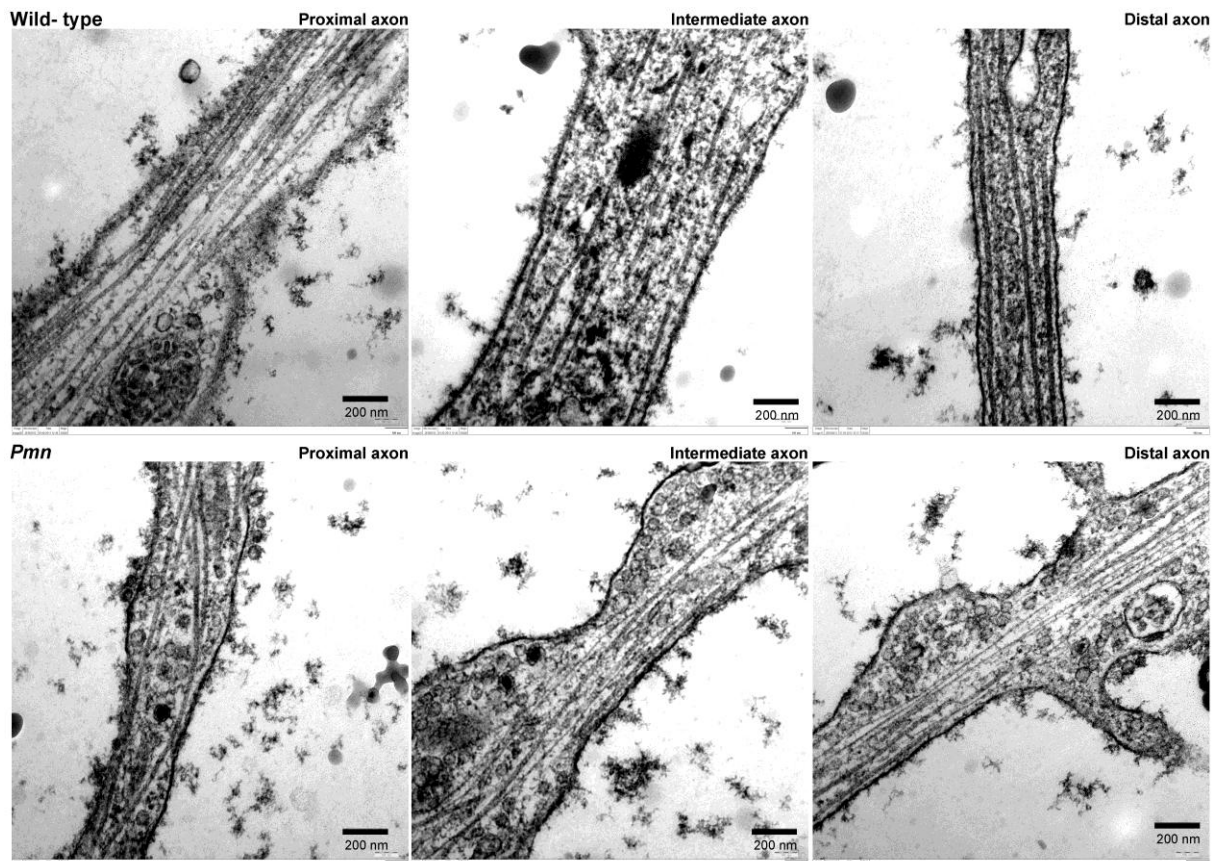
Figure 8: Intermediate filaments and microtubules in 7 days *in vitro* motoneurons

Electron micrograph showing proximal, intermediate and distal axonal compartments of 7 days *in vitro* cultured wild-type (upper panel) and *pmn* (lower panel) motoneurons, scale bar, 200 nm.

Levels of neurofilament proteins in the peripheral nerve of adult *pmn* mice were analyzed. For this purpose, sciatic nerves were isolated from 34 days old *pmn* mutant mice, representing an advanced stage of the disease. Nerve lysates were subjected to western blot analysis for NFL and NFH protein. *Pmn* mutant mice showed a significant increase in NFL protein levels in comparison to wild-type mice (Fig. 9A and 9B*; n = 5; t = 3.210; df = 4; P = 0.0326*). Also the levels of NFH protein increased in comparison to the wild-type mice (Fig. 9A and 9C*; n =5, t = 2.781; df = 4; P = 0.0498*).

In order to study the role of NFL upregulation for the disease phenotype, *pmn* mutant mice were crossbred with *Nefl* knockout mice. Deletion of one *Nefl* allele reduced the levels of NFL in *Nefl+/-;pmn* littermates to control levels (Fig. 9A-B*; t = 0.8864; df = 2; P = 0.4689*).

Also, the increased levels of NFH protein in *pmn* mice were normalized to wild-type levels in *Nefl+/-;pmn* mice (Fig. 9A and C*; t = 0.5821; df = 2; P = 0.6194*). Western blot analysis confirmed the absence of NFL in *Nefl-/-;pmn* mouse and showed highly reduced levels of NFH protein (Fig. 9A) (Zhu, Couillard-Despres et al. 1997).
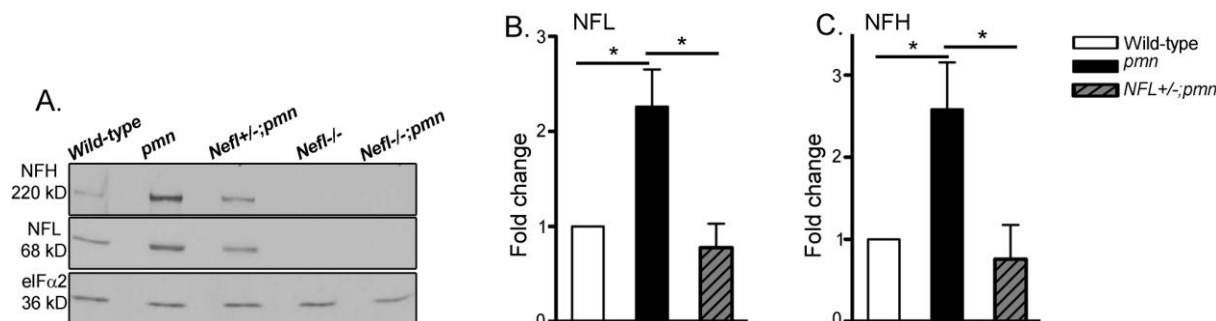

Figure 9: Increased neurofilament protein levels in sciatic nerve extracts of *pmn* mice

(A) Western blot analysis of tissue homogenates from the sciatic nerve of 34 days old mice using neurofilament-light (NFL) and neurofilament-heavy (NFH) antibody. (A-C) *Pmn* mutant mice showed increased levels of (B) NFL ($t = 3.210$, $P = 0.0326$) and (C) NFH ($t = 2.781$, $P = 0.0498$) proteins as compared to the wild-type. Bars represent mean ± SEM, (n = 5 wild-type and *pmn* and n = 3 *Nefl+/- ;pmn* mice analyzed, *$P < 0.05$; one sample t-test). Levels of NFL and NFH proteins were reduced to wild-type levels on deletion of one allele of *Nefl* from *pmn* mice.

3.1.2   *Nefl* deletion prolongs life span and improves behavior of *pmn* mutant mice

Homozygous *pmn* mice start to show first symptoms of disease within third week after birth and most of the *pmn* homozygous mice die at an age of 5-6 weeks (Schmalbruch, Jensen et al. 1991, Sendtner, Schmalbruch et al. 1992). *Nefl* knockout *per se* does not reduce survival of the mice, and *Nefl-/-* mice do not show an overt disease phenotype (Zhu, Couillard-Despres et al. 1997). In order to study the effect of NFL depletion in *pmn* mice, the life span of *Nefl-/- ;pmn* mice was followed. *Nefl-/-;pmn* mice showed a significant extension of life span with an average increase of ~21% in median survival (Fig. 10A; $\chi^2 = 6.460$, $P = 0.0110$) as compared to the *Nefl+/+;pmn* mice. Median survival of *Nefl-/-;pmn* (n = 22 mice) was 45 days, that of *Nefl+/-;pmn* (n = 27 mice) 40 days and in *Nefl+/+;pmn* (n = 22 mice) 37 days. Of the 22 mice analyzed at postnatal day 41; 18 *Nefl-/-;pmn* mice were still alive. At the same time point only 6 out of 22 *Nefl+/+;pmn* were alive. The average weight of *Nefl-/-;pmn* at the age of 27-29 days was comparatively higher than the weight of *pmn* mice though the data did not reach statistical significane (Fig. 10B). Hind limbs of the *Nefl-/-:pmn* were still functional at the age of 29 days when the hind limb of *pmn* mice were completely atrophied (Fig. 9C-D).
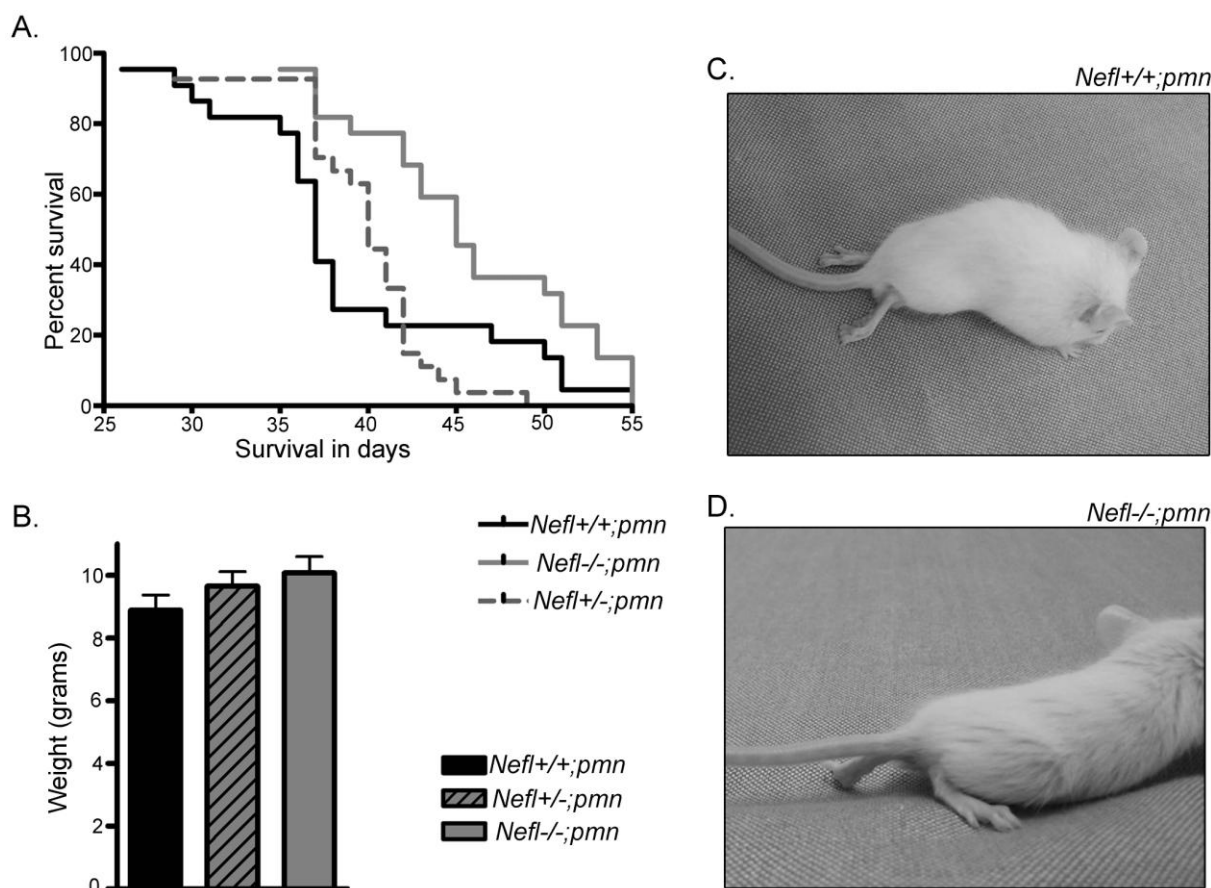
Figure 10: Survival and phenotype of NFL deficient *pmn* mice

NFL depletion extends the life span of *pmn* mice and improves their motor performance (A) Kaplan-Meier curve for comparison of life span of mutant mice; log rank test; n = 22 *pmn* and *Nefl-/-;pmn* mice and n = 27 *Nefl+/-;pmn* mice analyzed, $P = 0.0110$, $\chi^2 = 6.460$. (B) Mice were weighed at postnatal day 27-29 and showed no significant difference in the average weight. (C-D) Representative images of 29 days old (C*) Nefl+/+:pmn* and (D) *Nefl-/-;pmn* mice born in the same litter.

In order to assess the motor performance and disease progression in *Nefl-/-;pmn* mice, the performance of these mice were tested on rotarod. On a constant speed rotarod, *Nefl+/-;pmn* (Fig. 11A; n = 6; t = 4.663; *P* < 0.001) and *Nefl-/-;pmn* mice (Fig. 11A; n = 6; t = 1.476; not significant) showed an increase in the latency to fall as compared to *Nefl+/+;pmn,* suggesting higher strength and a better motor co-ordination in *pmn* mice when *Nefl* was deleted. Interestingly, *Nefl+/-;pmn* mice with normalized NFL levels performed better than *Nefl-/-;pmn* mice in this test. On an accelerating rotarod, *Nefl-/-;pmn* (Fig. 11B; t = 2.735, *P* < 0.05) and *Nefl+/-;pmn* (Fig. 11B; t = 5.206; *P* < 0.001) mice showed an increase in the latency to fall off the rotating rod, as compared to *Nefl+/+;pmn* mice. *Nefl-/-;pmn* could stay up to 50 sec when the rotating speed of the rotarod reaches to 40 rpm in contrast to *pmn* mice which could not sustain the higher rotating speed.
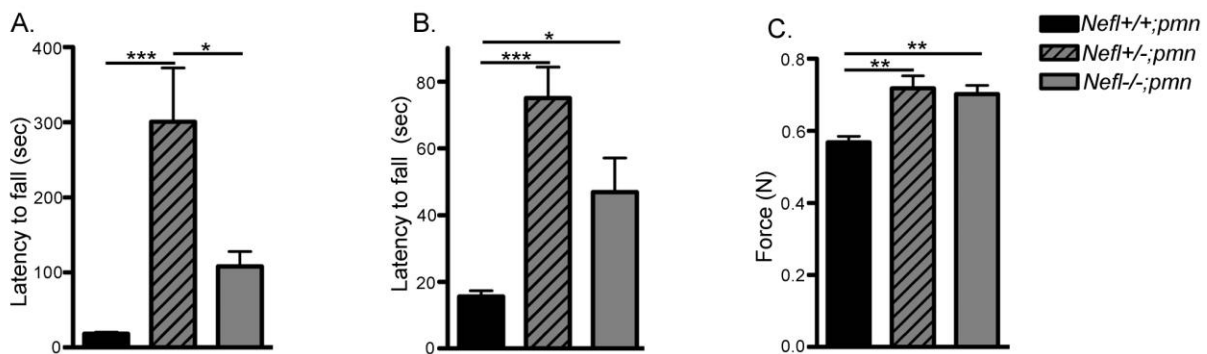
Figure 11: Rotarod and grip strength of NFL deficient *pmn* mouse

Both (A) on constant speed rotarod, *Nefl+/-;pmn* ($t = 4.663$) and *Nefl-/-;pmn* ($t = 1.476$) and (B) on an accelerating speed rotarod, *Nefl+/-;pmn* ($t = 5.206$) and *Nefl-/-;pmn* ($t = 2.735$) mice showed an increase in the latency to fall as compared to *Nefl+/+;pmn* mice. (C) Peak forelimb grip strength of mice was measured (in Newton N), *Nefl+/-;pmn* (t = 4.007) and *Nefl-/-;pmn* ($t = 3.578$) mice exhibited higher grip strength as compared to *Nefl+/+;pmn* mice. (A-C) Bars represent mean ± SEM (one-way ANOVA and Bonferroni's post hoc test, n = 6 mice per genotype, *$P < 0.05$, **$P < 0.01$, ***$P < 0.001$). Bars show average of the tests on postnatal day 27, 28 and 29 days

Next, the fore limb grip strength of *pmn* mice was measured using a grip strength meter. In this test, both *Nefl-/-;pmn* (Fig. 11C; n = 6; $t = 3.578$; $P < 0.01$) and *Nefl+/-;pmn* (n = 6; $t = 4.007$; $P < 0.01$) mice showed higher grip strength as compared to the *pmn* mice. For rotarod and grip strength test, six mice per genotype were tested for three consecutive days (at the age of 27, 28 and 29 day). This period was chosen because it marks a period of rapid disease progression in *pmn* mutant mice.

3.1.3 *Nefl* deletion increases axon length and microtubule density of *pmn* motoneurons

Isolated motoneurons from *pmn* mutant mice show reduced axon outgrowth when cultured for 7 days *in vitro* (Bommel, Xie et al. 2002), which could be rescued by CNTF application (Selvaraj, Frank et al. 2012). In order to study the effect of NFL depletion on axon elongation in *pmn* motoneurons, axon length of 7 days *in vitro* cultured *Nefl+/+;pmn* and *Nefl-/-;pmn* motoneurons in presence of BDNF, was measured. CNTF was not present in these cultures. *Pmn* motoneurons showed significantly shorter axons when cultured with BDNF (Fig. 12A-B; n = 3; $t = 10.84$; $P < 0.001$) whereas axons from *Nefl-/-* motoneurons ($t = 2.580$; $P > 0.05$) grew comparably to those of wild-type motoneurons. *Nefl* deletion completely rescued axon elongation in *pmn* mutant motoneurons. *Nefl-/-;pmn* motoneurons grew significantly longer as compared to the *pmn* motoneurons (n = 3; $t = 9.573$; $P < 0.001$) and showed axon length comparable to those of the wild-type motoneurons (Fig.12A-B; n = 3; $t = 0.5491$; $P > 0.05$;

60

ANOVA with Bonferroni's posthoc test). *Nefl-/-* deletion did not affect survival of the motoneurons (Fig.12C).
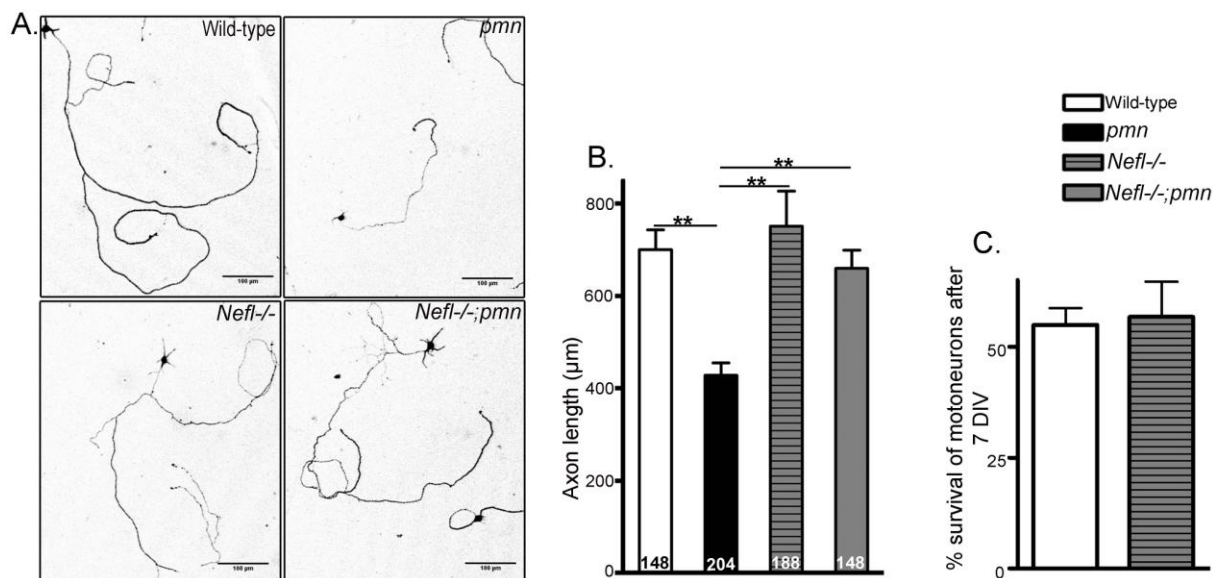
Figure 12: NFL depletion causes axon elongation of *in vitro* cultured *pmn* motoneurons

Representative images of 7 days *in vitro* cultured motoneurons. Scale bar 100 µm. (B) *Pmn* motoneurons showed reduced axon length ($t = 6.845$). *Nefl-/-;pmn* motoneurons grew significantly longer than *pmn* motoneurons ($t = 5.830$) (n = 3 independent experiments). Numbers in the bars represents total number of motoneurons analyzed. Bars represent mean ± SEM (one-way ANOVA and Bonferronis's posthoc test, *$P < 0.05$, **$P < 0.01$, ***$P < 0.001$). (C) Bar graph showing no change in the survival percentage of *Nefl* motoneurons after 7 days *in vitro* culture.

Pmn mutant mice exhibit reduced axonal microtubule density in the distal part of phrenic nerves (Martin, Jaubert et al. 2002, Schaefer, Schmalbruch et al. 2007). Similarly, cultured motoneurons from *pmn* mutant mice show reduced axonal microtubule density in the proximal part of the axons (Selvaraj, Frank et al. 2012). On the other hand, *Nefl-/-* mice show increased microtubule numbers in axons within spinal cord and higher α-tubulin protein levels in the cerebral cortex (Ishihara, Higuchi et al. 2001). In order to study the microtubule dynamics in *Nefl-/-;pmn* mice, ultrastructure of distal phrenic nerves in 34 days old wild-type, *pmn*, *Nefl-/-* and *Nefl-/-;pmn* mice was analyzed. As expected, *pmn* mice showed a reduction in number of microtubules per axon (Fig. 13-14A-B; n = 3 mice; 10 axons counted from each; $t = 4.453$; $P < 0.05$) as compared to the wild-type mice. Reduced microtubule density was also noted between these genotypes but did not reach significance in our analyses.
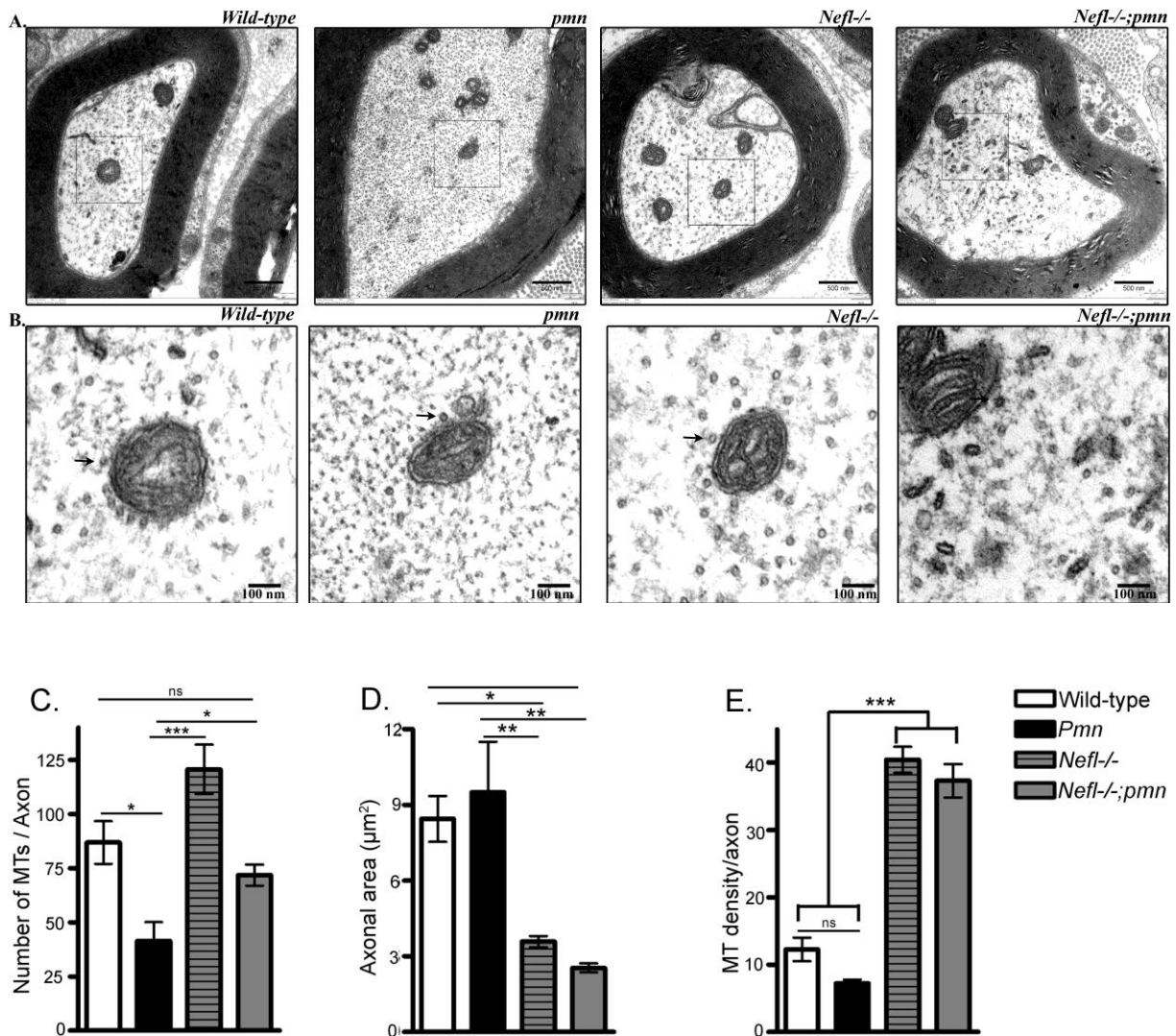
Figure 13: NFL depletion increases MT number and density in *pmn* mouse

NFL depletion increases microtubule (MT) density and axon length in *pmn* mutant motoneurons. (A) Electron micrographs of distal phrenic nerve cross-sections from 34 days old mice (top), scale bar 500 nm. Square boxes indicate the region enlarged in (B) bottom lane, scale bar 100 nm. Arrows show MTs. (C) Number of MTs per axon in *pmn* ($t = 3.640$) decreased whereas *Nefl-/-;pmn* mice ($t = 2.701$) showed MT number comparable to wild-type mice. (D) Cross-sectional area of *Nefl-/-* ($t = 3.416$) and *Nefl-/-;pmn* ($t = 4.488$) reduced as compared to wild-type axons. (E) Density of MT per axon in *Nefl-/-* ($t = 10.05$) and *Nefl-/-;pmn* ($t = 9.649$) mice increased (n = 3 *pmn* and *Nefl-/-* mice and n = 4 wild-type and *Nefl-/-;pmn* mice analyzed).

Depletion of NFL significantly increased the number of microtubules per axon in phrenic nerves of *Nefl-/-;pmn* mice (Fig. 13C; $t = 3.314$; $P < 0.05$) as compared to *pmn* mice. Also, the number of microtubules in *Nefl-/-* axons was higher than in wild-type but the data did not reach significance. This might suggest that depletion of NFL resulted in maintenance of stabilization of microtubules but not in the generation of additional microtubules. NFL is the major determinant of axonal caliber (Hoffman, Cleveland et al. 1987). Accordingly, NFL

depletion led to a drastic reduction in the cross-sectional area of axons in *Nefl-/-* (Fig. 13D; $t = 5.121$; $P < 0.01$) and *Nefl-/-;pmn* axons (Fig. 13D; $t = 6.642$; $P < 0.001$) as compared to wild-type and *pmn* axons. Consequently, the density of microtubules per axon was increased in *Nefl-/-* (Fig. 13E; $t = 4.490$; $P < 0.01$) and *Nefl-/-;pmn* (Fig. 13E; $t = 5.689$; $P < 0.01$) as compared to wild-type axons. MT density was also increased in *Nefl-/-* ($t = 5.587$; $P < 0.01$) and *Nefl-/-;pmn* ($t = 6.750$; $P < 0.001$) as compared to those of *pmn* axons. These data suggest that NFL depletion prevents destabilization of microtubules in *pmn* mice and leads to an increased density of microtubules in axons by reducing the axonal caliber in both wild-type and *pmn* mice.

Also, the *in vitro* cultured *Nefl-/-* and *Nefl-/-;pmn* motoneurons were analyzed using electron microscopy (Fig.14). An increase in microtubule number was observed but the data needs to be quantified using more axons.
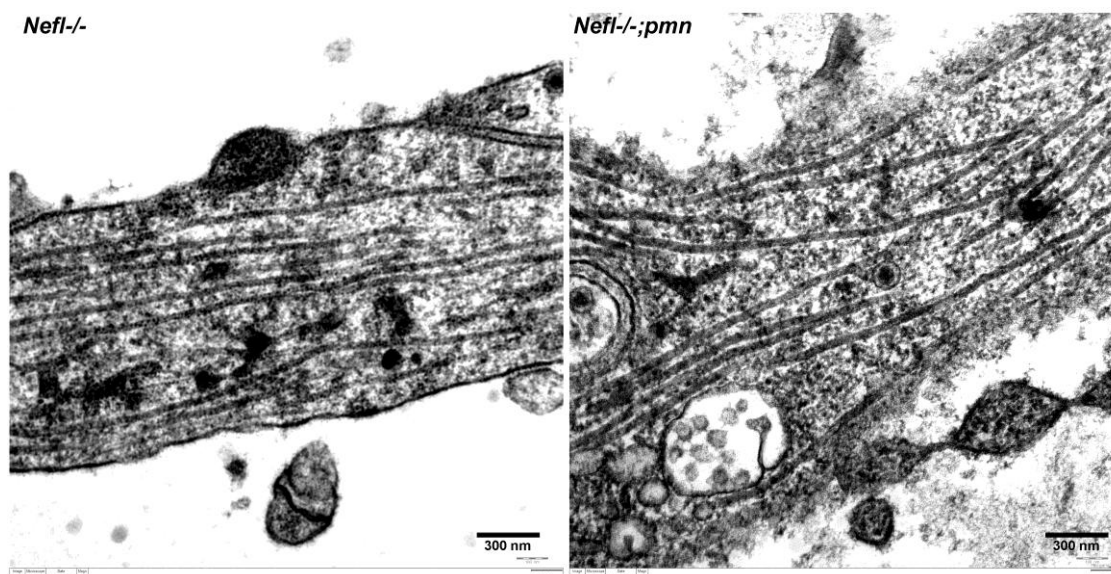
Figure 14: Electron micrograph of NFL deficient *in vitro* cultured motoneurons
Electron micrograph of axons from 7 days *in vitro* cultured motoneurons from *Nefl-/-* and *Nefl-/-;pmn*.

3.1.4 *Nefl* deletion increases microtubule regrowth in *pmn* motoneurons

In order to study microtubule dynamics in *Nefl-/-* motoneurons, microtubule regrowth and polymerization in cultured motoneurons after complete disintegration of microtubules was investigated. For this purpose, an established protocol for MT regrowth after nocodazole treatment was used (Ahmad and Baas 1995, Schaefer, Schmalbruch et al. 2007). Motoneurons were plated in culture dishes for 6 hours and the established microtubule network was

completely depolymerized by applying 10 µM nocodazole for 6 hours. Nocodazole was then completely washed off and the microtubules were allowed to grow.
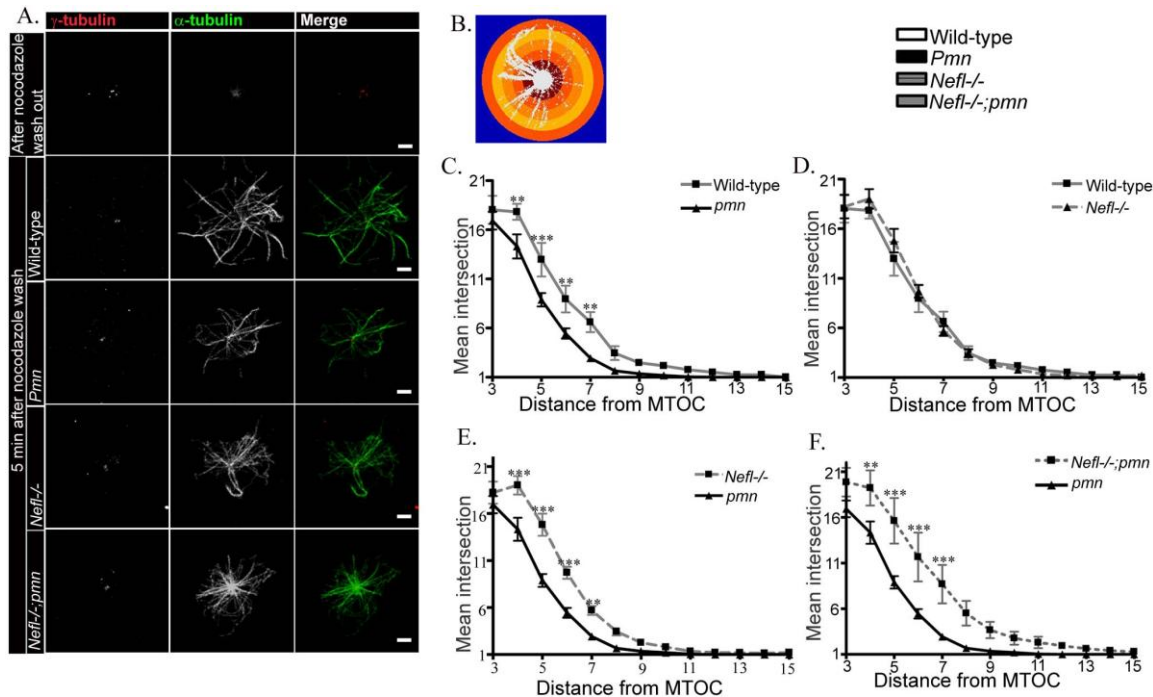
Figure 15: NFL depletion enhances microtubule regrowth in *pmn* motoneurons *in vitro*.

(A) Representative images of motoneurons showing depolymerized microtubules (MT) after nocodazole treatment and MT regrowth after 5 minutes of nocodazole washout. Microtubules are labelled using α-tubulin (green) and centrosome by γ-tubulin (red). Bars, 2 µm (B) Representative image of Sholl analysis performed to count the number of MTs with 1 µm concentric circles step. (C-E) Number of MT intersections (y axis) at increasing distance (x axis) from microtubule organizing center (MTOC) was counted. Line graphs showing mean ± SEM (two-way ANOVA with Bonferroni's posthoc test, n = 4 independent experiments, $**P < 0.01$, $***P < 0.001$)

Sholl analysis was performed to quantify MT polymerization, average MT length and total length of MT after regrowth. *Pmn* mutant motoneurons showed reduced MT regrowth when compared to wild-type or *Nefl* -/- motoneurons (Fig.15 A-C, E; n = 4). *Nefl-/-* motoneurons showed no change in MT repolymerization and the MT intersections appeared comparable to wild-type neurons (Fig. 15). NFL depletion significantly increased MT regrowth and repolymerization in *pmn* motoneurons, and *Nefl-/-;pmn* motoneurons showed microtubule regrowth comparable to wild-type and *Nefl-/-* motoneurons (Fig. 15A- F; *; $P < 0.05$; **, $P < 0.01$; *** $P < 0.001$;) when cultured with BDNF.

Next, the average length of microtubules was measured. For this purpose, length of all the microtubules growing from the microtubule organizing center (MTOC) was measured and the average length was calculated. *Pmn* mutant motoneurons exhibited shorter average

microtubule length and total microtubule length compared to wild-type neurons. The average microtubule length (Fig. 16A) and total microtubule length (Fig. 16B) within *Nefl-/-;pmn* motoneurons was longer than the length of microtubules in *pmn* but the data didn't reach statistical significance.
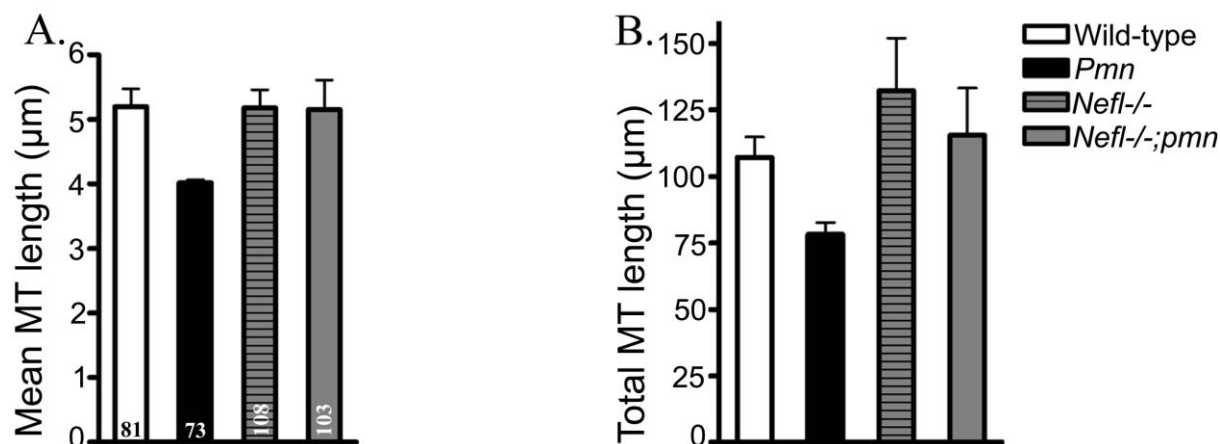
Figure 16: Length of MT regrowth after nocodazole treatment

(A) Bar graph showing the average length of microtubules regrown from MTOC in *in vitro* cultured motoneurons. Number in bars represents the number of analyzed motoneurons. (B) Graph showing the total length of microtubules originating from each MTOC. Error bars represent mean ± SEM from four independent experiments.

3.1.5   NFL interacts with stathmin and affects Stat3-stathmin interaction

CNTF mediated restoration of axon length and maintenance of *pmn* motoneurons has been shown to be mediated via local axonal function of Stat3. Stat3 is activated upon CNTF application and the activated Stat3 interacts with stathmin thereby inhibiting its microtubule destabilizing activity and preventing the axonal degeneration in *pmn* motoneurons (Selvaraj, Frank et al. 2012). Stat3-stathmin interaction has been shown to be increased in motoneurons upon CNTF application (Selvaraj, Frank et al. 2012). I therefore studied the interaction of Stat3-stathmin in *Nefl-/-* mice. Using a stathmin antibody, immunoprecipitation was performed and interaction partners of stathmin were investigated. This pulldown experiment revealed that NFL is also a binding partner of stathmin (Fig. 17A). In order to study the effect of NFL depletion, immunoprecipitation from protein lysates of sciatic nerves from one month old *Nefl-/-* mice was performed using stathmin antibody. An increase in Stat3-stathmin interaction in nerves from *Nefl-/-* mice was observed as compared to wild-type mice (Fig. 17A-B; $n = 3$, $t = 17.08$; df = 2; $P = 0.0034$). Hence, deletion of NFL increases the interaction of Stat3-stathmin that antagonizes the MT-destabilizing activity of stathmin (Ng, Lin et al. 2006). We measured the levels of Stat3 in relation to stathmin protein levels in the sciatic nerve extracts of wild-type and *Nefl-/-* mouse and found no difference (Fig. 17C). This

shows that the protein levels of Stat3 per stathmin are unchanged in *Nefl-/-* and only the interaction between the two proteins is affected on NFL depletion.
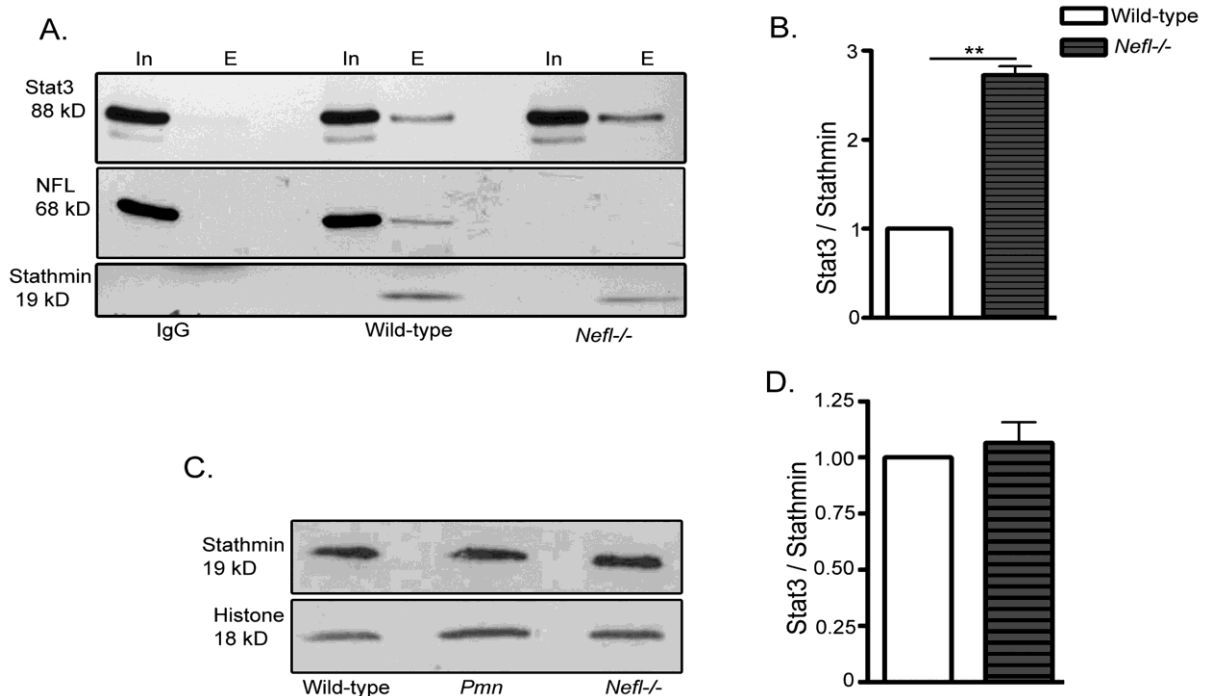
Figure 17: NFL interacts with stathmin and affects Stat3-stathmin interaction

(A) *Nefl* deletion increases Stat3-stathmin interaction. (A) Stathmin was immunoprecipitated from sciatic nerve extracts of 34 days old mice. Western blot shows from left to right, input (Ip) and eluate (E) from wild-type and *Nefl-/-* mice nerve extracts after anti-IgG control and anti-stathmin pulldown. (B) Quantification of band intensities in the eluate showed an increased interaction of Stat3 and stathmin in *Nefl-/-* mice ($t = 17.08$; $P = 0.0034$). Bars represent mean ± SEM (one sample t-test, n = 3 independent experiments. (C) Western blot analyses show levels of stathmin in the sciatic nerve extracts of 34 days old wild-type, *pmn* and *Nefl-/-* mice. Histone levels were determined to ensure equal loading of proteins. (D) Quantification of Stat3 per stathmin levels in the sciatic nerve extracts (input before immunoprecipitation) from 34 days old wild-type and *Nefl-/-* mice (n = 3 independent experiments).

Analysis of Stat3 and stathmin distribution in axons of wild-type and *Nefl-/-* motoneurons using SIM microscopy showed that the distribution of Stat3 is tubular and is along the tyrosinated tubules in wild-type. In *Nefl-/-* motoneurons Stat3 was more along the cytosol and not along the microtubules. This suggested that in *Nefl-/-* motoneurons Stat3 is distributed in the cytosol similar to stathmin, which also shows cytosolic distribution and is not along the tubules as was observed in wild-type motoneurons (Fig. 18).
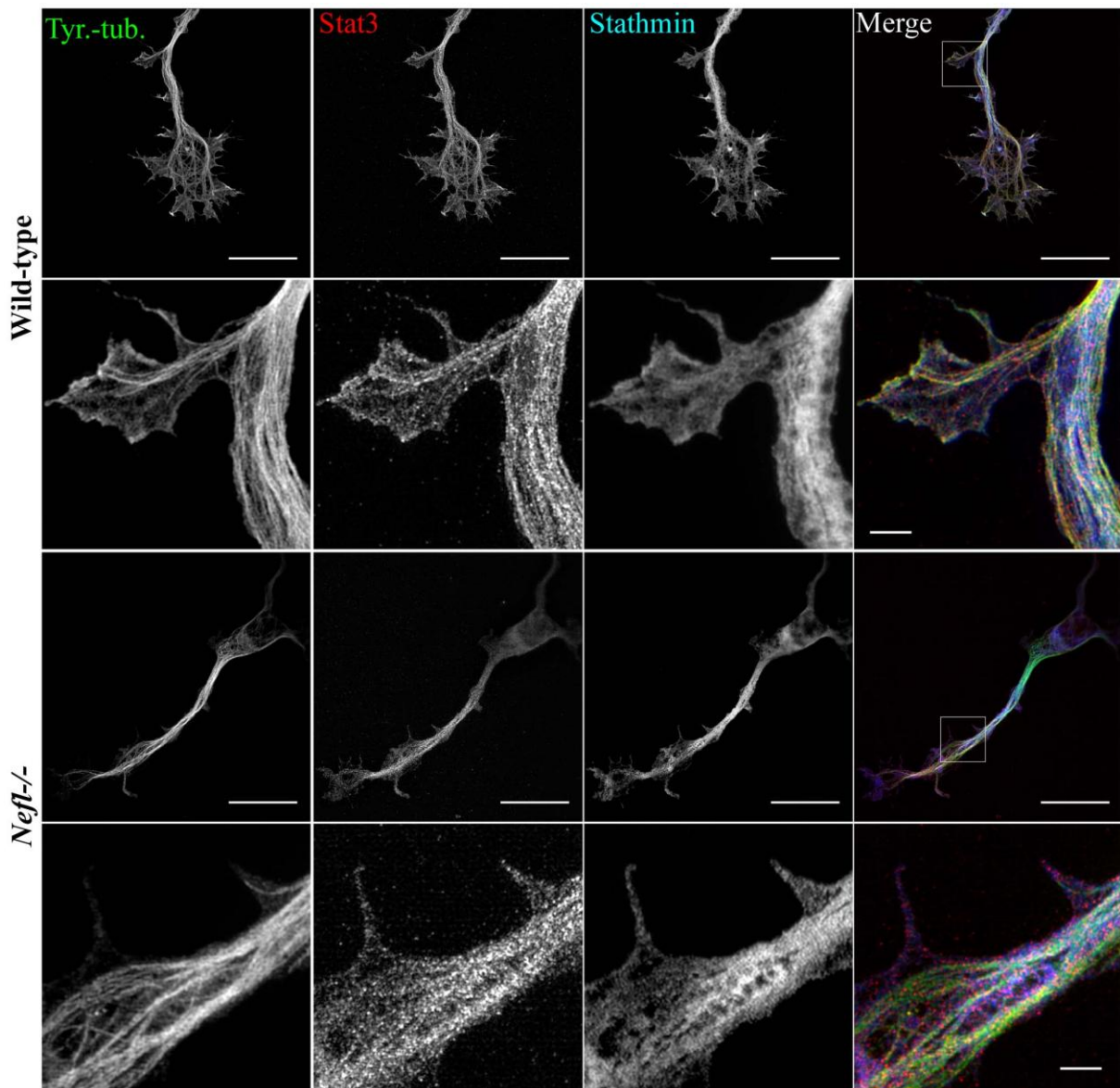
Figure 18: Distribution of Stat3 and stathmin in axons of wild-type and *Nefl-/-* motoneurons

Motoneurons were cultured for 3 days *in vitro*. Representative images of wild-type and *Nefl-/-* motoneurons, stained with antibodies against tyrosinated α-tubulin (green), Stat3 (red), and stathmin (blue). The antibody against tyrosinated α-tubulin stains both soluble αβ- tubulin heterodimers and polymerized highly dynamic microtubules. Scale bar 20 μm (first and third lane). White square boxes indicate the regions enlarged in the second and fourth lane, scale bar 2 μm.

3.1.6 Increased tubulin acetylation in *in vitro* cultured *Nefl-/-* motoneurons

αβ-tubulin heterodimer are the basic components of microtubules. These heterodimers undergo a variety of post-translational modifications which assign specific functions to the tubulin subunits. Acetylation of α-tubulin occurs in polymerized microtubules and acetylated tubulins are enriched in stable microtubules that have a low turnover whereas tyrosinated α-tubulin marks recently assembled more dynamic microtubules with a high turnover (Westermann and Weber 2003).
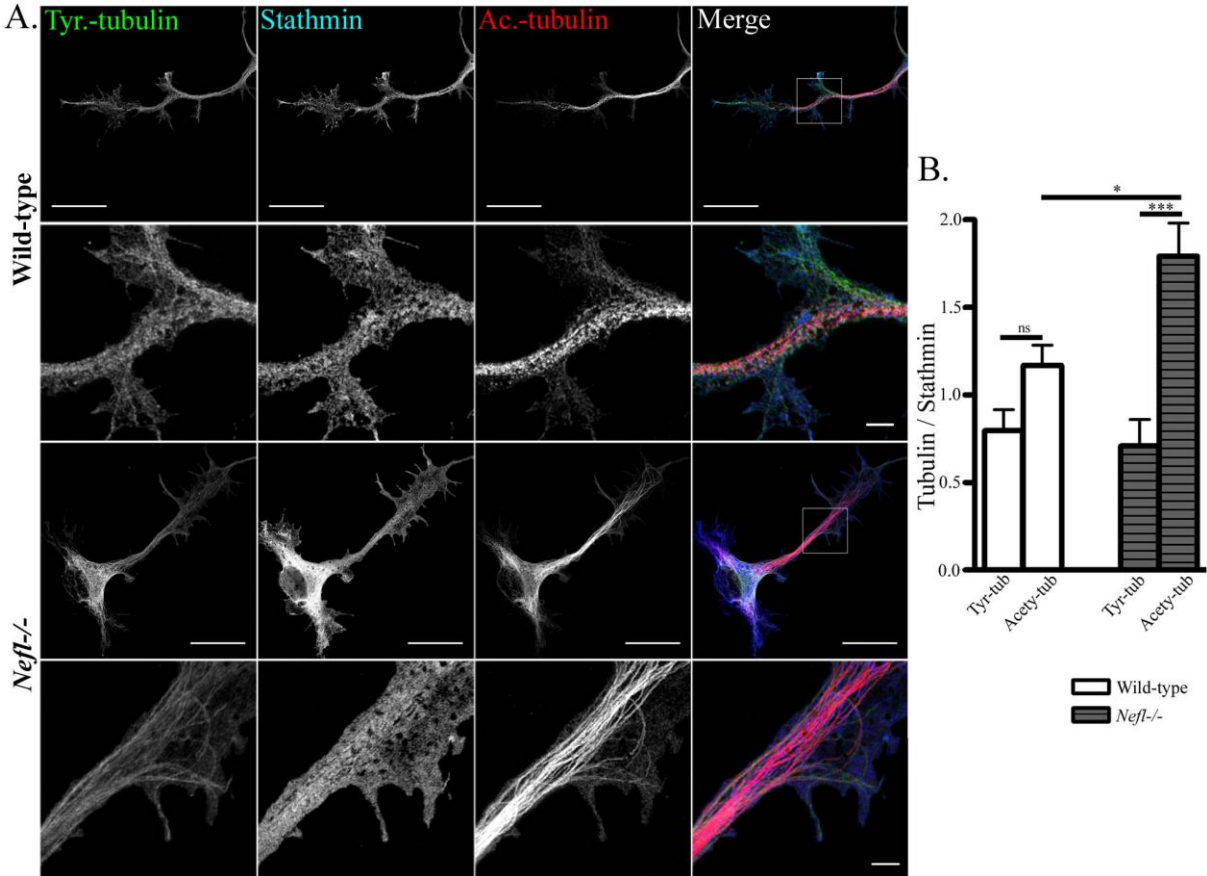
Figure 19: Increased tubulin acetylation in *in vitro* cultured *Nefl-/-* motoneurons

(A) Representative images of motoneurons showing increased acetylated microtubules in *Nefl-/-* motoneurons after 3 days *in vitro* culture. Neurons were stained with antibodies against tyrosinated α-tubulin (green), stathmin (blue) and acetylated α-tubulin (red). Scale bar 20 µm (first and third lane). White square boxes indicate the regions enlarged in the second and fourth lane, scale bar 2 µm. (B) Quantification of fluorescence intensities showed increased acetylated microtubules in *Nefl-/-* (t = 3.011) as compared to wild-type motoneurons, whereas tyrosinated microtubules remained unchanged. Intensity of stathmin is used as control. Bars represent mean ± SEM (one-way ANOVA, n = 10 motoneurons from three independent experiments, $*P < 0.05$, $***P < 0.001$).

Pmn mutant motoneurons exhibit increased levels of tyrosinated tubulin in axons whereas acetylated stable tubulin levels remain unchanged (Selvaraj, Frank et al. 2012). In wild-type neurons acetylated tubulins are found in more proximal parts of axons where microtubules are thought to be stable, and they appear to be excluded from axonal growth cones and dendrites (Witte, Neukirchen et al. 2008, Selvaraj, Frank et al. 2012). In these highly dynamic structures, tyrosinated tubulins are found (Selvaraj, Frank et al. 2012). Depletion of NFL increased the levels of acetylated microtubules in the axons of *Nefl-/-* motoneurons (Fig. 19), indicating that NFL influences MT dynamics, and its depletion stabilizes the MTs presumably by increasing the stathmin-Stat3 interaction and reducing the MT destabilizing activity of stathmin.

3.2 Smn deficiency alters expression and splicing of a presynaptic protein Nrxn2 in a mouse model of SMA

These results have already been published in the manuscript titled; *Smn-deficiency alters Nrxn2 expression and splicing in zebrafish and mouse models of Spinal Muscular Atrophy* (See, Yadav et al. 2013). This work was performed using the *Smn$^{-/-}$;SMN2* mouse model to study the alteration in neurexin expression and splicing. *Smn$^{-/-}$;SMN2* is a mouse model of SMA which expresses 2 copies of the human SMN2 gene on a mouse *Smn* null background and thus resembles the most severe form of SMA in humans (Monani, Coovert et al. 2000). The mice show severe signs of paralysis at birth and most of them die within 5 days of birth.

3.2.1 *Nrxn2* expression in *in vitro* cultured SMA mouse motoneurons

Isolated motoneurons from *Smn$^{-/-}$;SMN2* mouse exhibit significant reduction in axon length when cultured 7 days *in vitro,* in presence of BDNF (Fig. 19A). Survival of the cultured *Smn* deficient motoneurons is not affected (Rossoll, Jablonka et al. 2003). These motoneurons also show defects in spontaneous excitability due to altered clustering of VGCCs in growth cones (Jablonka, Beck et al. 2007). These findings suggested that axon growth and maintenance is primarily affected in SMA which ultimately leads to the loss of motoneurons.

SMN is a ubiquitously expressed protein but SMN deficiency affects the motoneurons particularly. In order to understand the particular vulnerability of motoneurons upon Smn deficiency, *Nrxn2* expression in *in vitro* cultured *Smn$^{-/-}$;SMN2* mouse motoneurons was studied. For this purpose, motoneurons were isolated at embryonic day 13.5 (E13.5) and cultured for 7 days *in vitro*. Quantitative real time PCR was performed using cDNA isolated from the cultured motoneurons, for *Nrxn2* specific primers. No change in the expression of *Nrxn2α* (Fig. 20B; *Nrxn2α*; $104.0 \pm 8.8\%$; t = 0.453, df = 3, $P = 0.6811$) in SMA motoneurons was observed. Next, the expression of shorter *Nrxn2* isoform; *Nrxn2β* in SMA motoneurons was analyzed and its expression also remained unchanged (Fig. 20B; *Nrxn2β*: $98.7 \pm 5.4\%$; t = 0.229, df = 3, $P = 0.8330$; n = 4 independent experiments, one sample t-test) when compared with control mice (*Smn$^{+/+}$;SMN2*; control: 100%).
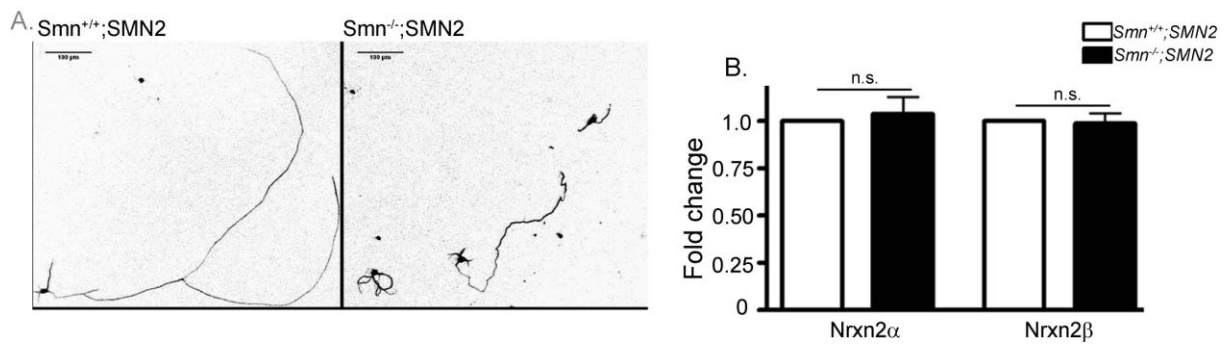
Figure 20: Nrxn2 expression in *in vitro* cultured SMA mouse motoneurons

(A) Motoneurons isolated from wild-type and *Smn⁻/⁻;SMN2* mice at embryonic day 13.5 cultured 7 days *in vitro,* show reduced axon growth in *Smn⁻/⁻;SMN2* motoneurons. (B) Bar graph showing no change in *Nrxn2α* and *Nrxn2β* expression as quantified by quantitative real time RT-PCR of cDNA from E13.5 motoneurons isolated from wild-type and *Smn⁻/⁻;SMN2* mice, cultured 7 days *in vitro.*

3.2.2   *Nrxn2* expression in embryonic day 14 and 18 SMA mouse spinal cord

SMA is mainly considered to be a disease primarily affecting motoneurons but neurons other than motoneuron might also contribute to the disease phenotype. Damage in multiple neuronal and non-neuronal supporting cells could converge into disease initiation and progression, leading to neuronal defects. Recent studies on ALS mouse models showed that other spinal cord cells such as astrocytes could also contribute to the disease, suggesting that interactions between motoneurons and other partner cells may be important contributing factor to a motoneuron disease (Ilieva, Polymenidou et al. 2009, Imlach, Beck et al. 2012).

Studies on mice have shown that motoneuron specific genetic reduction of Smn is not lethal (Park, Maeno-Hikichi et al. 2010) but causes aberration in structure and electrophysiology of the neuromuscular junction. Also, restoration of Smn in motoneurons of SMA mice is not sufficient to rescue the mutant lethality (Gogliotti, Quinlan et al. 2012, Martinez, Kong et al. 2012). In fact, Drosophila *Smn* mutants continued to show the disease phenotype of reduced muscle growth, defects in motor output rhythm, neuromuscular and transmission even after transgenic restoration of Smn protein in muscle or motoneurons but the phenotype was rescued when Smn was restored in both proprioceptive neurons and cholinergic interneurons (Imlach, Beck et al. 2012). These findings showed that Smn deficiency causes sensory-motor network dysfunction and as a result of this motoneurons are affected. An alternative explanation could be that Drosophila has only one *Smn* gene and any type of cell will die when it is completely devoid of Smn protein.
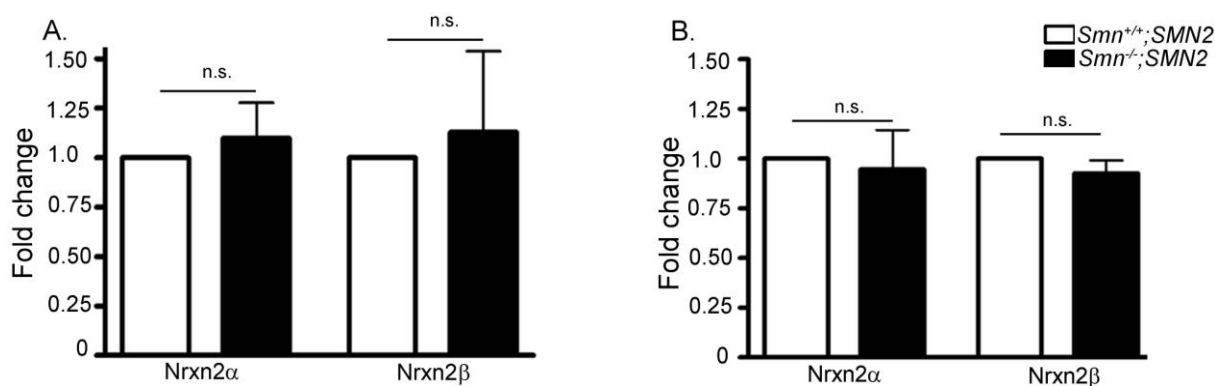
Figure 21: *Nrxn2* expression in spinal cord of embryonic SMA mouse

Bar graph showing no change in expression of *Nrxn2* in lumbar spinal cord of embryonic day (A) 14 and (B) 18 SMA mice, as compared to wild-type mice.

Considering that neurexin expression in Smn deficient mice might be influenced by factors from contacting cells, i.e. sensory neurons, neurons that project to spinal MNs or make contacts with muscle the expression of Nrxn2 in the spinal cord of SMA mice was studied. *Nrxn2* expression was analyzed in cDNA isolated from lumbar spinal cord of E14 and E18 SMA mice using qRT-PCR. No alteration in *Nrxn2α* or *Nrxn2β* expression in the early embryonic stage E14 SMA mice spinal cord (Fig. 21A; *Nrxn2α*: 109.9 + 17.8%; t = 0.556, df = 2, *P* = 0.6338 and *Nrxn2β*: 112.9% + 40.8%; t = 0.3157, df = 2, *P* = 0.7821; n = 3) and also at the late embryonic stage E18 (Fig.21B; *Nrxn2α*: 94.6+19.7%; t = 0.270, df = 2, *P* = 0.8125; *Nrxn2β:* 92.6+6.5%; t = 1.123, df = 2, *P* = 0.3780; n = 3) spinal cord from SMA mice as compared to the wild-type mice was observed. *Gapdh, Hmbs* and *Hprt1* were used as housekeeping genes.

3.2.3 Expression of *Nrxn1, Nrxn2* and *Nrxn3* in 2 days old SMA mice

In *Smn*^{-/-};*SMN2* mice, the number of motoneurons at the time of birth and even a day after birth are normal. Loss of motoneurons begins at postnatal day 3 when the disease phenotype starts to appear. Despite the fact these mice are severely sick at birth, and many of them die immediately after birth, postnatal day 2 is considered to be the presymptomatic stage of *Smn*^{-/-};*SMN2* mice where motoneurons do not die but salient degenerative changes might occur which later can lead to their death. Therefore, *Nrxn* expression in the lumbar spinal cord of postnatal day 2 SMA mice was studied using qRT-PCR. A significant reduction in *Nrxn2α* expression (Fig. 22; *Nrxn2α*: 72.7 + 3.7%; t = 7.170, df = 2, *P* = 0.0189) was observed in SMA mice as compared to the age-matched wild-type mice at postnatal day 2. *Nrxn2β*

expression remained unchanged (*Nrxn2β*: 97.8 + 14%; t = 0.150, df = 2, *P* = 0.8939; n = 3). *Gapdh, Hmbs* and *Hprt1* were used as housekeeping genes.
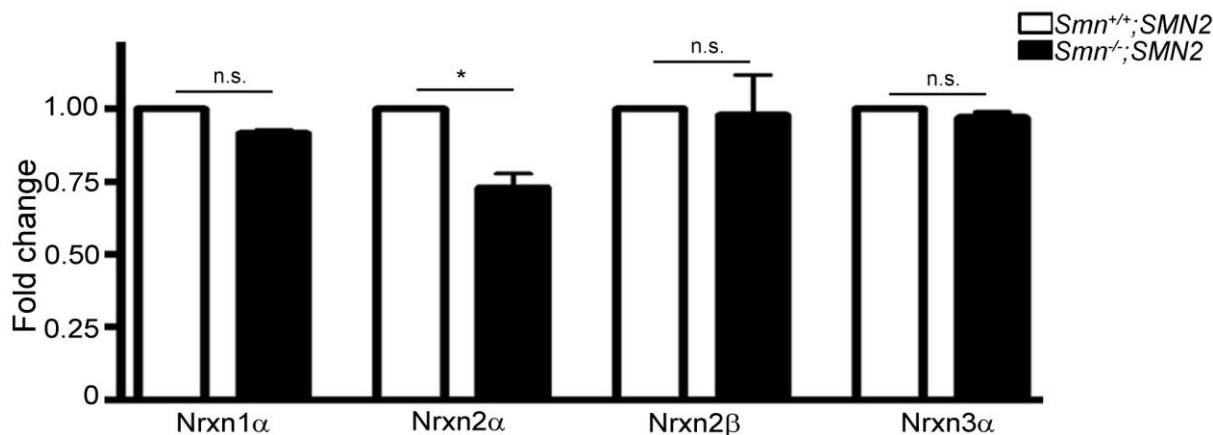
Figure 22: *Nrxn1, Nrxn2* and *Nrxn3* expression in 2 days old SMA mouse

Bar graph depicting changes in the expression of *Nrxn1α, Nrxn2α, Nrxn2β* and *Nrxn3α*, in 2 days old SMA mice lumbar spinal cords.

Because of the potential for redundancy in structure and function of *Nrxn1, Nrxn2 and Nrxn3* (Missler, Fernandez-Chacon et al. 1998), the expression of *Nrxn1α* and *3α* was studied in Smn deficient mice. Spinal cords from 2 days old SMA mice showed no alteration in *Nrxn1α* expression (Fig. 22; *Nrxn1α*: 91.4 + 2.1%; t = 3.999, df = 2, *P* = 0.0572; n = 3) or *Nrxn3α* expression (*Nrxn3α*: 96.8 + 0.5%; t = 5.301, df = 2, *P* = 0.0338; n = 3) by qRT-PCR, indicating that the effect is *Nrxn2* specific. This finding was in line with the findings of (Missler, Zhang et al. 2003) who showed that different combinations of *α-Nrxn* knockout mice exhibited different effects on survival and that the functions of α-neurexin overlap only partly.

3.2.4   Nrxn2 expression in 2 days old SMA mouse motoneurons

Both in human SMA and mouse SMA models, the disease turn to be motoneuron specific only after motoneurons have started to make contacts with the skeletal muscle. Number of motoneurons is normal at birth but decreases at the postnatal days 3 to 5, when differentiation of motor endplates takes place (Monani, Sendtner et al. 2000, Jablonka, Beck et al. 2007). *In vitro* cultured motoneurons start to show defects in axon elongation and excitability only after 4 days of culture, which corresponds to the *in vivo* developmental stage when axon elongation has reached its maximum and pre-synaptic terminals have started to differentiate into motor endplates. Hence, SMA phenotype is motoneuron specific but is dependent on both the contacting neurons and developmental stage.
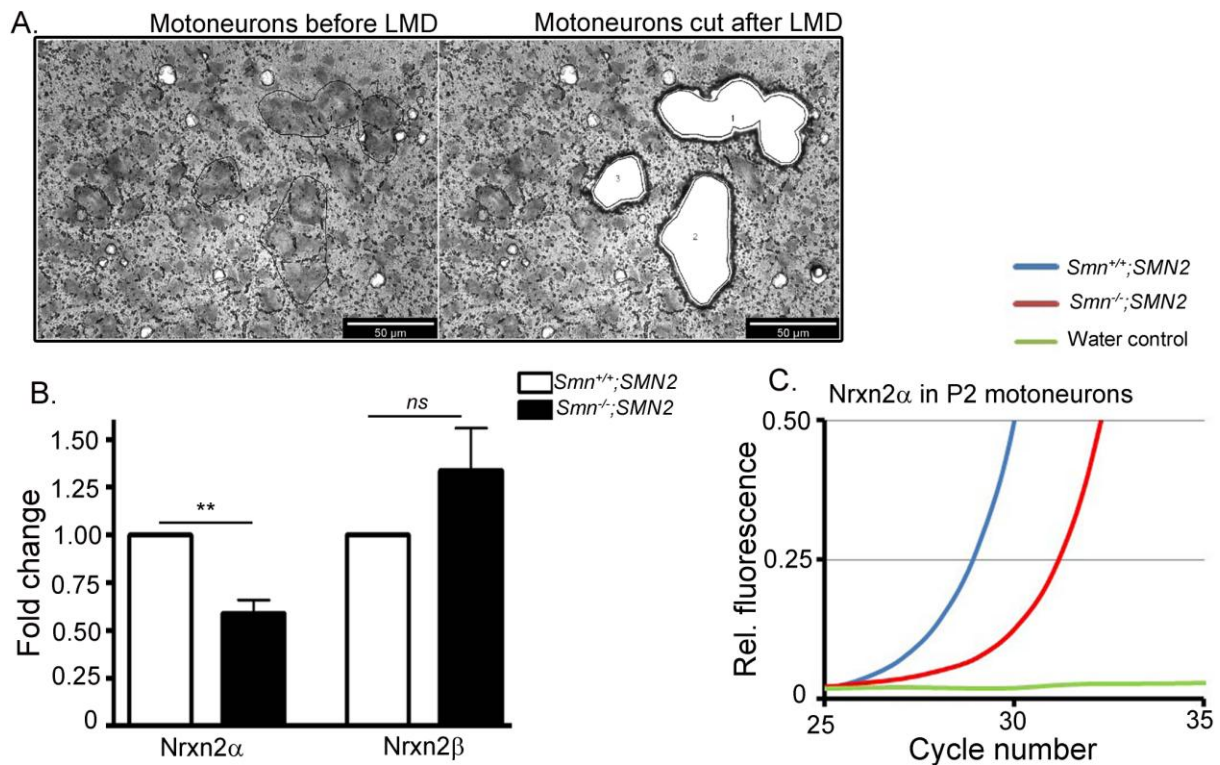
Figure 23: *Nrxn2* expression in motoneurons of 2 days old SMA mouse

(A) Cryosections of P2 lumbar spinal cord stained with cresyl violet, showing motoneurons before laser microdissection (encircled by red line) and spinal cord section after microdissection of motoneurons (B) Bar graph showing fold change in Nrxn2 expression in laser microdissected motoneurons from postnatal day 2 mice, by quantitative real time RT-PCR (C) Curve showing change in relative fluorescence with the cycle number in during qRT-PCR using cDNA from wild -type and Smn motoneurons.

Therefore, 2 days old motoneurons were studied, in vivo. For this purpose, motoneurons were dissected out from 2 days old mice by using laser capture microdissection technique. Although this corresponds to a stage of isolated E14 MNs cultured for 7 days in vitro, this technique allows motoneurons to be isolated at a similar stage in vivo under conditions when they have contact with their natural environment. The microdissected motoneurons showed a 40% reduction in *Nrxn2α* expression (Fig. 23A-C; *Nrxn2α:* 51.6 + 1.5%; $t = 31.86$, df = 2, $P = 0.0010$; n = 3) as compared to the corresponding wild-type motoneurons. Expression of *Nrxn2β* was not altered (*Nrxn2β*: 164.1 + 37.8%; $t = 1.696$, df = 2, $P = 0.2320$; n = 3). These data indicate that *Nrxn2* expression is altered in *Smn* deficient mice similar as in *Smn* deficient zebrafish but with species specific differences.

3.2.5 *Nrxn2α* splicing defects at SS3 in 2 days old SMA mice

All three neurexin transcripts, *Nrxn1, Nrxn2* and *Nrxn3*, show extensive alternative splicing (Ushkaryov, Petrenko et al. 1992) at 5 alternative splice sites. Splicing at these sites could potentially generate thousands of neurexin isoforms each exhibiting different functions and synaptic coupling properties (Ullrich, Ushkaryov et al. 1995). When cultured mouse cortical neurons are depolarized, splicing of *Nrxn2α* is altered at splice site 1 and 3; exclusion of exon11 at splice site 3 is calcium dependent (Rozic-Kotliroff and Zisapel 2007). These findings suggested that splicing of *Nrxn2α* could be affected by neuronal activity. Therefore, the alteration in splicing patterns of neurexin2α in the SMA mouse was analyzed.
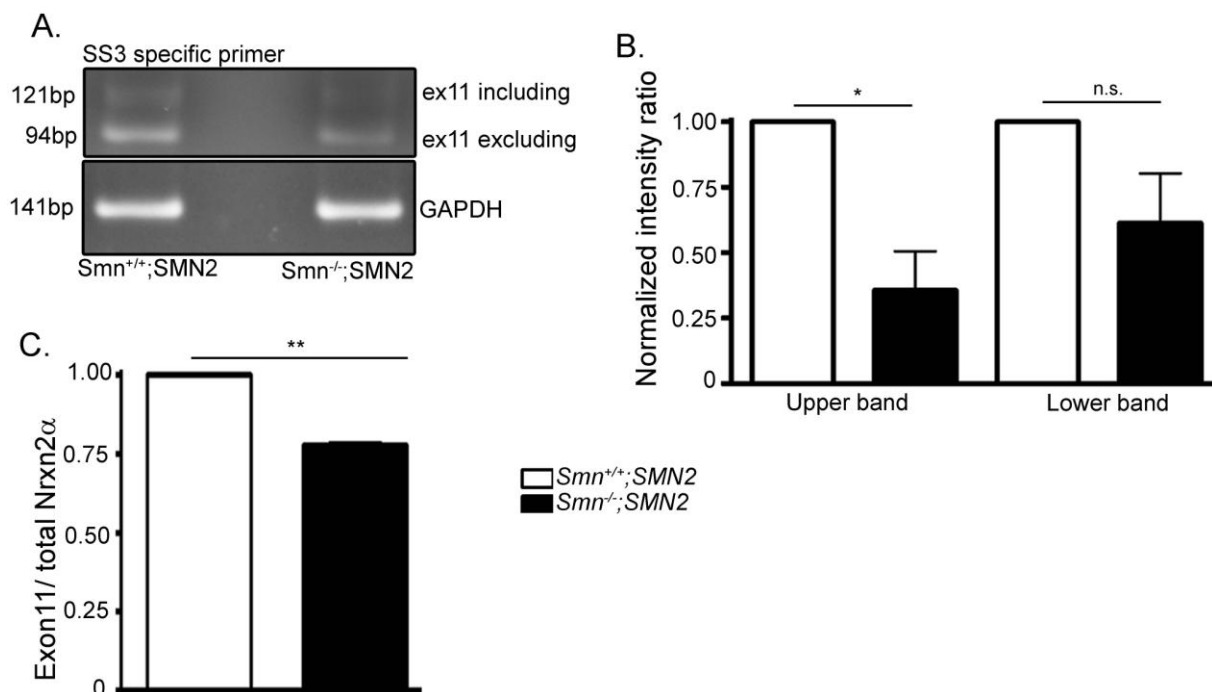
Figure 24: Splicing defects at SS3 of *Nrxn2α* of 2 days old SMA mice

Analysis of exon11 skipping at SS3 in Nrxn2α transcripts: (A-B) Alternative splicing assay using RT-PCR from postnatal day 2 spinal cord cDNA shows increased reduction of PCR products that include exon 11 (upper band) as compared to reduction in transcripts that exclude exon11 (lower band) in *Smn-/-;SMN2* mouse as compared to the wild-type controls. *Gapdh* was used as normalization control. Data shown represents mean ± S.E.M., n = at least 3 independent experiments in each case. (C) Quantitative RT-PCR shows increased skipping of exon 11 of *Nrxn2α* transcripts in $Smn^{-/-};SMN2$ (n = 2) postnatal day 2 spinal cord.

To characterize the alternative splicing patterns, primers were designed to bind exon 10 and exon 13 at the splice site 3 of mouse *Nrxn2α*. The four possible splice products included exons 10, 11, 12, 13 (121 bp), exons 10, 11, 13 (112 bp), exons 10, 12, 13 (94 bp) and exons 10, 13 (85 bp). PCR products were run on a 3% TAE agarose gel for better resolution. Band

intensity of each splice product was quantified using gel densitometry analysis with ImageJ. Using the technique of semi-quantitative RT–PCR, cDNAs from spinal cord of 2 days old SMA mice were analyzed for splicing alterations. A reduction in both exon11- including and exon11- excluding PCR products was observed. Levels of exon11- including transcripts were reduced to a larger extent than those of exon11- excluding transcripts (Fig. 24A-B; *Nrxn2α* exon11-including transcript: 35.7 + 14.8%; t = 4.327, df = 3, *P* = 0.0228; *Nrxn2α* exon11-excluding transcript: 61.6+18.7%; t = 2.044, df = 3, *P* = 0.1336; n = 4).

In order to confirm the splicing defects at SS3, qRT–PCR with primers to detect *Nrxn2α* exon11 levels relative to total *Nrxn2α* transcripts was utilized. Primers for exon 11 were designed over the exon11 and the exon1 primers were used for total neurexin expression levels. A significant reduction in exon11 containing transcripts was observed relative to total *Nrxn2α* in postnatal day 2 *Smn*$^{-/-}$;SMN2 mouse spinal cord (Fig. 24C; 77.76+0.8%; t = 27.68, df = 1, *P* = 0.0230; n = 2). These data show altered splicing of *Nrxn2α* in 2 days old SMA mice.

4 Discussion

In this study, I observed that number of intermediate filaments is increased in *pmn* mutant motoneurons both in embryonic and adult mouse. Deletion of *Nefl* from *pmn* mice rescues the axon elongation defects of *in vitro* cultured *pmn* motoneurons and rescues the defective microtubule regrowth of *in vitro* motoneurons after nocodazole treatment. Neurofilament depletion also improves disease severity in *pmn* mutant mice and prolongs their life-span. The rescue effect was observed both in *Nefl+/-;pmn* mice in which elevated NF expression was brought back to control levels and in *Nefl-/-;pmn* motoneurons in which axonal neurofilament was completely lost. In *pmn* mutant motoneurons, NFL depletion resulted in increased number of microtubules and markedly increased the microtubule density due to massive reduction in axonal diameter upon neurofilament depletion. Further, I observed that NFL binds to stathmin complex and depletion of NFL enhances the interaction of Stat3 with stathmin. This results in increased levels of stable pool of acetylated microtubules suggesting that stathmin induces the catastrophe of microtubules in *pmn* mice which is prevented by Stat3 interaction upon *Nefl* deletion. This analysis of *pmn* mutant mice provides an insight into the mechanism involved in neurodegeneration which could be relevant for understanding the pathogenesis of diverse neurodegenerative diseases that involve the aggregation of intermediate filaments.

4.1.1 Increased intermediate filaments in *pmn* mutant motoneurons

Accumulation of intermediate filaments has been observed in a variety of neurodegenerative diseases and in corresponding mouse models (Julien and Mushynski 1998, Liu, Xie et al. 2011, Lu, Petzold et al. 2012). Thus neurofilament pathology represents a point where pathomechanisms of distinct neurodegenerative disorders converge (Lepinoux-Chambaud and Eyer 2013). Here in this study I observed a drastic increase in levels of intermediate filaments in *pmn* mutant motoneurons.

The precise mechanism of neurofilament accumulation is not fully understood so far. It could be a result of increased IF protein synthesis, defective post-translational modifications or could be due to defective degradation of IF proteins. The possibility of increased protein synthesis could at least be ruled out in degenerating neurons of ALS and Alzheimer disease which showed downregulation of *NEFL* mRNA (McLachlan, Lukiw et al. 1988, Bergeron, Beric-Maskarel et al. 1994, Wong, He et al. 2000) whereas the transcript levels for NFM or

NFH remained unchanged (Wong, He et al. 2000). Also, the elevation of NFL and peripherin IF proteins in patients with giant axonal neuropathy (GAN) or motoneurons derived from GAN iPSCs did not correlate with increased mRNA expression as mRNA levels remained unchanged (Dequen, Bomont et al. 2008, Johnson-Kerner, Ahmad et al. 2015). This indicates that posttranscriptional mechanisms including deregulated translation or posttranslational mechanisms such as reduced degradation of NFL (Robberecht and Philips 2013) could be responsible for the phenotype. Defective degradation of intermediate filaments could also lead to the accumulation as in the case of giant axonal neuropathy (GAN). This disease is characterized by axonal swellings caused by massive neuronal intermediate filament accumulation and aggregation in neurons and non-neuronal cells. It is caused by mutation in the *GAN* gene that codes for Gigaxonin that has been shown to regulate the degradation of IF proteins via the proteasome (Mahammad, Murthy et al. 2013, Opal and Goldman 2013). The accumulated pool of IF in iPSCs derived motoneurons from GAN patients is lost on Gigaxonin restoration suggesting a role of defective proteasome degradation in IF accumulation (Johnson-Kerner, Ahmad et al. 2015).

The precise mechanism how NFL accumulation participates in the neurodegenerative mechanisms also remained speculative so far. The possibility that increased NF could act as toxic intermediates in the pathogenesis of neurodegenerative diseases was ruled out when NFL or NFH overexpression in *tg(SOD1*693A)* mice delayed the disease and prolonged the survival of mutant mice (Kong and Xu 2000). One suggested possible explanation for this beneficial effect of increased neurofilaments was that these proteins might serve as a sink that absorbs oxidative free radicals and reduce the peroxidation or nitration damage to other organelles (Wiedau-Pazos, Goto et al. 1996, Crow, Ye et al. 1997). *Tg(SOD1*G37R)* mice, a model for a common form of familial human ALS, are characterized by inclusion bodies containing peripherin along with neurofilament proteins in the cell body and axon of degenerating motoneurons (Corbo and Hays 1992, Tu, Raju et al. 1996). Overexpression or deletion of the peripherin gene in these mice had no influence on onset, severity or progression of disease caused by the mutant SOD1 suggesting that intermediate filaments and peripherin are not a key component of motoneuron degeneration in this mouse model (Corbo and Hays 1992). NFs control the radial growth of large myelinated axons (Hoffman, Cleveland et al. 1987), which in turn can affect the conduction velocity and transport of NFs in the axons (Hoffman, Griffin et al. 1985, Yamasaki, Itakura et al. 1991, Eyer and Peterson 1994, Burghes and Beattie 2009).

In this study, I observed that increase in intermediate filaments in *pmn* mutant motoneurons occurs both in embryonic motoneurons and at the late stage of the disease progression. The increase could be a cause or a consequence of neurodegeneration. *Pmn* motoneurons isolated at embryonic day 13.5 when cultured for seven days *in vitro* showed an increase in intermediate filaments suggesting that the IF abnormality starts at an early stage of disease progression. Also, increased IFs were observed at day 34 which represents a late stage in *pmn* mouse pathology. IF accumulation was observed in proximal, intermediate and distal compartments of the *in vitro* cultured motoneurons suggesting that disturbed transport along the axon should not be a reason for the accumulation. Also, distal phrenic nerves of *pmn* mutant mice showed an increase in intermediate filaments at late stages of disease. These findings suggested that abnormal neurofilament accumulation starts at an early stage in *pmn* mice and it continues until last stages of disease, and it affects all the axonal compartments of the mutant neurons. This suggests that IF accumulation should not be only a consequence of the neurodegeneration but could be a major factor contributing to the neurodegeneration and also that the reason for IF accumulation is more complex than disturbed transport or disturbed stoichiometry.

4.1.2   Physiological consequence of NFL depletion in motoneurons

Several other mouse models of neurodegenerative disorders, in addition to *pmn* mice (in this study) have provided enough support for the hypothesis that accumulation of NFL could be an early event in neurodegeneration. This is also supported by the finding that overexpression of *Nefl, Nefm* or *Nefh* transgenes causes NF aggregation and motoneuron dysfunction resembling motoneuron disease in mouse models (Cote, Collard et al. 1993, Xu, Cork et al. 1993, Julien, Couillard-Despres et al. 1998, Gama Sosa, Friedrich et al. 2003). Similarly, depletion of neurofilaments leads to rescue of the disease phenotype for e.g. in mutant *SOD1* mice, *Nefl* deletion delayed the onset of disease and slowed the disease progression (Williamson, Bruijn et al. 1998) and in *tau* transgenic mouse it reduces the abnormal tau accumulation and motoneuron degeneration (Ishihara, Higuchi et al. 2001). In line with these findings, I observed that deletion of only one *Nefl* allele in *pmn* mutant mouse normalized NFL and NFH protein levels in sciatic nerves. It also increased the life span of *pmn* mutant mice and increased their motor performance, thus providing evidence that elevation of endogenous neurofilament levels contributes to axon destabilization and loss of motor function. Despite the drastic reduction of IFs and the resultant reduction in axon diameter in peripheral nerves,

Nefl-/-;pmn mice survived longer than *Nefl+/-;pmn* or *pmn* mutant mice. Thus, loss of IFs delays axon destabilization.

Interaction of NFL with NFM or NFH is essential for the assembly of neurofilaments (Ching and Liem 1993, Lee, Xu et al. 1993). In line with this hypothesis, I observed highly reduced levels of 10 nm IFs in phrenic nerves of NFL deficient mice. These findings further confirm that *Nefl* deletion causes depletion of functional IF from axons. The deletion of one or both the alleles of *Nefl* prolonged the life span of the mice. *Nefl-/-;pmn* mutant mice survived longer than *Nefl+/-;pmn* and *pmn* mutant mice. The increase in the survival could be attributed to lower levels of NF aggregates in motor axons of *pmn* mutant mice throughout development which could delay the neurodegeneration. Alternatively, the reduced levels of neurofilament could affect other components of the cytoskeleton, in particular microtubules. NFH are also necessary for cross-bridging the NF fibers and probably for the interaction with other cytoskeletal elements like microtubules and microfilaments (Elder, Friedrich et al. 1998, Elder, Friedrich et al. 1999, Jacomy, Zhu et al. 1999). Therefore, reduced levels of IFs could affect other components of the cytoskeleton, in particular microtubules.

4.1.3 NFL removal improves the microtubule dynamics of the neurons

In *pmn* mutant mice the underlying gene defect leads to a massive reduction of αβ- tubulin heterodimers, the basic components of microtubules. This makes the microtubules unstable (Martin, Jaubert et al. 2002). In cultured *pmn* motoneurons, this leads to defective axon elongation (Schaefer, Schmalbruch et al. 2007, Selvaraj, Frank et al. 2012), and levels of tyrosinated microtubules are increased in the axons of these motoneurons. Intermediate filaments are anatomically and functionally linked with microtubules. Neurofilament interacts with tubulin (Minami, Murofushi et al. 1982) and stimulates microtubule polymerization in mature neurons (Bocquet, Berges et al. 2009). Any disturbance of NF protein levels does not only affect assembly of NF fibers, it also influences microtubules and the actin cytoskeleton (Elder, Friedrich et al. 1998, Elder, Friedrich et al. 1999, Jacomy, Zhu et al. 1999). NFM and NFH make cross bridges between adjacent NFs and microtubules. Thus, also removal of NFM and NFH sidearms delays the disease in *SOD1* mutant mice (Lobsiger, Garcia et al. 2005) in a similar manner as deletion of the *Nefl* gene in this mouse model (Williamson, Bruijn et al. 1998). Disease onset is also delayed in the same mouse model after treatment with microtubule stabilizing agents (Fanara, Banerjee et al. 2007). However, it has not been shown so far whether stabilization of microtubules contributes to the beneficial effects of NFL depletion or removal of NFM and NFH sidearms in mutant *SOD1* mice. The observation

that levels of acetylated tubulin increase in axons of *Nefl* deficient motoneurons points to this possibility, and indicates that the beneficial effects of normalizing IF levels, or by massive reduction of functional IFs could be due to stabilization of microtubules.

NFs have been shown to interact with tubulin (Minami, Murofushi et al. 1982). They can affect microtubule polymerization in mature neurons by binding unpolymerized tubulin (Bocquet, Berges et al. 2009), an interaction mediated by proteins such as microtubule associated proteins (Hisanaga and Hirokawa 1990). In transgenic mice in which transport of NFs from cell bodies to axons was prevented, microtubules assembled in a very high number but the total amount of tubulin was unaffected (Bocquet, Berges et al. 2009). This suggested that presence of NFs controls the rate of MT polymerization in axons by reducing the polymerization of soluble tubulins or it increases the catastrophe of polymerized microtubules.

In our study, distal phrenic nerve of *pmn* mutant mice showed drastic reduction in number of microtubules. *In vitro* cultured *pmn* mutant motoneurons showed a reduction in MT regrowth after nocodazole treatment. Depletion of NFL in *pmn* mutant mouse led to an increase in the number of microtubules and also rescued the defect in MT regrowth after nocodazole treatment. Also, the total and average length of microtubules that were decreased in *pmn* mutant motoneurons was rescued upon NFL depletion, indicating an effect of NFL on microtubule dynamics in these neurons. This led to the conclusion that either NFL depletion increases the number of MTs that grow after disintegration of the complete MT network in the motoneurons, or individual MTs elongate faster because catastrophe events are reduced. The second hypothesis is more plausible when catastrophe-induced endogenous MT deregulators such as stathmin proteins are functionally blocked.

4.1.4 Microtubule dynamics is related to NFL via Stat3-stathmin pathway

Stathmin plays a central role in the regulation of microtubule stability (Chauvin and Sobel 2015). It acts in two distinct ways on microtubule dynamics. First, in *in vitro* condition, it destabilizes existing microtubules by inducing microtubule catastrophes in a dose-dependent fashion (Belmont, Mitchison et al. 1996, Marklund, Larsson et al. 1996, Horwitz, Shen et al. 1997). Second, it binds αβ-tubulin heterodimers and sequesters them in a way that microtubule polymerization is inhibited (Jourdain, Curmi et al. 1997). Stat3 modulates the MT network by binding to stathmin that inactivates its MT-destabilizing activity (Ng, Lin et al. 2006). *In vitro*, a change in pH of the buffer can lead to a shift in role of stathmin from

sequestration of tubulin affecting microtubule elongation to increase microtubule catastrophes thus disintegrating the existing microtubules (Howell, Deacon et al. 1999). N-terminal of stathmin is required for the catastrophic role whereas the C-terminal is essential for the inhibition of MT-polymerization (Lawler 1998, Holmfeldt, Larsson et al. 2001). These effects of microtubule dynamics regulation apparently are involved in plasticity processes when neurons change their shape and new neuronal connections are made, for example during learning and memory processes. Mice that lack stathmin show severe defects in fear memory formation in the amygdala (Shumyatsky, Malleret et al. 2005, Uchida, Martel et al. 2014) and this process correlates with high levels of stathmin expression found in this brain region. Surprisingly, the hippocampus, an another region with high neuronal plasticity, has only low levels of stathmin expression, and hippocampus related forms of learning such as spatial learning in the water maze are not affected in stathmin deficient mice. Motoneurons also express high levels of stathmin, as shown in our own results and a previous study (Selvaraj, Frank et al. 2012). Thus, stathmin could play a role in axonal plasticity under physiological and pathophysiological conditions when axons grow or enhanced axonal sprouting occurs. However, enhanced stathmin activity could also contribute to axonal destabilization and degradation in motoneuron diseases. Proof for this possibility has been given by the observation that the expression of stathmin is enhanced in models of spinal muscular atrophy, and that microtubule disintegration in *Smn* deficient neuronal cells which correlates with enhanced stathmin expression can be reduced when stathmin is inactivated (Wen, Lin et al. 2010).

In *pmn* mutant mice, CNTF treatment reduces motor axon loss and degeneration (Sendtner, Schmalbruch et al. 1992) and this beneficial effect of CNTF is attributed to its local activating effect on Stat3 that modifies the axonal cytoskeleton (Selvaraj, Frank et al. 2012). CNTF activates Stat3 at tyrosine 705 and the activated Stat3, instead of moving to the nucleus remains mostly in the axonal cytoplasm. Here it interacts with stathmin and regulates MT dynamics by antagonizing its depolymerization activity (Ng, Lin et al. 2006). This effect appears to be mediated via a local and also transcription independent mechanism (Selvaraj, Frank et al. 2012). But the effect of NFL depletion on Stat3-stathmin interaction is more likely to affect the catastrophic activity of stathmin and not the release of tubulin heterodimers as observed by increased acetylation of the microtubules in cultured motoneurons by SIM images.

Not much is known about how stathmin function is regulated, but its spatial distribution within cells seems to play a role (Selvaraj and Sendtner 2013). Several members of the

stathmin family are associated with membranous structures via GPI anchors which restrict their subcellular distribution (Chauvin and Sobel 2015). Stathmin does not have such a GPI anchor, but this protein is not evenly distributed in the cytoplasm. SIM images showed that that stathmin is mostly localized with microtubules in axons of wild-type motoneurons. High resolution structured illumination microscopy (SIM) allowing resolution of structures down to nearly 100 nm reveals close interaction of stathmin with tyrosinated microtubules in the axons of wild-type motoneurons. This colocalization seems to be changed in *Nefl-/-* motoneurons, and stathmin colocalization with Stat3 and microtubules also increases. I further confirmed this increased interaction of stathmin with Stat3 by biochemical immunoprecipitation assays. This assay showed that NFL is also a part of stathmin-Stat3 complex, indicating that IFs play a role in the formation of complexes between Stat3 and stathmin, which is important for microtubule dynamics in the cell. This could explain how IF depletion modulates microtubule stability.

4.1.5   Tubulin dynamics and interaction of stathmin-Stat3 in *Nefl-/-* motoneurons

In cells, free tubulin heterodimers and MT polymers exist in rapid dynamic equilibrium (Fanara, Turner et al. 2004). Post-translational modifications of tubulins reflect specific functional properties, for e.g. tyrosinated tubulins represent highly dynamic MTs, whereas acetylated tubulins represent stable, long-lived microtubule. These modifications of tubulins are found to be affected in neurodegenerative diseases. Acetylated α-tubulin, is strongly reduced in the NFT-bearing neurons in Alzheimer's disease, even at an early stage of phospho-tau bearing neurons, suggesting that reduction in microtubule stability could be an early event in these cells (Hempen and Brion 1996). Tubulin acetylation is also reduced in patients with Huntington's disease, which then can reduce the trafficking of BDNF vesicles (Dompierre, Godin et al. 2007). Tubulin tyrosine ligase (TTL) is the enzyme that adds a C-terminal tyrosine to α-tubulin and rapidly tyrosinates the detyrosinated tubulins that are released from depolymerizing MTs (Wloga and Gaertig 2010, Janke and Bulinski 2011). Stathmin and TTL compete for binding on tubulin dimers. A recent study showed that Stathmin inhibits tubulin tyrosination activity of TTL (Szyk, Piszczek et al. 2013).

Previous findings in our lab showed that CNTF application to *pmn* motoneurons reduces the levels of tyrosinated tubulin, whereas the levels of acetylated tubulins remain unchanged (Selvaraj, Frank et al. 2012). These findings suggested that CNTF influences the dynamics of MTs and stabilizes them by deactivating the MT-destabilizing activity of stathmin. Upon NFL depletion the levels of stable acetylated tubulins increased whereas the levels of tyrosinated

tubulins remained unchanged. Therefore, in wild-type motoneurons, NFL depletion had a much more pronounced effect on the stability of existing microtubules that are acetylated at relatively high levels when compared to microtubule regrowth after nocodazole treatment. In *pmn* mutant motoneurons in which the availability of αβ- tubulin heterodimers is reduced, NFL depletion also restored defective microtubule regrowth after nocodazole treatment. This differential effect of NFL depletion could be explained by the reduced availability of αβ- tubulin heterodimers in *pmn* mutant motoneurons, which increases upon release of αβ- tubulin heterodimers when stathmin is inactivated by enhanced interaction with Stat3 (Selvaraj, Frank et al. 2012). Thus, the increased interaction of Stat3 and stathmin in NFL depleted motoneurons enhances the capacity for microtubule regrowth and microtubule plasticity in motoneurons from *pmn* mutant mice. This also indicates that enhanced neurofilament levels in neurodegenerative diseases reduce the capacity for microtubule regrowth and microtubule plasticity. Our data provide evidence that the destabilizing activity of stathmin is enhanced when neurofilaments are increased in neurodegenerative disorders, and this could make a major contribution to axonal degeneration.

When this idea is followed up towards therapeutic implications, this would mean that catastrophe-inducing endogenous MT deregulators such as stathmin proteins should be functionally blocked in order to stabilize microtubules and to enhance stability of axons. In neurons, altered MT-based transport and aggregation of proteins is often associated with neurodegenerative disorders (Pigino, Morfini et al. 2003, Stokin, Lillo et al. 2005). Despite the fact that axons exhibit smaller diameter, the improvement in MT network in *Nefl-/-;pmn* motoneurons apparently stabilizes the axon and possibly also improves the transport of cargoes, leading to prolonged survival and delay of the decline of motor function. In summary, our findings suggest that NF accumulation contributes to axonal destabilization in the *pmn* mouse model of motoneuron disease and possibly also other forms of neurodegenerative disorders. NFL depletion stabilizes the MT structure and leads to enhanced axon growth in *pmn* mutant motoneurons via increased Stat3-stathmin interaction. Thus, targeting the NFL accumulation in neurodegenerative diseases could be a target for therapy in neurodegenerative disorders.

4.1.6 Effect of local axonal signaling and RNA transport on axon maintenance

Though the mechanisms behind the pathology of *pmn* mutant and *SMA* mice are completely distinct but both mouse models for different forms of motoneuron disease are characterized by destabilization of axon terminals and eventually axon degeneration. In neurodegenerative

diseases, the neuronal cytoskeleton along with local axonal signaling plays an important role in axonal maintenance. Local axonal regulation is not only achieved by local Stat3-stathmin signaling. Also RNA transport and local protein synthesis play important roles. Local protein synthesis has started to emerge as an important factor that could link the pathology of distinct neurodegenerative disorders such as *Smn* and *pmn* pathology.

Local translation provides the cell a spatial and temporal control of the protein composition at the site of translation in different compartments of a cell. Axons contain local protein synthesis capacity and possess the machinery for translation including ribosomes and RNAs (Koenig and Martin 1996, Bassell, Zhang et al. 1998). The translational machinery and mRNA could also be transported to the axons where translation is then regulated by local stimuli. After injury some of the locally synthesized proteins are transported back to the cell body to provide information of events occurring in distal axons, such as injury (Perry and Fainzilber 2009) and to start regeneration responses in the cell body. The local translation of mRNAs also could help in constructing the post-synaptic structure by modulating the local cytoskeleton. For example, ß- actin mRNA that encodes for a cytoskeleton protein forming microfilaments has been observed in dendrites in response to neurotrophic factors and also in axonal growth cones of *in vitro* cultured neurons (Yoon, Zivraj et al. 2009). It regulates actin morphology during neuronal development and growth cone movement upon NT3 stimulation (Zhang, Singer et al. 1999, Zhang, Eom et al. 2001).

The *Nefl* mRNA levels are reduced in degenerating spinal motoneurons of ALS models (Bergeron, Beric-Maskarel et al. 1994, Wong, He et al. 2000, Menzies, Grierson et al. 2002). However, the stability of *hNEFL* mRNA is enhanced when exposed to spinal cord protein homogenates from ALS patients (Strong, Leystra-Lantz et al. 2004). This suggested that motoneuron specific determinants of *hNEFL* mRNA stability exist (Ge, Leystra-Lantz et al. 2003) and it has been identified to be the ubiquitously expressed DNA/RNA binding protein human TAR DNA-binding protein (TDP43) (Buratti and Baralle 2001) that prevents the degradation of hNFL mRNA.

In cytoplasm, TDP43 forms mRNP granules that can be bidirectionally transported along the microtubules, and this helps in transporting the mRNA to target compartment of the neurons (Alami, Smith et al. 2014). A TDP43 mutation that causes ALS impairs its mRNA transport activity and it could affect the translocation of mRNAs binding to it. TDP43 is mostly nuclear in motoneurons but in ALS motoneurons it is mostly cytosolic and is incorporated into the ubiquitinated aggregates (Arai, Hasegawa et al. 2006, Neumann, Sampathu et al. 2006). It

interacts directly with 3'UTR of hNFL mRNA and could contribute to the formation of NF aggregates in ALS through alterations in NF stoichiometry (Strong, Volkening et al. 2007). Nerve injury can also activate transcription of genes required for regeneration and survival of the axons through retrograde signaling (Michaelevski, Segal-Ruder et al. 2010) by local synthesis of transcription factors such as Stat3 at the injury site (Ben-Yaakov, Dagan et al. 2012). Locally synthesized Stat3 is activated upon injury and is retrogradely transported to the nucleus providing a direct link between axon and nucleus upon injury. Activated Stat3 is highly increased in *pmn* mutant motoneurons.

RNA binding proteins and proteins involved in formation of RNA binding complexes such as Smn, Gemin2 and hnRNPR are also observed in the axonally localized beta actin mRNA transport granules (Rossoll, Kroning et al. 2002, Carrel, McWhorter et al. 2006). hnRNPR interacts directly with the 3'-UTR of beta-actin mRNA in a complex with Smn and is probably required for axonal growth of motoneurons (Glinka, Herrmann et al. 2010). Translocation of mRNAs or the translational machinery to the axonal compartment could make them susceptible to degeneration. Translocation of mRNAs decreases in the axons of spinal muscular atrophy mouse motoneurons (Glinka, Herrmann et al. 2010) and dendrites of Alzheimer's disease models (Meyer-Luehmann, Mielke et al. 2009). Smn protein is involved in assembling snRNP complexes (Eggert, Chari et al. 2006, Burghes and Beattie 2009) by a direct or indirect interaction as with beta actin mRNA through hnRNPR (Mourelatos, Abel et al. 2001, Rossoll, Jablonka et al. 2003). Smn also plays a major role in modulating the axonal transport of mRNAs such as beta actin and perhaps it could affect the translocation of NF mRNA via TDP43 or hnPNPR.

4.1.7 Presynaptic membrane protein, neurexin, a new candidate in SMA

Smn is an ubiquitously expressed protein, but its general depletion leads to a motoneuron specific disease. Two main hypotheses have been proposed for the motoneuron specific effect of Smn depletion. The first hypothesis proposes that Smn depletion could affect a MN-specific role in subcellular mRNA transport and regulation of axonal translation in neurons (Jablonka, Bandilla et al. 2001, Rossoll, Jablonka et al. 2003). A second hypotheses proposes that its role in U snRNP assembly is essentially affected, thus leading to functional deficits due to altered pre-mRNA splicing of MN-specific genes (Fischer, Liu et al. 1997, Pellizzoni, Kataoka et al. 1998, Pellizzoni, Yong et al. 2002, Chari, Golas et al. 2008). In the present study I observed that both the expression and splicing of *nrxn2α*, a presynaptic protein, is disturbed in SMA mice. Since the changes in neurexin expression were observed only at the

late stages of the disease, this study establishes *Nrxn2α* as a new downstream target of Smn and provided evidence for particular vulnerability of motoneurons as observed by increased effect on motoneurons.

Our collaborators (See, Yadav et al. 2014) had found that both the longer and shorter isoform of *nrxn2a* is strongly down-regulated in Smn morphant zebrafish, with isoform specific differences in the expression pattern of *nrxn2aa* and *nrxn2ab*. In order to support this finding in a mammalian model of SMA, I investigated the *Smn$^{-/-}$;SMN2* mice and found a strong down-regulation of *Nrxn2α* in such motoneurons.

Neurexins are a family of highly polymorphic cell membrane proteins which are specifically found in the nervous system (Ushkaryov, Petrenko et al. 1992). Mammals have three genes for neurexins, each with two promoters; proteins encoded by the longer mRNAs are called α-neurexins and those encoded by the shorter mRNAs are called β-neurexins (Ullrich, Ushkaryov et al. 1995). α-neurexins are alternatively spliced at five canonical positions and β-neurexins at two, providing the basis for the potential to express more than 1000 isoforms for neurexins (Ullrich, Ushkaryov et al. 1995). Neurexins play important roles in mediating cell adhesion at the synapse (Ushkaryov, Petrenko et al. 1992), synapse formation, synapse maturation (Graf, Zhang et al. 2004, Li, Ashley et al. 2007) and in triggering neurotransmitter release at the NMJ synapse (Missler, Zhang et al. 2003, Sons, Busche et al. 2006).

4.1.8 *Nrxn2α* expression and SMA disease progression

Here, I reported that expression and splicing of *Nrxn2α* are unchanged at early embryonic stages in SMA mice, representing pre-symptomatic stages for the disease. This indicates that the altered pre-mRNA splicing is not a general effect that can be attributed to defects in spliceosomal U snRNA assembly, because then these changes in *Nrxn2α* splicing are also expected to occur at such early stages. But later, when the mouse starts to show the initial symptoms of SMA i.e. at postnatal day 2, altered splicing starts to appear suggesting that this observation could be a consequence of the disease process, or at least that there is a correlation between the altered expression and disease severity. Postnatal day 2 is also a stage when neurons are differentiated, have formed functional neuromuscular synapses and have received afferent synaptic inputs from the spinal cord.

No change in expression pattern of *Nrxn2α* was observed in isolated mouse motoneurons that were cultured for 7 days *in vitro*, which is equivalent to the stage of postnatal day 2 motoneurons *in vivo*. Interestingly, the expression of *Nrxn2α* was affected in postnatal day 2

motoneurons dissected from mouse spinal cord, indicating that the alterations only appear in the motoneurons when they are able to form active neuromuscular connections *in vivo*.

4.1.9 Differential neurexin α and β expression changes in SMA

Only *Nrxn2α* expression is reduced in the SMA mouse model whereas the expression of *Nrxn2β* remained unchanged. Notably, there are separate promoters driving transcription of α and β Nrxn isoforms. The possible explanation for the differential change in the expression of two Nrxn2 isoforms could be the differential regulation of the two promoters or aberrant splicing. *Nrxn2α* and *Nrxn2β* are differently distributed in different classes of neurons and possibly have different roles, for e.g. in rat brain the two isoforms have different expression pattern and are expressed independently of each other. *Nrxn2β* isoform exhibited a more uniform expression pattern compared to *Nrxn2α*, which appeared to be highly expressed only in selective cell types (Ullrich, Ushkaryov et al. 1995). Also, in spinal cord of zebrafish, the expression of *nrxn2b* was stronger and more uniform than the expression of *nrxn2a* (See, Yadav et al. 2014).

4.1.10 Alternative splicing of *Nrxn2α* changes in mouse model of SMA

Neurexins undergo extensive alternative splicing forming products that differ in their roles in synaptic coupling. There are 5 splice sites in *Nrxn2α* and 3 in *Nrxn2β* in mouse. Different splice variants of neurexin have different roles in synapse formation and maintenance. External stimuli can also evoke changes in the splicing of *Nrxns*. Alternative splicing of *Nrxn1* in mouse brain is found to be temporally and spatially controlled by neuronal activity via calcium/calmodulin-dependent kinase IV signaling (Iijima, Wu et al. 2011). Depolarization of neurons also modulates splicing of *Nrxn2α* at splice site 1 and 3. Neuronal activity can also influence splicing of *Nrxn2α*; exon 11 at splice site 3 (SS3) of rat is excluded in a calcium-dependent manner, which suggests a role in maintenance of mature neuronal circuits (Rozic-Kotliroff and Zisapel 2007).

I also observed a change in the pattern of alternative splicing of *Nrxn2α* at SS3 in SMA mice similar to that found for its ortholog *Nrxn2α* in rat. I observed an increase in exon 11 skipping at SS3 of *Nrxn2α* in SMA mice; this could be dependent on Ca2+ and could thus be affected by altered neuronal activity. This alteration in *Nrxn2α* splicing was observed only at a late postnatal stage indicating that the changes could be a consequence of the reduction in Ca2+ influx as is observed in SMA mouse models (Ruiz, Casanas et al. 2010). The main function of neurexins at the synapses is to act as a cell recognition molecule (Nguyen and Sudhof 1997).

This function is most likely performed by its interaction with isoform-specific ligands through its extracellular domain, which is also involved in its role in triggering neurotransmitter release at synapses (Ushkaryov, Petrenko et al. 1992, Zhang, Rohlmann et al. 2005). Alternative SS3 in *Nrxn2α* is also affecting this extracellular domain; therefore it is possible that the exon11 skipping at SS3 changes its interaction with synaptic ligands and thus modulates it synaptic coupling properties. Therefore, in *Smn⁻ᐟ⁻;SMN2* mice the alternative splicing of *Nrxn2α* could alter its binding to synaptic ligands and thus influence intracellular Ca2+ levels affecting neuronal activity. Also our collaborators found that the knock-down of *nrxn2a* morphants in zebrafish showed defective Ca2+ influx that does not correlate with axon outgrowth defects. This effect could take place when synapses become functional and need to be strengthened. *Nrxnα* triple knock-out mouse show impaired synaptic vesicle release, reduced evoked transmitter release and reduced quantal content at NMJ synapses similar to the SMA mice (Zhang, Rohlmann et al. 2005, Sons, Busche et al. 2006, Kariya, Park et al. 2008, Kong, Wang et al. 2009). Similar to the SMA mouse, *Nrxn* knockout mice also displayed defects in breathing and showed compromised survival (Missler, Zhang et al. 2003).

In this study, I observed a downregulation and altered splicing at exon 11 of Neurexin in SMA mice. I suggest that defects in splicing of Neurexin and reduced expression lead to defects in calcium channel clustering and synaptic release at the NMJ in SMA that contribute to disease progression. Our findings suggest that *Nrxn2α* could be a molecule downstream of Smn pathology that is involved in the pathophysiology of Spinal Muscular Atropy. Smn deficiency causes downregulation of *Nrxn2α* in SMA mice and also leads to altered splicing, probably in a Ca^{2+}-dependent manner, which might then lead to lack of splice variants essential for synapse strengthening and maintenance thus causing the synaptic defects in SMA.

References

Abe, A., C. Numakura, K. Saito, H. Koide, N. Oka, A. Honma, Y. Kishikawa and K. Hayasaka (2009). "Neurofilament light chain polypeptide gene mutations in Charcot-Marie-Tooth disease: nonsense mutation probably causes a recessive phenotype." J Hum Genet **54**(2): 94-97.

Ahmad, F. J. and P. W. Baas (1995). "Microtubules released from the neuronal centrosome are transported into the axon." J Cell Sci **108 (Pt 8)**: 2761-2769.

Alami, N. H., R. B. Smith, M. A. Carrasco, L. A. Williams, C. S. Winborn, S. S. Han, E. Kiskinis, B. Winborn, B. D. Freibaum, A. Kanagaraj, A. J. Clare, N. M. Badders, B. Bilican, E. Chaum, S. Chandran, C. E. Shaw, K. C. Eggan, T. Maniatis and J. P. Taylor (2014). "Axonal transport of TDP-43 mRNA granules is impaired by ALS-causing mutations." Neuron **81**(3): 536-543.

Arai, T., M. Hasegawa, H. Akiyama, K. Ikeda, T. Nonaka, H. Mori, D. Mann, K. Tsuchiya, M. Yoshida, Y. Hashizume and T. Oda (2006). "TDP-43 is a component of ubiquitin-positive tau-negative inclusions in frontotemporal lobar degeneration and amyotrophic lateral sclerosis." Biochem Biophys Res Commun **351**(3): 602-611.

Baas, P. W. and A. Brown (1997). "Slow axonal transport: the polymer transport model." Trends Cell Biol **7**(10): 380-384.

Barra, H. S., J. A. Rodriguez, C. A. Arce and R. Caputto (1973). "A soluble preparation from rat brain that incorporates into its own proteins (14 C)arginine by a ribonuclease-sensitive system and (14 C)tyrosine by a ribonuclease-insensitive system." J Neurochem **20**(1): 97-108.

Beaulieu, J. M., J. Robertson and J. P. Julien (1999). "Interactions between peripherin and neurofilaments in cultured cells: disruption of peripherin assembly by the NF-M and NF-H subunits." Biochem Cell Biol **77**(1): 41-45.

Belmont, L., T. Mitchison and H. W. Deacon (1996). "Catastrophic revelations about Op18/stathmin." Trends Biochem Sci **21**(6): 197-198.

Bergeron, C., K. Beric-Maskarel, S. Muntasser, L. Weyer, M. J. Somerville and M. E. Percy (1994). "Neurofilament light and polyadenylated mRNA levels are decreased in amyotrophic lateral sclerosis motor neurons." J Neuropathol Exp Neurol **53**(3): 221-230.

Biederer, T. and T. C. Sudhof (2000). "Mints as adaptors. Direct binding to neurexins and recruitment of munc18." J Biol Chem **275**(51): 39803-39806.

Bocquet, A., R. Berges, R. Frank, P. Robert, A. C. Peterson and J. Eyer (2009). "Neurofilaments bind tubulin and modulate its polymerization." J Neurosci **29**(35): 11043-11054.

Bommel, H., G. Xie, W. Rossoll, S. Wiese, S. Jablonka, T. Boehm and M. Sendtner (2002). "Missense mutation in the tubulin-specific chaperone E (Tbce) gene in the mouse mutant progressive motor neuronopathy, a model of human motoneuron disease." J Cell Biol **159**(4): 563-569.

Brettschneider, J., A. Petzold, S. D. Sussmuth, A. C. Ludolph and H. Tumani (2006). "Axonal damage markers in cerebrospinal fluid are increased in ALS." Neurology **66**(6): 852-856.

Brown, A., Y. Li, T. Slaughter and M. M. Black (1993). "Composite microtubules of the axon: quantitative analysis of tyrosinated and acetylated tubulin along individual axonal microtubules." J Cell Sci **104 (Pt 2)**: 339-352.

Buratti, E. and F. E. Baralle (2001). "Characterization and functional implications of the RNA binding properties of nuclear factor TDP-43, a novel splicing regulator of CFTR exon 9." J Biol Chem **276**(39): 36337-36343.

Burghes, A. H. and C. E. Beattie (2009). "Spinal muscular atrophy: why do low levels of survival motor neuron protein make motor neurons sick?" Nat Rev Neurosci **10**(8): 597-609.

Bussaglia, E., O. Clermont, E. Tizzano, S. Lefebvre, L. Burglen, C. Cruaud, J. A. Urtizberea, J. Colomer, A. Munnich, M. Baiget and et al. (1995). "A frame-shift deletion in the survival motor neuron gene in Spanish spinal muscular atrophy patients." Nat Genet **11**(3): 335-337.

Campo, R., A. Fontalba, L. M. Sanchez and J. C. Zabala (1994). "A 14 kDa release factor is involved in GTP-dependent beta-tubulin folding." FEBS Lett **353**(2): 162-166.

Carden, M. J., J. Q. Trojanowski, W. W. Schlaepfer and V. M. Lee (1987). "Two-stage expression of neurofilament polypeptides during rat neurogenesis with early establishment of adult phosphorylation patterns." J Neurosci **7**(11): 3489-3504.

Chari, A., M. M. Golas, M. Klingenhager, N. Neuenkirchen, B. Sander, C. Englbrecht, A. Sickmann, H. Stark and U. Fischer (2008). "An assembly chaperone collaborates with the SMN complex to generate spliceosomal SnRNPs." Cell **135**(3): 497-509.

Chauvin, S. and A. Sobel (2015). "Neuronal stathmins: a family of phosphoproteins cooperating for neuronal development, plasticity and regeneration." Prog Neurobiol **126**: 1-18.

Chih, B., L. Gollan and P. Scheiffele (2006). "Alternative splicing controls selective trans-synaptic interactions of the neuroligin-neurexin complex." Neuron **51**(2): 171-178.

Ching, G. Y. and R. K. Liem (1993). "Assembly of type IV neuronal intermediate filaments in nonneuronal cells in the absence of preexisting cytoplasmic intermediate filaments." J Cell Biol **122**(6): 1323-1335.

Cifuentes-Diaz, C., S. Nicole, M. E. Velasco, C. Borra-Cebrian, C. Panozzo, T. Frugier, G. Millet, N. Roblot, V. Joshi and J. Melki (2002). "Neurofilament accumulation at the motor endplate and lack of axonal sprouting in a spinal muscular atrophy mouse model." Hum.Mol.Genet. **11**(12): 1439-1447.

Coovert, D. D., T. T. Le, P. E. McAndrew, J. Strasswimmer, T. O. Crawford, J. R. Mendell, S. E. Coulson, E. J. Androphy, T. W. Prior and A. H. Burghes (1997). "The survival motor neuron protein in spinal muscular atrophy." Hum Mol Genet **6**(8): 1205-1214.

Corbo, M. and A. P. Hays (1992). "Peripherin and neurofilament protein coexist in spinal spheroids of motor neuron disease." J Neuropathol Exp Neurol **51**(5): 531-537.

Cote, F., J. F. Collard and J. P. Julien (1993). "Progressive neuronopathy in transgenic mice expressing the human neurofilament heavy gene: a mouse model of amyotrophic lateral sclerosis." Cell **73**(1): 35-46.

Couillard-Despres, S., Q. Zhu, P. C. Wong, D. L. Price, D. W. Cleveland and J. P. Julien (1998). "Protective effect of neurofilament heavy gene overexpression in motor neuron disease induced by mutant superoxide dismutase." Proc Natl Acad Sci U S A **95**(16): 9626-9630.

Crow, J. P., Y. Z. Ye, M. Strong, M. Kirk, S. Barnes and J. S. Beckman (1997). "Superoxide dismutase catalyzes nitration of tyrosines by peroxynitrite in the rod and head domains of neurofilament-L." J Neurochem **69**(5): 1945-1953.

Darnell, J. E., Jr. (1994). "Spending to save: financial reform for the medicine of the future." Ann N Y Acad Sci **729**: 127.

De Jonghe, P., I. Mersivanova, E. Nelis, J. Del Favero, J. J. Martin, C. Van Broeckhoven, O. Evgrafov and V. Timmerman (2001). "Further evidence that neurofilament light chain gene mutations can cause Charcot-Marie-Tooth disease type 2E." Ann Neurol **49**(2): 245-249.

Delisle, M. B. and S. Carpenter (1984). "Neurofibrillary axonal swellings and amyotrophic lateral sclerosis." J Neurol Sci **63**(2): 241-250.

Dequen, F., P. Bomont, G. Gowing, D. W. Cleveland and J. P. Julien (2008). "Modest loss of peripheral axons, muscle atrophy and formation of brain inclusions in mice with targeted deletion of gigaxonin exon 1." J Neurochem **107**(1): 253-264.

Desai, A. and T. J. Mitchison (1997). "Microtubule polymerization dynamics." Annu Rev Cell Dev Biol **13**: 83-117.

DiDonato, C. J., X. N. Chen, D. Noya, J. R. Korenberg, J. H. Nadeau and L. R. Simard (1997). "Cloning, characterization, and copy number of the murine survival motor neuron gene: homolog of the spinal muscular atrophy-determining gene." Genome Res **7**(4): 339-352.

Dompierre, J. P., J. D. Godin, B. C. Charrin, F. P. Cordelieres, S. J. King, S. Humbert and F. Saudou (2007). "Histone deacetylase 6 inhibition compensates for the transport deficit in Huntington's disease by increasing tubulin acetylation." J Neurosci **27**(13): 3571-3583.

Eggert, C., A. Chari, B. Laggerbauer and U. Fischer (2006). "Spinal muscular atrophy: the RNP connection." Trends Mol Med **12**(3): 113-121.

Elder, G. A., V. L. Friedrich, Jr., P. Bosco, C. Kang, A. Gourov, P. H. Tu, V. M. Lee and R. A. Lazzarini (1998). "Absence of the mid-sized neurofilament subunit decreases axonal calibers, levels of light neurofilament (NF-L), and neurofilament content." J Cell Biol **141**(3): 727-739.

Elder, G. A., V. L. Friedrich, Jr., C. Kang, P. Bosco, A. Gourov, P. H. Tu, B. Zhang, V. M. Lee and R. A. Lazzarini (1998). "Requirement of heavy neurofilament subunit in the development of axons with large calibers." J Cell Biol **143**(1): 195-205.

Elder, G. A., V. L. Friedrich, Jr., D. Pereira, P. H. Tu, B. Zhang, V. M. Lee and R. A. Lazzarini (1999). "Mice with disrupted midsized and heavy neurofilament genes lack axonal neurofilaments but have unaltered numbers of axonal microtubules." J Neurosci Res **57**(1): 23-32.

Eyer, J. and J. F. Leterrier (1988). "Influence of the phosphorylation state of neurofilament proteins on the interactions between purified filaments in vitro." Biochem J **252**(3): 655-660.

Eyer, J. and A. Peterson (1994). "Neurofilament-deficient axons and perikaryal aggregates in viable transgenic mice expressing a neurofilament-beta-galactosidase fusion protein." Neuron **12**(2): 389-405.

Fan, L. and L. R. Simard (2002). "Survival motor neuron (SMN) protein: role in neurite outgrowth and neuromuscular maturation during neuronal differentiation and development." Hum Mol Genet **11**(14): 1605-1614.

Fanara, P., J. Banerjee, R. V. Hueck, M. R. Harper, M. Awada, H. Turner, K. H. Husted, R. Brandt and M. K. Hellerstein (2007). "Stabilization of hyperdynamic microtubules is neuroprotective in amyotrophic lateral sclerosis." J Biol Chem **282**(32): 23465-23472.

Fanara, P., S. Turner, R. Busch, S. Killion, M. Awada, H. Turner, A. Mahsut, K. L. Laprade, J. M. Stark and M. K. Hellerstein (2004). "In vivo measurement of microtubule dynamics using stable isotope labeling with heavy water. Effect of taxanes." J Biol Chem **279**(48): 49940-49947.

Fischer, U., Q. Liu and G. Dreyfuss (1997). "The SMN-SIP1 complex has an essential role in spliceosomal snRNP biogenesis." Cell **90**(6): 1023-1029.

Fletcher, D. A. and R. D. Mullins (2010). "Cell mechanics and the cytoskeleton." Nature **463**(7280): 485-492.

Fontalba, A., R. Paciucci, J. Avila and J. C. Zabala (1993). "Incorporation of tubulin subunits into dimers requires GTP hydrolysis." J Cell Sci **106 (Pt 2)**: 627-632.

Friede, R. L. and T. Samorajski (1970). "Axon caliber related to neurofilaments and microtubules in sciatic nerve fibers of rats and mice." Anat Rec **167**(4): 379-387.

Fuchs, E. and K. Weber (1994). "Intermediate filaments: structure, dynamics, function, and disease." Annu Rev Biochem **63**: 345-382.

Gabanella, F., M. E. Butchbach, L. Saieva, C. Carissimi, A. H. Burghes and L. Pellizzoni (2007). "Ribonucleoprotein assembly defects correlate with spinal muscular atrophy severity and preferentially affect a subset of spliceosomal snRNPs." PLoS One **2**(9): e921.

Gama Sosa, M. A., V. L. Friedrich, Jr., R. DeGasperi, K. Kelley, P. H. Wen, E. Senturk, R. A. Lazzarini and G. A. Elder (2003). "Human midsized neurofilament subunit induces motor neuron disease in transgenic mice." Exp Neurol **184**(1): 408-419.

Ge, W. W., C. Leystra-Lantz, W. Wen and M. J. Strong (2003). "Selective loss of trans-acting instability determinants of neurofilament mRNA in amyotrophic lateral sclerosis spinal cord." J Biol Chem **278**(29): 26558-26563.

Georgiou, D. M., J. Zidar, M. Korosec, L. T. Middleton, T. Kyriakides and K. Christodoulou (2002). "A novel NF-L mutation Pro22Ser is associated with CMT2 in a large Slovenian family." Neurogenetics **4**(2): 93-96.

Geuens, G., G. G. Gundersen, R. Nuydens, F. Cornelissen, J. C. Bulinski and M. DeBrabander (1986). "Ultrastructural colocalization of tyrosinated and detyrosinated alpha-tubulin in interphase and mitotic cells." J Cell Biol **103**(5): 1883-1893.

Ghosh-Roy, A., A. Goncharov, Y. Jin and A. D. Chisholm (2012). "Kinesin-13 and tubulin posttranslational modifications regulate microtubule growth in axon regeneration." Dev Cell **23**(4): 716-728.

Gogliotti, R. G., K. A. Quinlan, C. B. Barlow, C. R. Heier, C. J. Heckman and C. J. Didonato (2012). "Motor neuron rescue in spinal muscular atrophy mice demonstrates that sensory-motor defects are a consequence, not a cause, of motor neuron dysfunction." J Neurosci **32**(11): 3818-3829.

Gong, C. X., T. Lidsky, J. Wegiel, L. Zuck, I. Grundke-Iqbal and K. Iqbal (2000). "Phosphorylation of microtubule-associated protein tau is regulated by protein phosphatase 2A in mammalian brain. Implications for neurofibrillary degeneration in Alzheimer's disease." J Biol Chem **275**(8): 5535-5544.

Graf, E. R., X. Zhang, S. X. Jin, M. W. Linhoff and A. M. Craig (2004). "Neurexins induce differentiation of GABA and glutamate postsynaptic specializations via neuroligins." Cell **119**(7): 1013-1026.

Grundemann, J., F. Schlaudraff, O. Haeckel and B. Liss (2008). "Elevated alpha-synuclein mRNA levels in individual UV-laser-microdissected dopaminergic substantia nigra neurons in idiopathic Parkinson's disease." Nucleic Acids Res **36**(7): e38.

Gundersen, G. G., M. H. Kalnoski and J. C. Bulinski (1984). "Distinct populations of microtubules: tyrosinated and nontyrosinated alpha tubulin are distributed differently in vivo." Cell **38**(3): 779-789.

Gundersen, G. G., S. Khawaja and J. C. Bulinski (1987). "Postpolymerization detyrosination of alpha-tubulin: a mechanism for subcellular differentiation of microtubules." J Cell Biol **105**(1): 251-264.

Hafezparast, M., R. Klocke, C. Ruhrberg, A. Marquardt, A. Ahmad-Annuar, S. Bowen, G. Lalli, A. S. Witherden, H. Hummerich, S. Nicholson, P. J. Morgan, R. Oozageer, J. V. Priestley, S. Averill, V. R. King, S. Ball, J. Peters, T. Toda, A. Yamamoto, Y. Hiraoka, M. Augustin, D. Korthaus, S. Wattler, P. Wabnitz, C. Dickneite, S. Lampel, F. Boehme, G. Peraus, A. Popp, M. Rudelius, J. Schlegel, H. Fuchs, M. Hrabe de Angelis, G. Schiavo, D. T. Shima, A. P. Russ, G. Stumm, J. E. Martin and E. M. Fisher (2003). "Mutations in dynein link motor neuron degeneration to defects in retrograde transport." Science **300**(5620): 808-812.

Hahnen, E., J. Schonling, S. Rudnik-Schoneborn, H. Raschke, K. Zerres and B. Wirth (1997). "Missense mutations in exon 6 of the survival motor neuron gene in patients with spinal muscular atrophy (SMA)." Hum Mol Genet **6**(5): 821-825.

Hallak, M. E., J. A. Rodriguez, H. S. Barra and R. Caputto (1977). "Release of tyrosine from tyrosinated tubulin. Some common factors that affect this process and the assembly of tubulin." FEBS Lett **73**(2): 147-150.

Hata, Y., S. Butz and T. C. Sudhof (1996). "CASK: a novel dlg/PSD95 homolog with an N-terminal calmodulin-dependent protein kinase domain identified by interaction with neurexins." J Neurosci **16**(8): 2488-2494.

Heim, M. H., I. M. Kerr, G. R. Stark and J. E. Darnell, Jr. (1995). "Contribution of STAT SH2 groups to specific interferon signaling by the Jak-STAT pathway." Science **267**(5202): 1347-1349.

Heins, S. and U. Aebi (1994). "Making heads and tails of intermediate filament assembly, dynamics and networks." Curr Opin Cell Biol **6**(1): 25-33.

Hellal, F., A. Hurtado, J. Ruschel, K. C. Flynn, C. J. Laskowski, M. Umlauf, L. C. Kapitein, D. Strikis, V. Lemmon, J. Bixby, C. C. Hoogenraad and F. Bradke (2011). "Microtubule stabilization reduces scarring and causes axon regeneration after spinal cord injury." Science **331**(6019): 928-931.

Hempen, B. and J. P. Brion (1996). "Reduction of acetylated alpha-tubulin immunoreactivity in neurofibrillary tangle-bearing neurons in Alzheimer's disease." J Neuropathol Exp Neurol **55**(9): 964-972.

Herrmann, H. and U. Aebi (2000). "Intermediate filaments and their associates: multi-talented structural elements specifying cytoarchitecture and cytodynamics." Curr Opin Cell Biol **12**(1): 79-90.

Hirano, A., H. Donnenfeld, S. Sasaki and I. Nakano (1984). "Fine structural observations of neurofilamentous changes in amyotrophic lateral sclerosis." J Neuropathol Exp Neurol **43**(5): 461-470.

Hirokawa, N. (1997). "The mechanisms of fast and slow transport in neurons: identification and characterization of the new kinesin superfamily motors." Curr Opin Neurobiol **7**(5): 605-614.

Hisanaga, S. and N. Hirokawa (1990). "Dephosphorylation-induced interactions of neurofilaments with microtubules." J Biol Chem **265**(35): 21852-21858.

Hoffman, P. N., D. W. Cleveland, J. W. Griffin, P. W. Landes, N. J. Cowan and D. L. Price (1987). "Neurofilament gene expression: a major determinant of axonal caliber." Proc Natl Acad Sci U S A **84**(10): 3472-3476.

Hoffman, P. N., J. W. Griffin, B. G. Gold and D. L. Price (1985). "Slowing of neurofilament transport and the radial growth of developing nerve fibers." J Neurosci **5**(11): 2920-2929.

Hoffman, P. N. and R. J. Lasek (1975). "The slow component of axonal transport. Identification of major structural polypeptides of the axon and their generality among mammalian neurons." J Cell Biol **66**(2): 351-366.

Holmfeldt, P., N. Larsson, B. Segerman, B. Howell, J. Morabito, L. Cassimeris and M. Gullberg (2001). "The catastrophe-promoting activity of ectopic Op18/stathmin is required for disruption of mitotic spindles but not interphase microtubules." Mol Biol Cell **12**(1): 73-83.

Horwitz, S. B., H. J. Shen, L. He, P. Dittmar, R. Neef, J. Chen and U. K. Schubart (1997). "The microtubule-destabilizing activity of metablastin (p19) is controlled by phosphorylation." J Biol Chem **272**(13): 8129-8132.

Howell, B., H. Deacon and L. Cassimeris (1999). "Decreasing oncoprotein 18/stathmin levels reduces microtubule catastrophes and increases microtubule polymer in vivo." J Cell Sci **112 (Pt 21)**: 3713-3722.

Ichtchenko, K., Y. Hata, T. Nguyen, B. Ullrich, M. Missler, C. Moomaw and T. C. Sudhof (1995). "Neuroligin 1: a splice site-specific ligand for beta-neurexins." Cell **81**(3): 435-443.

Iijima, T., K. Wu, H. Witte, Y. Hanno-Iijima, T. Glatter, S. Richard and P. Scheiffele (2011). "SAM68 regulates neuronal activity-dependent alternative splicing of neurexin-1." Cell **147**(7): 1601-1614.

Ilieva, H., M. Polymenidou and D. W. Cleveland (2009). "Non-cell autonomous toxicity in neurodegenerative disorders: ALS and beyond." J Cell Biol **187**(6): 761-772.

Imlach, W. L., E. S. Beck, B. J. Choi, F. Lotti, L. Pellizzoni and B. D. McCabe (2012). "SMN is required for sensory-motor circuit function in Drosophila." Cell **151**(2): 427-439.

Ishihara, T., M. Higuchi, B. Zhang, Y. Yoshiyama, M. Hong, J. Q. Trojanowski and V. M. Lee (2001). "Attenuated neurodegenerative disease phenotype in tau transgenic mouse lacking neurofilaments." J Neurosci **21**(16): 6026-6035.

Ishihara, T., M. Hong, B. Zhang, Y. Nakagawa, M. K. Lee, J. Q. Trojanowski and V. M. Lee (1999). "Age-dependent emergence and progression of a tauopathy in transgenic mice overexpressing the shortest human tau isoform." Neuron **24**(3): 751-762.

Jablonka, S., M. Bandilla, S. Wiese, D. Buhler, B. Wirth, M. Sendtner and U. Fischer (2001). "Co-regulation of survival of motor neuron (SMN) protein and its interactor SIP1 during development and in spinal muscular atrophy." Hum Mol Genet **10**(5): 497-505.

Jablonka, S., M. Beck, B. D. Lechner, C. Mayer and M. Sendtner (2007). "Defective Ca2+ channel clustering in axon terminals disturbs excitability in motoneurons in spinal muscular atrophy." J Cell Biol **179**(1): 139-149.

Jacomy, H., Q. Zhu, S. Couillard-Despres, J. M. Beaulieu and J. P. Julien (1999). "Disruption of type IV intermediate filament network in mice lacking the neurofilament medium and heavy subunits." J Neurochem **73**(3): 972-984.

Janke, C. and J. C. Bulinski (2011). "Post-translational regulation of the microtubule cytoskeleton: mechanisms and functions." Nat Rev Mol Cell Biol **12**(12): 773-786.

Johnson-Kerner, B. L., F. S. Ahmad, A. G. Diaz, J. P. Greene, S. J. Gray, R. J. Samulski, W. K. Chung, R. Van Coster, P. Maertens, S. A. Noggle, C. E. Henderson and H. Wichterle (2015). "Intermediate filament protein accumulation in motor neurons derived from giant axonal neuropathy iPSCs rescued by restoration of gigaxonin." Hum Mol Genet **24**(5): 1420-1431.

Jordanova, A., P. De Jonghe, C. F. Boerkoel, H. Takashima, E. De Vriendt, C. Ceuterick, J. J. Martin, I. J. Butler, P. Mancias, S. Papasozomenos, D. Terespolsky, L. Potocki, C. W. Brown, M. Shy, D. A. Rita, I. Tournev, I. Kremensky, J. R. Lupski and V. Timmerman (2003). "Mutations in the neurofilament light chain gene (NEFL) cause early onset severe Charcot-Marie-Tooth disease." Brain **126**(Pt 3): 590-597.

Jourdain, L., P. Curmi, A. Sobel, D. Pantaloni and M. F. Carlier (1997). "Stathmin: a tubulin-sequestering protein which forms a ternary T2S complex with two tubulin molecules." Biochemistry **36**(36): 10817-10821.

Julien, J. P., S. Couillard-Despres and J. Meier (1998). "Transgenic mice in the study of ALS: the role of neurofilaments." Brain Pathol **8**(4): 759-769.

Julien, J. P., D. Meyer, D. Flavell, J. Hurst and F. Grosveld (1986). "Cloning and developmental expression of the murine neurofilament gene family." Brain Res **387**(3): 243-250.

Julien, J. P. and W. E. Mushynski (1998). "Neurofilaments in health and disease." <u>Prog Nucleic Acid Res Mol Biol</u> **61**: 1-23.

Kalebic, N., S. Sorrentino, E. Perlas, G. Bolasco, C. Martinez and P. A. Heppenstall (2013). "alphaTAT1 is the major alpha-tubulin acetyltransferase in mice." <u>Nat Commun</u> **4**: 1962.

Kariya, S., G. H. Park, Y. Maeno-Hikichi, O. Leykekhman, C. Lutz, M. S. Arkovitz, L. T. Landmesser and U. R. Monani (2008). "Reduced SMN protein impairs maturation of the neuromuscular junctions in mouse models of spinal muscular atrophy." <u>Hum Mol Genet</u> **17**(16): 2552-2569.

Kashima, T. and J. L. Manley (2003). "A negative element in SMN2 exon 7 inhibits splicing in spinal muscular atrophy." <u>Nat Genet</u> **34**(4): 460-463.

Kong, J., V. W. Tung, J. Aghajanian and Z. Xu (1998). "Antagonistic roles of neurofilament subunits NF-H and NF-M against NF-L in shaping dendritic arborization in spinal motor neurons." <u>J Cell Biol</u> **140**(5): 1167-1176.

Kong, J. and Z. Xu (2000). "Overexpression of neurofilament subunit NF-L and NF-H extends survival of a mouse model for amyotrophic lateral sclerosis." <u>Neurosci Lett</u> **281**(1): 72-74.

Kong, L., X. Wang, D. W. Choe, M. Polley, B. G. Burnett, M. Bosch-Marce, J. W. Griffin, M. M. Rich and C. J. Sumner (2009). "Impaired synaptic vesicle release and immaturity of neuromuscular junctions in spinal muscular atrophy mice." <u>J Neurosci</u> **29**(3): 842-851.

Kreitzer, G., G. Liao and G. G. Gundersen (1999). "Detyrosination of tubulin regulates the interaction of intermediate filaments with microtubules in vivo via a kinesin-dependent mechanism." <u>Mol Biol Cell</u> **10**(4): 1105-1118.

Kriz, J., Q. Zhu, J. P. Julien and A. L. Padjen (2000). "Electrophysiological properties of axons in mice lacking neurofilament subunit genes: disparity between conduction velocity and axon diameter in absence of NF-H." <u>Brain Res</u> **885**(1): 32-44.

Kumar, N. and M. Flavin (1981). "Preferential action of a brain detyrosinolating carboxypeptidase on polymerized tubulin." <u>J Biol Chem</u> **256**(14): 7678-7686.

L'Hernault, S. W. and J. L. Rosenbaum (1985). "Chlamydomonas alpha-tubulin is posttranslationally modified by acetylation on the epsilon-amino group of a lysine." <u>Biochemistry</u> **24**(2): 473-478.

Lavedan, C., S. Buchholtz, R. L. Nussbaum, R. L. Albin and M. H. Polymeropoulos (2002). "A mutation in the human neurofilament M gene in Parkinson's disease that suggests a role for the cytoskeleton in neuronal degeneration." <u>Neurosci Lett</u> **322**(1): 57-61.

Lawler, S. (1998). "Microtubule dynamics: if you need a shrink try stathmin/Op18." <u>Curr Biol</u> **8**(6): R212-214.

Lee, M. K., Z. Xu, P. C. Wong and D. W. Cleveland (1993). "Neurofilaments are obligate heteropolymers in vivo." <u>J Cell Biol</u> **122**(6): 1337-1350.

Lefebvre, S., L. Burglen, S. Reboullet, O. Clermont, P. Burlet, L. Viollet, B. Benichou, C. Cruaud, P. Millasseau, M. Zeviani and et al. (1995). "Identification and characterization of a spinal muscular atrophy-determining gene." <u>Cell</u> **80**(1): 155-165.

Lefebvre, S., P. Burlet, Q. Liu, S. Bertrandy, O. Clermont, A. Munnich, G. Dreyfuss and J. Melki (1997). "Correlation between severity and SMN protein level in spinal muscular atrophy." <u>Nat Genet</u> **16**(3): 265-269.

Lepinoux-Chambaud, C. and J. Eyer (2013). "Review on intermediate filaments of the nervous system and their pathological alterations." <u>Histochem Cell Biol</u> **140**(1): 13-22.

Lewis, S. A., G. Tian and N. J. Cowan (1997). "The alpha- and beta-tubulin folding pathways." <u>Trends Cell Biol</u> **7**(12): 479-484.

Li, J., J. Ashley, V. Budnik and M. A. Bhat (2007). "Crucial role of Drosophila neurexin in proper active zone apposition to postsynaptic densities, synaptic growth, and synaptic transmission." Neuron **55**(5): 741-755.

Liao, G. and G. G. Gundersen (1998). "Kinesin is a candidate for cross-bridging microtubules and intermediate filaments. Selective binding of kinesin to detyrosinated tubulin and vimentin." J Biol Chem **273**(16): 9797-9803.

Liem, R. K., S. H. Yen, G. D. Salomon and M. L. Shelanski (1978). "Intermediate filaments in nervous tissues." J Cell Biol **79**(3): 637-645.

Liu, Q. and G. Dreyfuss (1996). "A novel nuclear structure containing the survival of motor neurons protein." EMBO J **15**(14): 3555-3565.

Liu, Q., F. Xie, A. Alvarado-Diaz, M. A. Smith, P. I. Moreira, X. Zhu and G. Perry (2011). "Neurofilamentopathy in neurodegenerative diseases." Open Neurol J **5**: 58-62.

Liu, Q., F. Xie, S. L. Siedlak, A. Nunomura, K. Honda, P. I. Moreira, X. Zhua, M. A. Smith and G. Perry (2004). "Neurofilament proteins in neurodegenerative diseases." Cell Mol Life Sci **61**(24): 3057-3075.

Liu, Y., J. A. Staal, A. J. Canty, M. T. Kirkcaldie, A. E. King, O. Bibari, S. T. Mitew, T. C. Dickson and J. C. Vickers (2013). "Cytoskeletal changes during development and aging in the cortex of neurofilament light protein knockout mice." J Comp Neurol **521**(8): 1817-1827.

Lobsiger, C. S., M. L. Garcia, C. M. Ward and D. W. Cleveland (2005). "Altered axonal architecture by removal of the heavily phosphorylated neurofilament tail domains strongly slows superoxide dismutase 1 mutant-mediated ALS." Proc Natl Acad Sci U S A **102**(29): 10351-10356.

Lu, C. H., A. Petzold, B. Kalmar, J. Dick, A. Malaspina and L. Greensmith (2012). "Plasma neurofilament heavy chain levels correlate to markers of late stage disease progression and treatment response in SOD1(G93A) mice that model ALS." PLoS One **7**(7): e40998.

Mahammad, S., S. N. Murthy, A. Didonna, B. Grin, E. Israeli, R. Perrot, P. Bomont, J. P. Julien, E. Kuczmarski, P. Opal and R. D. Goldman (2013). "Giant axonal neuropathy-associated gigaxonin mutations impair intermediate filament protein degradation." J Clin Invest **123**(5): 1964-1975.

Marinkovic, P., M. S. Reuter, M. S. Brill, L. Godinho, M. Kerschensteiner and T. Misgeld (2012). "Axonal transport deficits and degeneration can evolve independently in mouse models of amyotrophic lateral sclerosis." Proc Natl Acad Sci U S A **109**(11): 4296-4301.

Marklund, U., N. Larsson, H. M. Gradin, G. Brattsand and M. Gullberg (1996). "Oncoprotein 18 is a phosphorylation-responsive regulator of microtubule dynamics." EMBO J **15**(19): 5290-5298.

Marszalek, J. R., T. L. Williamson, M. K. Lee, Z. Xu, P. N. Hoffman, M. W. Becher, T. O. Crawford and D. W. Cleveland (1996). "Neurofilament subunit NF-H modulates axonal diameter by selectively slowing neurofilament transport." J Cell Biol **135**(3): 711-724.

Martin, N., J. Jaubert, P. Gounon, E. Salido, G. Haase, M. Szatanik and J. L. Guenet (2002). "A missense mutation in Tbce causes progressive motor neuronopathy in mice." Nat Genet **32**(3): 443-447.

Martinez, T. L., L. Kong, X. Wang, M. A. Osborne, M. E. Crowder, J. P. Van Meerbeke, X. Xu, C. Davis, J. Wooley, D. J. Goldhamer, C. M. Lutz, M. M. Rich and C. J. Sumner (2012). "Survival motor neuron protein in motor neurons determines synaptic integrity in spinal muscular atrophy." J Neurosci **32**(25): 8703-8715.

Matten, W. T., M. Aubry, J. West and P. F. Maness (1990). "Tubulin is phosphorylated at tyrosine by pp60c-src in nerve growth cone membranes." J Cell Biol **111**(5 Pt 1): 1959-1970.

McLachlan, D. R., W. J. Lukiw, L. Wong, C. Bergeron and N. T. Bech-Hansen (1988). "Selective messenger RNA reduction in Alzheimer's disease." Brain Res **427**(3): 255-261.

Menzies, F. M., A. J. Grierson, M. R. Cookson, P. R. Heath, J. Tomkins, D. A. Figlewicz, P. G. Ince and P. J. Shaw (2002). "Selective loss of neurofilament expression in Cu/Zn superoxide dismutase (SOD1) linked amyotrophic lateral sclerosis." J Neurochem **82**(5): 1118-1128.

Mersiyanova, I. V., A. V. Perepelov, A. V. Polyakov, V. F. Sitnikov, E. L. Dadali, R. B. Oparin, A. N. Petrin and O. V. Evgrafov (2000). "A new variant of Charcot-Marie-Tooth disease type 2 is probably the result of a mutation in the neurofilament-light gene." Am J Hum Genet **67**(1): 37-46.

Minami, Y., H. Murofushi and H. Sakai (1982). "Interaction of tubulin with neurofilaments: formation of networks by neurofilament-dependent tubulin polymerization." J Biochem **92**(3): 889-898.

Missler, M., R. Fernandez-Chacon and T. C. Sudhof (1998). "The making of neurexins." J Neurochem **71**(4): 1339-1347.

Missler, M. and T. C. Sudhof (1998). "Neurexins: three genes and 1001 products." Trends Genet **14**(1): 20-26.

Missler, M., W. Zhang, A. Rohlmann, G. Kattenstroth, R. E. Hammer, K. Gottmann and T. C. Sudhof (2003). "Alpha-neurexins couple Ca2+ channels to synaptic vesicle exocytosis." Nature **423**(6943): 939-948.

Monani, U. R., D. D. Coovert and A. H. Burghes (2000). "Animal models of spinal muscular atrophy." Hum Mol Genet **9**(16): 2451-2457.

Monani, U. R., C. L. Lorson, D. W. Parsons, T. W. Prior, E. J. Androphy, A. H. Burghes and J. D. McPherson (1999). "A single nucleotide difference that alters splicing patterns distinguishes the SMA gene SMN1 from the copy gene SMN2." Hum Mol Genet **8**(7): 1177-1183.

Monani, U. R., M. Sendtner, D. D. Coovert, D. W. Parsons, C. Andreassi, T. T. Le, S. Jablonka, B. Schrank, W. Rossoll, T. W. Prior, G. E. Morris and A. H. Burghes (2000). "The human centromeric survival motor neuron gene (SMN2) rescues embryonic lethality in Smn(-/-) mice and results in a mouse with spinal muscular atrophy." Hum Mol Genet **9**(3): 333-339.

Mourelatos, Z., L. Abel, J. Yong, N. Kataoka and G. Dreyfuss (2001). "SMN interacts with a novel family of hnRNP and spliceosomal proteins." EMBO J **20**(19): 5443-5452.

Munoz, D. G., C. Greene, D. P. Perl and D. J. Selkoe (1988). "Accumulation of phosphorylated neurofilaments in anterior horn motoneurons of amyotrophic lateral sclerosis patients." J Neuropathol Exp Neurol **47**(1): 9-18.

Munsat, T. L. and K. E. Davies (1992). "International SMA consortium meeting. (26-28 June 1992, Bonn, Germany)." Neuromuscul Disord **2**(5-6): 423-428.

Neumann, M., D. M. Sampathu, L. K. Kwong, A. C. Truax, M. C. Micsenyi, T. T. Chou, J. Bruce, T. Schuck, M. Grossman, C. M. Clark, L. F. McCluskey, B. L. Miller, E. Masliah, I. R. Mackenzie, H. Feldman, W. Feiden, H. A. Kretzschmar, J. Q. Trojanowski and V. M. Lee (2006). "Ubiquitinated TDP-43 in frontotemporal lobar degeneration and amyotrophic lateral sclerosis." Science **314**(5796): 130-133.

Ng, D. C., B. H. Lin, C. P. Lim, G. Huang, T. Zhang, V. Poli and X. Cao (2006). "Stat3 regulates microtubules by antagonizing the depolymerization activity of stathmin." J Cell Biol **172**(2): 245-257.

Nguyen, M. D., R. C. Lariviere and J. P. Julien (2000). "Reduction of axonal caliber does not alleviate motor neuron disease caused by mutant superoxide dismutase 1." Proc Natl Acad Sci U S A **97**(22): 12306-12311.

Nguyen, T. and T. C. Sudhof (1997). "Binding properties of neuroligin 1 and neurexin 1beta reveal function as heterophilic cell adhesion molecules." J Biol Chem **272**(41): 26032-26039.

Niebroj-Dobosz, I., D. Dziewulska and P. Janik (2006). "Auto-antibodies against proteins of spinal cord cells in cerebrospinal fluid of patients with amyotrophic lateral sclerosis (ALS)." Folia Neuropathol **44**(3): 191-196.

Nixon, R. A. (1998). "The slow axonal transport debate." Trends Cell Biol **8**(3): 100.

Nixon, R. A. (1998). "The slow axonal transport of cytoskeletal proteins." Curr Opin Cell Biol **10**(1): 87-92.

Nixon, R. A. and T. B. Shea (1992). "Dynamics of neuronal intermediate filaments: a developmental perspective." Cell Motil Cytoskeleton **22**(2): 81-91.

Ohara, O., Y. Gahara, T. Miyake, H. Teraoka and T. Kitamura (1993). "Neurofilament deficiency in quail caused by nonsense mutation in neurofilament-L gene." J Cell Biol **121**(2): 387-395.

Opal, P. and R. D. Goldman (2013). "Explaining intermediate filament accumulation in giant axonal neuropathy." Rare Dis **1**: e25378.

Park, G. H., Y. Maeno-Hikichi, T. Awano, L. T. Landmesser and U. R. Monani (2010). "Reduced survival of motor neuron (SMN) protein in motor neuronal progenitors functions cell autonomously to cause spinal muscular atrophy in model mice expressing the human centromeric (SMN2) gene." J Neurosci **30**(36): 12005-12019.

Parsons, D. W., P. E. McAndrew, U. R. Monani, J. R. Mendell, A. H. Burghes and T. W. Prior (1996). "An 11 base pair duplication in exon 6 of the SMN gene produces a type I spinal muscular atrophy (SMA) phenotype: further evidence for SMN as the primary SMA-determining gene." Hum Mol Genet **5**(11): 1727-1732.

Pearn, J. (1978). "Incidence, prevalence, and gene frequency studies of chronic childhood spinal muscular atrophy." J Med Genet **15**(6): 409-413.

Pearn, J. H. (1973). "The gene frequency of acute Werdnig-Hoffmann disease (SMA type 1). A total population survey in North-East England." J Med Genet **10**(3): 260-265.

Pellizzoni, L., N. Kataoka, B. Charroux and G. Dreyfuss (1998). "A novel function for SMN, the spinal muscular atrophy disease gene product, in pre-mRNA splicing." Cell **95**(5): 615-624.

Pellizzoni, L., J. Yong and G. Dreyfuss (2002). "Essential role for the SMN complex in the specificity of snRNP assembly." Science **298**(5599): 1775-1779.

Perdiz, D., R. Mackeh, C. Pous and A. Baillet (2011). "The ins and outs of tubulin acetylation: more than just a post-translational modification?" Cell Signal **23**(5): 763-771.

Peris, L., M. Wagenbach, L. Lafanechere, J. Brocard, A. T. Moore, F. Kozielski, D. Job, L. Wordeman and A. Andrieux (2009). "Motor-dependent microtubule disassembly driven by tubulin tyrosination." J Cell Biol **185**(7): 1159-1166.

Perrin, F. E., G. Boisset, M. Docquier, O. Schaad, P. Descombes and A. C. Kato (2005). "No widespread induction of cell death genes occurs in pure motoneurons in an amyotrophic lateral sclerosis mouse model." Hum Mol Genet **14**(21): 3309-3320.

Perrot, R., R. Berges, A. Bocquet and J. Eyer (2008). "Review of the multiple aspects of neurofilament functions, and their possible contribution to neurodegeneration." Mol Neurobiol **38**(1): 27-65.

Perrot, R. and J. Eyer (2009). "Neuronal intermediate filaments and neurodegenerative disorders." Brain Res Bull **80**(4-5): 282-295.

Perrot, R. and J. P. Julien (2009). "Real-time imaging reveals defects of fast axonal transport induced by disorganization of intermediate filaments." FASEB J **23**(9): 3213-3225.

Perry, R. B. and M. Fainzilber (2009). "Nuclear transport factors in neuronal function." <u>Semin Cell Dev Biol</u> **20**(5): 600-606.

Petrenko, A. G., M. S. Perin, B. A. Davletov, Y. A. Ushkaryov, M. Geppert and T. C. Sudhof (1991). "Binding of synaptotagmin to the alpha-latrotoxin receptor implicates both in synaptic vesicle exocytosis." <u>Nature</u> **353**(6339): 65-68.

Pigino, G., G. Morfini, A. Pelsman, M. P. Mattson, S. T. Brady and J. Busciglio (2003). "Alzheimer's presenilin 1 mutations impair kinesin-based axonal transport." <u>J Neurosci</u> **23**(11): 4499-4508.

Rathod, R., S. Havlicek, N. Frank, R. Blum and M. Sendtner (2012). "Laminin induced local axonal translation of beta-actin mRNA is impaired in SMN-deficient motoneurons." <u>Histochem Cell Biol</u> **138**(5): 737-748.

Raybin, D. and M. Flavin (1977). "Enzyme which specifically adds tyrosine to the alpha chain of tubulin." <u>Biochemistry</u> **16**(10): 2189-2194.

Reich, N. C. and L. Liu (2006). "Tracking STAT nuclear traffic." <u>Nat Rev Immunol</u> **6**(8): 602-612.

Reid, E., M. Kloos, A. Ashley-Koch, L. Hughes, S. Bevan, I. K. Svenson, F. L. Graham, P. C. Gaskell, A. Dearlove, M. A. Pericak-Vance, D. C. Rubinsztein and D. A. Marchuk (2002). "A kinesin heavy chain (KIF5A) mutation in hereditary spastic paraplegia (SPG10)." <u>Am J Hum Genet</u> **71**(5): 1189-1194.

Reynolds, E. S. (1963). "The use of lead citrate at high pH as an electron-opaque stain in electron microscopy." <u>J Cell Biol</u> **17**: 208-212.

Robberecht, W. and T. Philips (2013). "The changing scene of amyotrophic lateral sclerosis." <u>Nat Rev Neurosci</u> **14**(4): 248-264.

Roberts, D. F., J. Chavez and S. D. Court (1970). "The genetic component in child mortality." <u>Arch Dis Child</u> **45**(239): 33-38.

Rossoll, W., S. Jablonka, C. Andreassi, A. K. Kroning, K. Karle, U. R. Monani and M. Sendtner (2003). "Smn, the spinal muscular atrophy-determining gene product, modulates axon growth and localization of beta-actin mRNA in growth cones of motoneurons." <u>J Cell Biol</u> **163**(4): 801-812.

Rossoll, W., A. K. Kroning, U. M. Ohndorf, C. Steegborn, S. Jablonka and M. Sendtner (2002). "Specific interaction of Smn, the spinal muscular atrophy determining gene product, with hnRNP-R and gry-rbp/hnRNP-Q: a role for Smn in RNA processing in motor axons?" <u>Hum Mol Genet</u> **11**(1): 93-105.

Rozic-Kotliroff, G. and N. Zisapel (2007). "Ca2+ -dependent splicing of neurexin IIalpha." <u>Biochem Biophys Res Commun</u> **352**(1): 226-230.

Ruiz, R., J. J. Casanas, L. Torres-Benito, R. Cano and L. Tabares (2010). "Altered intracellular Ca2+ homeostasis in nerve terminals of severe spinal muscular atrophy mice." <u>J Neurosci</u> **30**(3): 849-857.

Sagot, Y., S. A. Tan, J. P. Hammang, P. Aebischer and A. C. Kato (1996). "GDNF slows loss of motoneurons but not axonal degeneration or premature death of pmn/pmn mice." <u>J Neurosci</u> **16**(7): 2335-2341.

Sakaguchi, T., M. Okada, T. Kitamura and K. Kawasaki (1993). "Reduced diameter and conduction velocity of myelinated fibers in the sciatic nerve of a neurofilament-deficient mutant quail." <u>Neurosci Lett</u> **153**(1): 65-68.

Sasaki, S., S. Maruyama, K. Yamane, H. Sakuma and M. Takeishi (1989). "Swellings of proximal axons in a case of motor neuron disease." <u>Ann Neurol</u> **25**(5): 520-522.

Schaefer, M. K., H. Schmalbruch, E. Buhler, C. Lopez, N. Martin, J. L. Guenet and G. Haase (2007). "Progressive motor neuronopathy: a critical role of the tubulin chaperone TBCE in axonal tubulin routing from the Golgi apparatus." J Neurosci **27**(33): 8779-8789.

Scheiffele, P., J. Fan, J. Choih, R. Fetter and T. Serafini (2000). "Neuroligin expressed in nonneuronal cells triggers presynaptic development in contacting axons." Cell **101**(6): 657-669.

Schmalbruch, H., H. J. Jensen, M. Bjaerg, Z. Kamieniecka and L. Kurland (1991). "A new mouse mutant with progressive motor neuronopathy." J Neuropathol Exp Neurol **50**(3): 192-204.

Schmidt, M. L., M. J. Carden, V. M. Lee and J. Q. Trojanowski (1987). "Phosphate dependent and independent neurofilament epitopes in the axonal swellings of patients with motor neuron disease and controls." Lab Invest **56**(3): 282-294.

Schmidt, M. L., V. M. Lee and J. Q. Trojanowski (1989). "Analysis of epitopes shared by Hirano bodies and neurofilament proteins in normal and Alzheimer's disease hippocampus." Lab Invest **60**(4): 513-522.

Schmidt, M. L., V. M. Lee and J. Q. Trojanowski (1990). "Relative abundance of tau and neurofilament epitopes in hippocampal neurofibrillary tangles." Am J Pathol **136**(5): 1069-1075.

Schmidt, M. L., J. A. Martin, V. M. Lee and J. Q. Trojanowski (1996). "Convergence of Lewy bodies and neurofibrillary tangles in amygdala neurons of Alzheimer's disease and Lewy body disorders." Acta Neuropathol **91**(5): 475-481.

Schrank, B., R. Gotz, J. M. Gunnersen, J. M. Ure, K. V. Toyka, A. G. Smith and M. Sendtner (1997). "Inactivation of the survival motor neuron gene, a candidate gene for human spinal muscular atrophy, leads to massive cell death in early mouse embryos." Proc Natl Acad Sci U S A **94**(18): 9920-9925.

Schulze, E., D. J. Asai, J. C. Bulinski and M. Kirschner (1987). "Posttranslational modification and microtubule stability." J Cell Biol **105**(5): 2167-2177.

Schweizer, U., J. Gunnersen, C. Karch, S. Wiese, B. Holtmann, K. Takeda, S. Akira and M. Sendtner (2002). "Conditional gene ablation of Stat3 reveals differential signaling requirements for survival of motoneurons during development and after nerve injury in the adult." J Cell Biol **156**(2): 287-297.

See, K., P. Yadav, M. Giegerich, P. S. Cheong, M. Graf, H. Vyas, S. G. Lee, S. Mathavan, U. Fischer, M. Sendtner and C. Winkler (2013). "SMN deficiency alters Nrxn2 expression and splicing in zebrafish and mouse models of spinal muscular atrophy." Hum Mol Genet.

See, K., P. Yadav, M. Giegerich, P. S. Cheong, M. Graf, H. Vyas, S. G. Lee, S. Mathavan, U. Fischer, M. Sendtner and C. Winkler (2014). "SMN deficiency alters Nrxn2 expression and splicing in zebrafish and mouse models of spinal muscular atrophy." Hum Mol Genet **23**(7): 1754-1770.

Selvaraj, B. T., N. Frank, F. L. Bender, E. Asan and M. Sendtner (2012). "Local axonal function of STAT3 rescues axon degeneration in the pmn model of motoneuron disease." J Cell Biol **199**(3): 437-451.

Selvaraj, B. T. and M. Sendtner (2013). "CNTF, STAT3 and new therapies for axonal degeneration: what are they and what can they do?" Expert Rev Neurother **13**(3): 239-241.

Sendtner, M. (2014). "Motoneuron disease." Handb Exp Pharmacol **220**: 411-441.

Sendtner, M., H. Schmalbruch, K. A. Stockli, P. Carroll, G. W. Kreutzberg and H. Thoenen (1992). "Ciliary neurotrophic factor prevents degeneration of motor neurons in mouse mutant progressive motor neuronopathy." Nature **358**(6386): 502-504.

Shankar, S. K., R. Yanagihara, R. M. Garruto, I. Grundke-Iqbal, K. S. Kosik and D. C. Gajdusek (1989). "Immunocytochemical characterization of neurofibrillary tangles in amyotrophic lateral sclerosis and parkinsonism-dementia of Guam." Ann Neurol **25**(2): 146-151.

Shaw, G. and K. Weber (1982). "Differential expression of neurofilament triplet proteins in brain development." Nature **298**(5871): 277-279.

Shumyatsky, G. P., G. Malleret, R. M. Shin, S. Takizawa, K. Tully, E. Tsvetkov, S. S. Zakharenko, J. Joseph, S. Vronskaya, D. Yin, U. K. Schubart, E. R. Kandel and V. Y. Bolshakov (2005). "stathmin, a gene enriched in the amygdala, controls both learned and innate fear." Cell **123**(4): 697-709.

Sobel, A., M. C. Boutterin, L. Beretta, H. Chneiweiss, V. Doye and H. Peyro-Saint-Paul (1989). "Intracellular substrates for extracellular signaling. Characterization of a ubiquitous, neuron-enriched phosphoprotein (stathmin)." J Biol Chem **264**(7): 3765-3772.

Song, Y. and S. T. Brady (2015). "Post-translational modifications of tubulin: pathways to functional diversity of microtubules." Trends Cell Biol **25**(3): 125-136.

Sons, M. S., N. Busche, N. Strenzke, T. Moser, U. Ernsberger, F. C. Mooren, W. Zhang, M. Ahmad, H. Steffens, E. D. Schomburg, J. J. Plomp and M. Missler (2006). "alpha-Neurexins are required for efficient transmitter release and synaptic homeostasis at the mouse neuromuscular junction." Neuroscience **138**(2): 433-446.

Steinmetz, M. O. (2007). "Structure and thermodynamics of the tubulin-stathmin interaction." J Struct Biol **158**(2): 137-147.

Sternberger, N. H., L. A. Sternberger and J. Ulrich (1985). "Aberrant neurofilament phosphorylation in Alzheimer disease." Proc Natl Acad Sci U S A **82**(12): 4274-4276.

Stokin, G. B., C. Lillo, T. L. Falzone, R. G. Brusch, E. Rockenstein, S. L. Mount, R. Raman, P. Davies, E. Masliah, D. S. Williams and L. S. Goldstein (2005). "Axonopathy and transport deficits early in the pathogenesis of Alzheimer's disease." Science **307**(5713): 1282-1288.

Strong, M. J., C. Leystra-Lantz and W. W. Ge (2004). "Intermediate filament steady-state mRNA levels in amyotrophic lateral sclerosis." Biochem Biophys Res Commun **316**(2): 317-322.

Strong, M. J., K. Volkening, R. Hammond, W. Yang, W. Strong, C. Leystra-Lantz and C. Shoesmith (2007). "TDP43 is a human low molecular weight neurofilament (hNFL) mRNA-binding protein." Mol Cell Neurosci **35**(2): 320-327.

Sudhof, T. C. (2008). "Neuroligins and neurexins link synaptic function to cognitive disease." Nature **455**(7215): 903-911.

Sugita, S., F. Saito, J. Tang, J. Satz, K. Campbell and T. C. Sudhof (2001). "A stoichiometric complex of neurexins and dystroglycan in brain." J Cell Biol **154**(2): 435-445.

Szaro, B. G. and M. J. Strong (2010). "Post-transcriptional control of neurofilaments: New roles in development, regeneration and neurodegenerative disease." Trends Neurosci **33**(1): 27-37.

Szyk, A., A. M. Deaconescu, G. Piszczek and A. Roll-Mecak (2011). "Tubulin tyrosine ligase structure reveals adaptation of an ancient fold to bind and modify tubulin." Nat Struct Mol Biol **18**(11): 1250-1258.

Szyk, A., G. Piszczek and A. Roll-Mecak (2013). "Tubulin tyrosine ligase and stathmin compete for tubulin binding in vitro." J Mol Biol **425**(14): 2412-2414.

Takeda, K., K. Noguchi, W. Shi, T. Tanaka, M. Matsumoto, N. Yoshida, T. Kishimoto and S. Akira (1997). "Targeted disruption of the mouse Stat3 gene leads to early embryonic lethality." Proc Natl Acad Sci U S A **94**(8): 3801-3804.

Talbot, K., C. P. Ponting, A. M. Theodosiou, N. R. Rodrigues, R. Surtees, R. Mountford and K. E. Davies (1997). "Missense mutation clustering in the survival motor neuron gene: a role for a conserved tyrosine and glycine rich region of the protein in RNA metabolism?" Hum Mol Genet **6**(3): 497-500.

Tortelli, R., M. Ruggieri, R. Cortese, E. D'Errico, R. Capozzo, A. Leo, M. Mastrapasqua, S. Zoccolella, R. Leante, P. Livrea, G. Logroscino and I. L. Simone (2012). "Elevated cerebrospinal fluid neurofilament light levels in patients with amyotrophic lateral sclerosis: a possible marker of disease severity and progression." Eur J Neurol **19**(12): 1561-1567.

Tu, P. H., P. Raju, K. A. Robinson, M. E. Gurney, J. Q. Trojanowski and V. M. Lee (1996). "Transgenic mice carrying a human mutant superoxide dismutase transgene develop neuronal cytoskeletal pathology resembling human amyotrophic lateral sclerosis lesions." Proc Natl Acad Sci U S A **93**(7): 3155-3160.

Tuszynski, J. A., E. J. Carpenter, J. T. Huzil, W. Malinski, T. Luchko and R. F. Luduena (2006). "The evolution of the structure of tubulin and its potential consequences for the role and function of microtubules in cells and embryos." Int J Dev Biol **50**(2-3): 341-358.

Uchida, S., G. Martel, A. Pavlowsky, S. Takizawa, C. Hevi, Y. Watanabe, E. R. Kandel, J. M. Alarcon and G. P. Shumyatsky (2014). "Learning-induced and stathmin-dependent changes in microtubule stability are critical for memory and disrupted in ageing." Nat Commun **5**: 4389.

Ullrich, B., Y. A. Ushkaryov and T. C. Sudhof (1995). "Cartography of neurexins: more than 1000 isoforms generated by alternative splicing and expressed in distinct subsets of neurons." Neuron **14**(3): 497-507.

Ushkaryov, Y. A., A. G. Petrenko, M. Geppert and T. C. Sudhof (1992). "Neurexins: synaptic cell surface proteins related to the alpha-latrotoxin receptor and laminin." Science **257**(5066): 50-56.

Ushkaryov, Y. A. and T. C. Sudhof (1993). "Neurexin III alpha: extensive alternative splicing generates membrane-bound and soluble forms." Proc Natl Acad Sci U S A **90**(14): 6410-6414.

Verma, N. K., J. Dourlat, A. M. Davies, A. Long, W. Q. Liu, C. Garbay, D. Kelleher and Y. Volkov (2009). "STAT3-stathmin interactions control microtubule dynamics in migrating T-cells." J Biol Chem **284**(18): 12349-12362.

Viollet, L., S. Bertrandy, A. L. Bueno Brunialti, S. Lefebvre, P. Burlet, O. Clermont, C. Cruaud, J. L. Guenet, A. Munnich and J. Melki (1997). "cDNA isolation, expression, and chromosomal localization of the mouse survival motor neuron gene (Smn)." Genomics **40**(1): 185-188.

Webster, D. R., G. G. Gundersen, J. C. Bulinski and G. G. Borisy (1987). "Differential turnover of tyrosinated and detyrosinated microtubules." Proc Natl Acad Sci U S A **84**(24): 9040-9044.

Wen, H. L., Y. T. Lin, C. H. Ting, S. Lin-Chao, H. Li and H. M. Hsieh-Li (2010). "Stathmin, a microtubule-destabilizing protein, is dysregulated in spinal muscular atrophy." Hum Mol Genet **19**(9): 1766-1778.

Werdnig, G. (1971). "Two early infantile hereditary cases of progressive muscular atrophy simulating dystrophy, but on a neural basis. 1891." Arch Neurol **25**(3): 276-278.

Westermann, S. and K. Weber (2003). "Post-translational modifications regulate microtubule function." Nat Rev Mol Cell Biol **4**(12): 938-947.

Wiedau-Pazos, M., J. J. Goto, S. Rabizadeh, E. B. Gralla, J. A. Roe, M. K. Lee, J. S. Valentine and D. E. Bredesen (1996). "Altered reactivity of superoxide dismutase in familial amyotrophic lateral sclerosis." Science **271**(5248): 515-518.

Wiese, S., T. Herrmann, C. Drepper, S. Jablonka, N. Funk, A. Klausmeyer, M. L. Rogers, R. Rush and M. Sendtner (2010). "Isolation and enrichment of embryonic mouse motoneurons from the lumbar spinal cord of individual mouse embryos." Nat Protoc **5**(1): 31-38.

Williamson, T. L., L. I. Bruijn, Q. Zhu, K. L. Anderson, S. D. Anderson, J. P. Julien and D. W. Cleveland (1998). "Absence of neurofilaments reduces the selective vulnerability of motor neurons and slows disease caused by a familial amyotrophic lateral sclerosis-linked superoxide dismutase 1 mutant." Proc Natl Acad Sci U S A **95**(16): 9631-9636.

Williamson, T. L. and D. W. Cleveland (1999). "Slowing of axonal transport is a very early event in the toxicity of ALS-linked SOD1 mutants to motor neurons." Nat Neurosci **2**(1): 50-56.

Winkler, C., C. Eggert, D. Gradl, G. Meister, M. Giegerich, D. Wedlich, B. Laggerbauer and U. Fischer (2005). "Reduced U snRNP assembly causes motor axon degeneration in an animal model for spinal muscular atrophy." Genes Dev **19**(19): 2320-2330.

Witte, H., D. Neukirchen and F. Bradke (2008). "Microtubule stabilization specifies initial neuronal polarization." J Cell Biol **180**(3): 619-632.

Wloga, D. and J. Gaertig (2010). "Post-translational modifications of microtubules." J Cell Sci **123**(Pt 20): 3447-3455.

Wong, N. K., B. P. He and M. J. Strong (2000). "Characterization of neuronal intermediate filament protein expression in cervical spinal motor neurons in sporadic amyotrophic lateral sclerosis (ALS)." J Neuropathol Exp Neurol **59**(11): 972-982.

Wong, P. C., J. Marszalek, T. O. Crawford, Z. Xu, S. T. Hsieh, J. W. Griffin and D. W. Cleveland (1995). "Increasing neurofilament subunit NF-M expression reduces axonal NF-H, inhibits radial growth, and results in neurofilamentous accumulation in motor neurons." J Cell Biol **130**(6): 1413-1422.

Xu, Z., L. C. Cork, J. W. Griffin and D. W. Cleveland (1993). "Increased expression of neurofilament subunit NF-L produces morphological alterations that resemble the pathology of human motor neuron disease." Cell **73**(1): 23-33.

Yamasaki, H., C. Itakura and M. Mizutani (1991). "Hereditary hypotrophic axonopathy with neurofilament deficiency in a mutant strain of the Japanese quail." Acta Neuropathol **82**(6): 427-434.

Yuan, A., M. V. Rao, T. Sasaki, Y. Chen, A. Kumar, Veeranna, R. K. Liem, J. Eyer, A. C. Peterson, J. P. Julien and R. A. Nixon (2006). "Alpha-internexin is structurally and functionally associated with the neurofilament triplet proteins in the mature CNS." J Neurosci **26**(39): 10006-10019.

Zhang, W., A. Rohlmann, V. Sargsyan, G. Aramuni, R. E. Hammer, T. C. Sudhof and M. Missler (2005). "Extracellular domains of alpha-neurexins participate in regulating synaptic transmission by selectively affecting N- and P/Q-type Ca2+ channels." J Neurosci **25**(17): 4330-4342.

Zhao, C., J. Takita, Y. Tanaka, M. Setou, T. Nakagawa, S. Takeda, H. W. Yang, S. Terada, T. Nakata, Y. Takei, M. Saito, S. Tsuji, Y. Hayashi and N. Hirokawa (2001). "Charcot-Marie-Tooth disease type 2A caused by mutation in a microtubule motor KIF1Bbeta." Cell **105**(5): 587-597.

Zhao, J. X., A. Ohnishi, C. Itakura, M. Mizutani, T. Yamamoto, H. Hayashi and Y. Murai (1994). "Greater number of microtubules per axon of unmyelinated fibers of mutant quails deficient in neurofilaments: possible compensation for the absence of neurofilaments." Acta Neuropathol **87**(4): 332-336.

Zhu, Q., S. Couillard-Despres and J. P. Julien (1997). "Delayed maturation of regenerating myelinated axons in mice lacking neurofilaments." Exp Neurol **148**(1): 299-316.

Zhu, Q., M. Lindenbaum, F. Levavasseur, H. Jacomy and J. P. Julien (1998). "Disruption of the NF-H gene increases axonal microtubule content and velocity of neurofilament transport: relief of axonopathy resulting from the toxin beta,beta'-iminodipropionitrile." <u>J Cell Biol</u> **143**(1): 183-193.

Affidavit

I hereby confirm that my thesis entitled "Studying Neuronal Cytoskeleton Defects and Synaptic Defects in Mouse Model of Amyotrophic Lateral Sclerosis and Spinal Muscular Atrophy" is the result of my own work. I did not receive any help or support from commercial consultants. All sources and / or materials applied are listed and specified in the thesis. Furthermore, I confirm that this thesis has not yet been submitted as part of another examination process neither in identical nor in similar form.

Wuerzburg, _____

Place, Date   Signature

Eidesstattliche Erklärung

Hiermit erkläre ich an Eides statt, die Dissertation mit dem Titel "Die Analyse des neuronalen Zytoskeletts und synaptischer Defekte im Mausmodel der Amyotrophen Lateralsklerose und der Spinalen Muskelatrophie " eigenständig, d.h. insbesondere selbständig und ohne Hilfe eines kommerziellen Promotionsberaters, angefertigt und keine anderen als die von mir angegebenen Quellen und Hilfsmittel verwendet zu haben.

Ich erkläre außerdem, dass die Dissertation weder in gleicher noch in ähnlicher Form bereits in einem anderen Prüfungsverfahren vorgelegen hat.

Würzburg, _____

Ort, Datum   Unterschrift

Curriculum Vitae

PERSONAL INFORMATION

Name   Preeti Yadav

Education

Apr 2010 – expected Jan 2016 PhD; University of Wuerzburg, Germany, Institute for Clinical Neurobiology, Fellow at Graduate School of Life Sciences (GSLS)

Nov 2008 – Jan 2010, Project Assistant; National Brain Research Centre, India**,** Major research area: Learning and Memory

Jun 2006 – May 2008, Master of Science, Jawaharlal Nehru University, New Delhi, India, Courses: Biotechnology, Immunology, Molecular Biology

Jul 2003 – Apr 2006, Bachelor of Science, Maharani's College, University of Rajasthan**, Courses**: Biotechnology, Botany and Chemistry.

Research experience

Apr 2010 - Jan 2016, University of Würzburg, Germany**,** Institute for Clinical Neurobiology, PhD title: Studying neuronal cytoskeleton alteration and synaptic defects in mouse models of amyotrophic lateral sclerosis and spinal muscular atrophy.

Nov 2008 - Jan 2010, National Brain Research Centre, India, Research project: Depolarization induces acetylation of histone H2B in the hippocampus.

Jun 2006 – May 2008, Jawaharlal Nehru University, New Delhi, India, Master thesis: Studying the effect of various process parameters on recombinant protein production in bacteria and studying quiescent bacterial cells.

Posters

Oct 2011; presented a scientific poster; **"**Altered mRNA expression for a presynaptic protein Neurexin in spinal muscular atrophy'', at International symposium Bio-Bang, 2011, organized by GSLS, Wuerzburg. Germany**.**

Jun 2012; presented a scientific poster, **"**Differential expression and altered splicing of Neurexin, a presynaptic protein, in spinal muscular atrophy'', at International meeting NGF, 2012, Wuerzburg, Germany.

Oct 2012; presented a scientific poster, Differential expression and altered splicing of Neurexin, a presynaptic protein, in spinal muscular atrophy, at the Society for Neuroscience meeting, 2012 in New Orleans, US.

Scholarships and Courses

Apr 2010 - Oct 2013; Scholarship from Graduate school of life sciences, University of Würzburg.

Jun 2006 – May 2008; Scholarship from Department of Biotechnology (DBT, India) for Master thesis at Jawaharlal Nehru University.

Oct 2012; attended the course work and cleared the exams for Clinical Neurobiology course for Masters with a grade of 1.3.

Publications

Aug 2012; Subramanian N, Wetzel A, Dombert B, Yadav P, Havlicek S, Jablonka S, Nassar MA, Blum R, Sendtner M. Role of Na(v)1.9 in activity-dependent axon growth in motoneurons. Hum Mol Genet. 2012, Aug 15; 21(16):3655-67.

Apr 2014; See K, Yadav P, Giegerich M, Cheong PS, Graf M, Vyas H, Lee SG, Mathavan S, Fischer U, Sendtner M, Winkler C**.** Altered Splicing of mRNA for Presynaptic Protein Neurexin in Spinal Muscular Atrophy. Hum Mol Genet. 2014 Apr; 23(7):1754-70.

Acknowledgements

At the end of my PhD, I am using this opportunity to express my deepest appreciation and gratitude to all those who supported me in successfully completing this research work. This work is made possible with the help and trust of several individuals who directly or indirectly supported me in achieving this goal. The journey has been a wonderful learning experience on both personal and professional level and I thank God for giving me the strength to complete this journey with all the patience.

Firstly, I am thankful to Prof. Michael Sendtner for his aspiring guidance during this doctoral dissertation. It was a great pleasure and a thorough learning experience to work under his supervision. His approach was extraordinarily motivating, his constructive criticism and friendly advices led to the success of this thesis. His continued support, his vision and scientific knowledge led me to accomplish this excellent research work. Thanks to him for showing the trust in me, encouraging my research and for allowing me to grow as a research scientist.

I thank Professor Erich Buchner for serving as my committee member and for all his advices for the project. I also want to thank him for his brilliant comments and suggestions during the lab meetings and supervisory meetings.

Next my special appreciation and thanks to Dr. Robert Blum for being my committee member and for his excellent suggestions and help during my PhD. I am sincerely grateful to him for all the emotional support he has provided during this time. The excellent technical approach and an organized way for scientific experiments that I learned from him will be very helpful for me throughout my scientific career.

I also thank Prof. Asan Esther for the collaborative work done with her and for her promptness and interest to discuss the results. Similarly, I thank Dr. Christoph Winkler and Prof. Markus Sauer for the collaborative works I performed with them.

Next, I thank the animal house for the help especially Regine Sendtner, Victor Buterus, Richard, Verena and Joachim Horschig. Without their help this tedious work on a double knockout line would have been a nightmare. All of them were there to support me when I needed mice and crossings for my PhD work and I sincerely appreciate this more than they will ever know.